REPUBLIQUE ALGERIENNE DEMOCRATIQUE ET POPULAIRE

MINISTERE DE L'ENSEIGNEMENT SUPERIEUR ET DE LA RECHERCHE SCIENTIFIQUE

UNIVERSITE FERHAT ABBAS – SETIF 1
UFAS 1 (ALGERIE)

THESE

Présentée à l'Institut d'Optique et de Mécanique de Précision

Pour l'obtention du diplôme de

Doctorat En Science

Option : Optique et Mécanique de Précision

Par:

Mr. GUESSOUM AMIR

THÈME:

**Étude de l'interaction acousto-optique dans un milieu perturbé
par un signal modulé en fréquence et en phase**

**Study of acousto-optic interaction in a medium perturbed by
a frequency and phase modulated signal**

Soutenu le ………………. devant la commission d'examen composée de:

Président	BOUAFIA Mohamed	Professeur	Université de Sétif 1
Rapporteur	LAOUAR Naamane	MCA	Université de Sétif 1
Examinateurs	HAMADOU Abdelouahab	MCA	Université de BBA
	BENCHEIKH Abdelhalim	MCA	Université de BBA

التشكرات :

الحمد لله الذي وفقنا لطلب العلم ورتب عليه الأجر الكبير لمن أخلص و نفع به نفسه وغيره . إننا لن نكون أقوياء في العمل إلا إذا كنا أقوياء في العلم ولن نكون أقوياء في العلم إلا إذا إنقطعنا له ووقفنا له الوقت كله ، إن العلم لا يعطي القياد إلا لمن مهره السهاد وصرف إليه أعنة الإجتهاد . العالم و المتعلم شريكان في الخير وسائر الناس همج لا خير فيهم .

الشكر الكبير لكل من ساهم في تطوير العلم من عالم و متعلم ، وكل الشكر للأساتذة الذين تتلمذت على أيديهم من الطور الإبتدائي إلى غاية حصولي على شهادة التخرج وعلى رأسهم الأستاذ **لعور نعمان** الذي كان له الفضل الكبير في إدخالنا في دوامة تداخل الأمواج الصوتية والضوئية .

كذلك تشكراتي الكبيرة و الخالصة للأستاذ والزميل **قويدر فرية** على سعة رحابة صدره ووقوفه معنا إلى غاية إنهاء هذا المقال العلمي وكذا توفيره للعتاد الذي مكننا من تحقيق التجربة .

كل الشكر لكل أعضاء لجنة التقييم الذين تحملوا المشاق في فهم ، تصحيح وتقييم هذه الأطروحة .

وإن كنت أنسى فلست أنسى أن أوجه جزيل الشكر **لوالدي** حفظهما الله اللذين سهرا علي منذ نعومة أظافري .

بالطبع فإنني لا أنسى نصائح زملائي الأساتذة:بلخير نبيل، بلقاسم بخوش، واحدي رشيد وكل من سار على دأبهم، والعفو الكبير من كل من نسينا ذكره .

والحمد لله أولا وأخيرا

CONTENTS

CHAPTER I

MODULATED ELECTRICAL SIGNALS

CHAPTER II

THE ULTRASOUND EFFECT ON REFRACTIVE INDEX

CHAPTER III

THEORETICAL STUDY OF ACOUSTO-OPTIC INTERACTION

CHAPTER IV

EXPERIMENTAL STUDY OF THE LIGHT DEFLECTION

LIST OF FIGURES

LIST OF TABLES

INTRODUCTION

Before we begin to present the main goal of this research and the thesis outline, it is of interest to briefly review the historical development and some of the important milestones in acousto-optic field. This field was studied extensively in the past century, where in 1922, Brillouin predicted that the light can be diffracted by ultrasound [1]. It was not possible to confirm this prediction experimentally until ten years later. Surprisingly, simultaneously and for the first time a large number of diffracted orders was observed, symmetrically spaced about the undiffracted beam, independently by the Americans Debye and Sears, and the French Lucas and Biquard in 1932 [2-3]. Various efforts were made by them to describe the presence of multiple diffracted orders but unfortunately the intensities wandering of the various components has not found explanation in any of their theories [4].

In 1935 Raman and Nath succeeded to explain this diffraction where they demonstrated that the propagation of an ultrasonic wave in elastic medium creates dilation and compression regions according to the rhythm of this ultrasonic wave. This variation produces a periodic modulation of the refractive index via the elasto-optic effect. Accordingly, the medium which was initially homogeneous transformed into inhomogeneous one providing a dynamic phase grating. This last may diffract portions of an incident light into one or more directions. The theoretical analysis of this diffraction showed that the intensity and the position, of each diffracted order, are constant when ultrasonic wave is sinusoidal [4-5].

In case where sinusoidal ultrasonic wave is amplitude modulated (AM), the diffraction orders position remains constant. Likewise, it was observed that besides these diffracted orders, the spectrum showed satellite diffracted orders. This diffraction was performed for the first time by Pancholy and Parthasarathy and explained mathematically by Mertens and Hereman in 1979 [6-7].

Meanwhile, the using of frequency modulated ultrasonic wave (FM) led to appear a variety of optical devices such as acousto-optic deflectors (AODs), which have in turn widespread applications in many fields. For instance, some authors used theses AODs to develop an

acousto-optic cylindrical lens with a very fast focal scanning [8] by using two adjacent counterpropagating acoustic waves carrying the same frequency chirp [9]. Recently, AODs attracted more attention for diverse applications as is quoted in [10-11].

In the same context, other diffraction can be obtained using sinusoidal ultrasonic wave of high frequency modulated by another sinusoidal one of low frequency. In this case the position of the diffracted order is no longer constant as the two first cases, sinusoidal and AM signal, but it oscillates around a central position with scanning frequency which increases proportionally with the modulating signal frequency. This deflection has long been known but it remained, to our knowledge, without explication.

In this work, we theoretically study this deflection, following the same steps of those who preceded us in this field, starting form acousto-optic interaction principle to finally reach a very important relationship between the diffracted order position and the modulating signal. Afterwards, in order to check the proposed theoretical development a series of experiments are conducted.

For better presentation and clear explanation of this research work, we are starting by studying modulated electrical signal which is used to generate ultrasound. After this, the determination of the relationship between the ultrasound and the medium refractive index is primordial to explain the diffraction phenomenon. Therefore, the thesis is organized as follows:

i.   The first chapter is interested to study the different electrical signals (amplitude modulated, frequency modulated and phase modulated). Particular attention is devoted to frequency modulated signal as well as the essential parameters that affect the acousto optic deflector such as; modulation frequency, frequency excursion and frequency modulation index.

ii. In the second chapter, which is considered the longest, we exploit electrical signals sited above to generate ultrasonic waves using piezoelectric transducer. This is followed by the study of ultrasounds propagation in elastic media and their effect on the refractive index.

iii. During the third chapter, which is considered the most important, we theoretically investigate the diffraction phenomenon obtained by the interaction of ultrasonic waves,

generated previously, and electromagnetic one. This treatment is performed for three types of ultrasonic waves (sinusoidal, amplitude modulated and frequency modulated).

iv.   The experimental part is the subject of the fourth chapter, which presents the different performed experiments in order to check the theoretical development proposed in the chapter number three. Such as the effect of modulating signal frequency on the scanning frequency and the angular excursion of each diffracted order. This is followed by a new method presentation enables us to measure the frequency modulation index. This operation was performed before using only a spectrum analyzer.

This thesis is ended with general conclusion in which we present the achieved results and future prospects in this field.

CHAPTER I

MODULATED ELECTRICAL SIGNALS

1-1) Introduction:

During the development of telecommunication devices, it quickly became necessary to code the information to be transmitted, either to adapt the information to the transmission channel or to simultaneously transmit several signals on the same channel. As a result, the coding of information is still being research subject. One of the forms of the information coding among the simplest and the oldest is to perform a frequency translation of the carrier. This type of coding is called analog modulation [12].

Analog modulation is the process of facilitating the transport of information over a carrier. For instance, the sound transmission in air has a limited range depends on sonic power. To extend the range of sound, we need to transmit it by another way, such as an electromagnetic wave. To perform that, it's enough to vary the amplitude, frequency or phase of a carrier in accordance with instantaneous value of information (modulating signal). Once the carrier is mapped with the information to be sent, it is no longer a carrier and we call it the modulated signal. We distinguish three types of modulation [13]:

Amplitude modulation (AM).

Exponential modulation: Frequency modulation (FM).

Phase modulation (PM).

AM and FM are ways of broadcasting radio signals. Both transmit the information in the form of electromagnetic waves. AM works by modulating the amplitude of the carrier according to the modulating signal being sent, while the frequency remains constant. This differs from FM technology in which information is encoded by varying the carrier frequency and its amplitude is kept constant [34].

Generally, the carrier frequency is very high compared to the modulating signal frequency. In the case where the two signals are sinusoidal, we write:

$$A(t) = A_a \cos(\omega_a t) \tag{1.1}$$

Where:

A_a : Carrier amplitude.

ω_a : Carrier pulsation.

The comparison of these different modulation types and the choice of one of them is based on numerous criteria (noise immunity, implementation, demodulation, range, cost, etc.) [20].

1-2) Amplitude modulation (AM):

Amplitude modulation was the earliest modulation method used in electronic communication, most commonly for transmitting voice. It was developed during the first two decades of the 20th century beginning. The amplitude of the carrier is varied in proportion to the modulating signal being transmitted. In our study, we will interest in a sinusoidal modulating signal.

1-2-1) Expression of amplitude modulated sinusoidal signal:

As its name implies, an amplitude modulated sinusoidal electrical signal $A(t)$ is a signal has an amplitude modifies according to a linear law by the modulating signal.

Let $S(t)$ represent the modulating signal with a frequency f_m and amplitude A_m:

$$S(t) = A_m \cos(\omega_m t) \tag{1.2}$$

So, the amplitude modulated signal is written as follows:

$$A(t) = [A_a + C_a S(t)] \cos(\omega_a t) \tag{1.3}$$

Where: C_a is the modulator proportionality factor, which sometimes takes the denomination modulator sensitivity.

If we replace equation (1.2) in equation (1.3), we obtain:

$$A(t) = [A_a + C_a A_m \cos(\omega_m t)] \cos(\omega_a t) = A_a \left[1 + \frac{C_a A_m}{A_a} \cos(\omega_m t) \right] \cos(\omega_a t)$$

$$= A_a [1 + \beta_a \cos(\omega_m t)] \cos(\omega_a t) \tag{1.4}$$

Where β_a is the amplitude modulation index (Amplitude modulation depth).

1-2-2) Time domain of AM signal:

To plot AM signal as a function of time, we choose for example a carrier with a frequency of $f_a = 10^6\, Hz$ and a modulating signal of frequency $f_m = 10^3\, Hz$. The graphs below represent the amplitude modulated signal for different values of β_a.

➢ t=0:.00000001:0.003;

A= $(1+\beta_a *\cos(2*\text{pi}*10\text{^}3*t)).*\cos(2*\text{pi}*10\text{^}6*t)$;

>> plot(A),grid

+50%

Original level

-50%

Time [s]
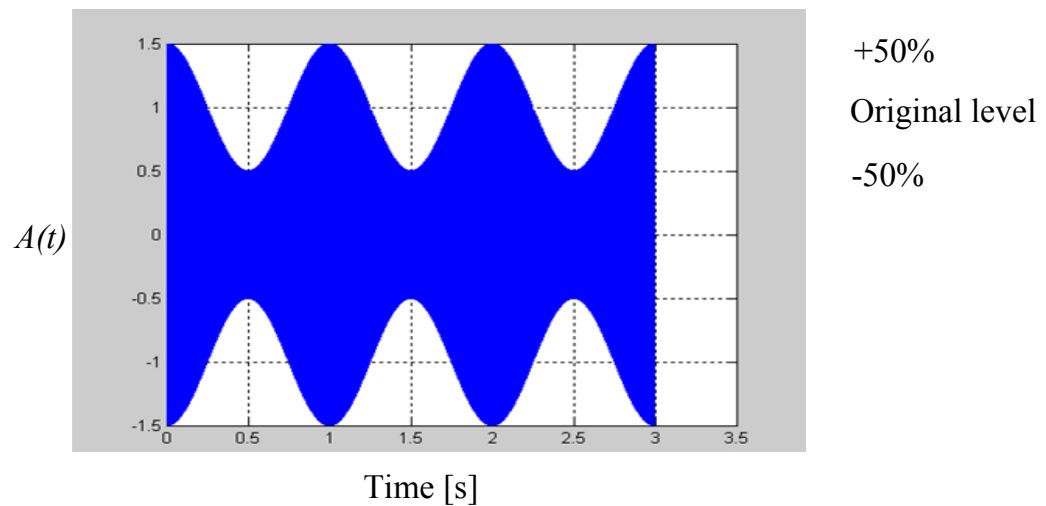
Figure 1.1: Time domain representation of AM signal for $\beta_a = 0.5$

Time [s]
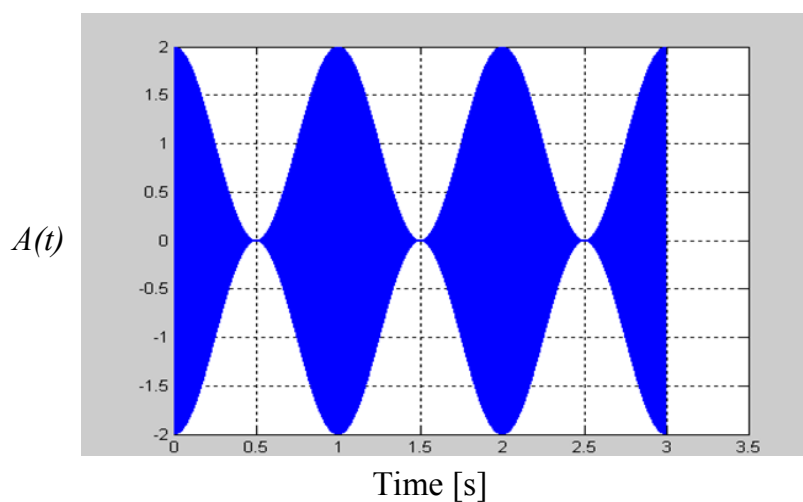
Figure 1.2: Time domain representation of AM signal for $\beta_a = 1$

9
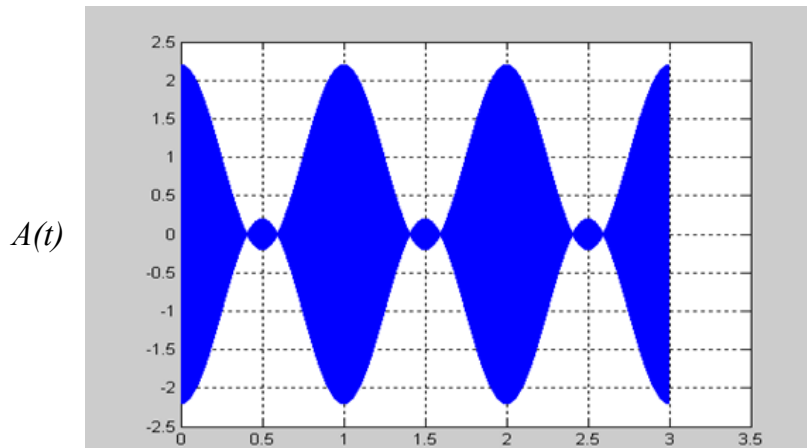
- From these figures, it can be seen that for an amplitude modulation index of 0.5, the modulation causes the signal to increase by a factor of 0.5 and decrease to 0.5 of its original level.

- When the modulation index reaches 1, the carrier level falls to zero and rises to twice its non-modulated level.

- Any increase of the modulation index above 1 causes over-modulation which gives rise to additional sidebands.

- Experimentally, we can easily extract the AM index value from the graphics, without knowing f_a and f_m, as follows:

We have: $A(t) = A_a \left[1 + \beta_a \cos(\omega_m t) \right] \cos(\omega_a t)$

So the new amplitude is $A'(t) = A_a \left[1 + \beta_a \cos(\omega_m t) \right]$

In the case where $\left[\cos(\omega_m t) = 1 \right] \Rightarrow A'(t) = A'_{max} = A_a \left[1 + \beta_a \right]$ 1.5

And if $\left[\cos(\omega_m t) = -1 \right] \Rightarrow A'(t) = A'_{min} = A_a \left[1 - \beta_a \right]$ 1.6

From (1.5) and (1.6) we can find:

$$\beta_a = \frac{A'_{max} - A'_{min}}{A'_{max} + A'_{min}}$$ 1.7

For example in figure (1.1), the amplitude modulation index equals:

$$\beta_a = \frac{A'_{max} - A'_{min}}{A'_{max} + A'_{min}} = \frac{1.5 - 0.5}{1.5 + 0.5} = 0.5$$

1-2-3) Frequency domain of AM signal:

In the frequency domain, amplitude modulation produces a signal with power concentrated at the carrier frequency and two adjacent sidebands. Each sideband is an image of the other as indicated below.

Using trigonometric relationship:

$$\cos(a)\,\cos(b) = \frac{1}{2}\left[\cos(a+b) + \cos(a-b)\right]$$

The equation $A(t)$ can be written as a sum of three sine waves [34]:

$$A(t) = A_a\left[1 + \beta_a \cos(\omega_m t)\right]\cos(\omega_a t)$$

$$= A_a \cos(\omega_a t) + A_0\,\beta_a \cos(\omega_m t)\,\cos(\omega_a t)$$

$$\Rightarrow A(t) = A_a \cos(\omega_a t) + \frac{A_a\,\beta_a}{2}\left[\cos(\omega_m t + \omega_a t) + \cos(\omega_m t - \omega_a t)\right] \qquad 1.8$$

Therefore, the modulated signal has three components: the carrier which is unchanged and two sine waves with frequencies slightly above and below the carrier frequency f_a.

The spectrum $\underline{A}(f)$ of the signal is then obtained by using the Fourier transform of this signal:

$$\underline{A}(f) = \frac{A_a}{2}\left[\delta(f - f_a) + \delta(f + f_a)\right] + \frac{A_a\,\beta_a}{4}\left[\delta(f - (f_a + f_m)) + \delta(f + (f_a + f_m))\right]$$

$$+ \frac{A_a\,\beta_a}{4}\left[\delta(f - (f_a - f_m)) + \delta(f + (f_a - f_m))\right] \qquad\qquad 1.9$$

Where $\delta(f)$ represents the Dirac Delta function (Appendix 1).

This gives rise to two identical spectra, one for negative frequencies, and the other for positive ones as indicated in figure (1.4). Each spectrum is composed of three lines, one of amplitude $A_a/2$ at frequency f_a, the two other are of amplitude $A_a\,\beta_a/4$ at frequencies; $(f_a - f_m)$ called Lower Side Band (LSB) and $(f_a + f_m)$ called Upper Side Band (USB) [12].

$$\underline{A}(f)$$

$$\frac{A_a}{2}$$

$$\frac{A_a\beta_a}{4}$$

$$-(f_a + f_m) \quad -f_a \quad -(f_a - f_m) \qquad\qquad f_a - f_m \quad f_a \quad f_a + f_m \quad f$$
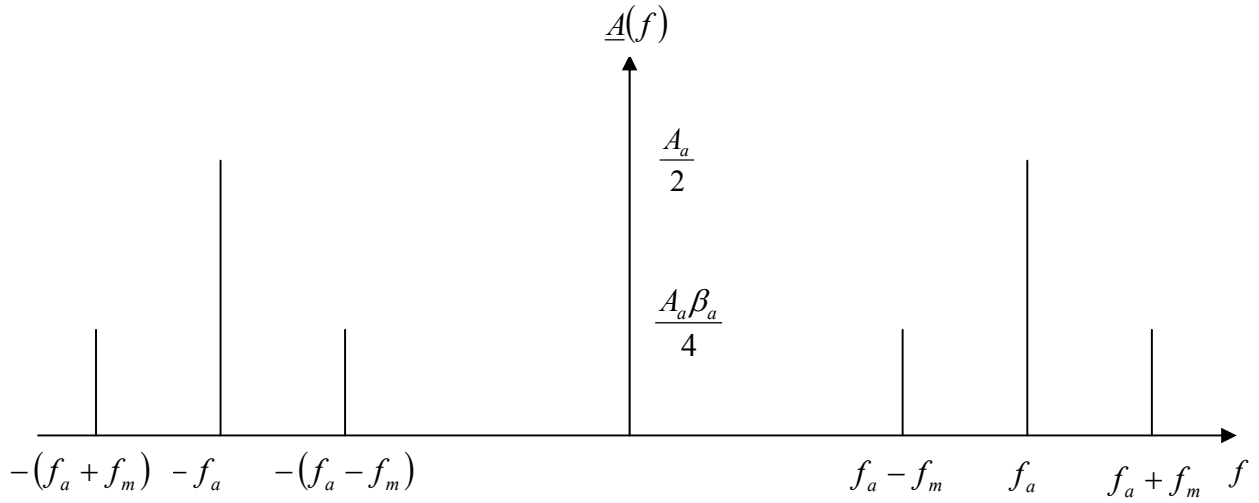
Figure 1.4: Frequency domain representation of AM signal

When the carrier is fully modulated ($\beta_a = 1$), the amplitude of line at frequency f_a is equal to half that of the carrier, the sum of the powers of the sidebands is equal to half that of the carrier. This means that each sideband is just a quarter of the total power. In other words, for transmitting 100 watts, the total sideband power would be 50 watts and each individual sideband would be 25 watts [34].

Therefore, the sidebands spread out either side of the carrier and the total required bandwidth to transmit the signal, preserving its integrity, is given by the following equation [12, 20]:

$$BP_a = 2f_m \qquad\qquad 1.10$$

1-3) Exponential modulation:

We have already seen that the AM principle is based on the amplitude modification of the carrier without the frequency modification. Another form of modulation is to keep the amplitude of the carrier constant and vary, as a function the modulating signal rhythm, the value of the instantaneous phase. This modulation is called exponential or angular modulation [12-20].

We can define the instantaneous pulsation as follows:

$$\omega(t) = \frac{d\varphi(t)}{dt} \qquad\qquad 1.11$$

12

These two quantities $\omega(t)$ and $\varphi(t)$ will be modified as a function of the modulating signal. According to the characteristics of this modification we will have two modulations; a frequency modulation which is linear action on the instantaneous pulsation $\omega(t)$ and a phase modulation which acts linearly on the instantaneous phase $\varphi(t)$. The advantage of these types of modulations is that the signals are less disturbed by the "noises" during their transmission, because the noises modify the amplitude, not the frequency of a signal.

1-3-1) Frequency modulation:

1-3-1-1) Expression of frequency modulated sinusoidal signal:

In this case, the amplitude of the transmitted signal is constant and the information signal is encoded linearly in carrier frequency as indicate these formulas:

$$A(t) = A_a \left[\cos\left(\omega_a\, t + 2\,\pi\, C_f \int S(t)\, dt \right) \right] \qquad 1.12$$

Where C_f being the modulator proportionality factor, this sometimes takes the denomination of modulator sensitivity [12].

The instantaneous phase, pulsation and frequency are given, respectively, by the following formulas:

$$\varphi(t) = \omega_a\, t + 2\,\pi\, C_f \int S(t)\, dt \qquad 1.13$$

$$\omega(t) = \omega_a + 2\,\pi\, C_f\, S(t) \qquad 1.14$$

$$f(t) = f_a + C_f\, S(t) \qquad 1.15$$

In the case where $S(t)$ is cosinusoidal, the formulas (1.12-1.15) become:

$$A(t) = A_a \left[\cos\left(\omega_a\, t + \frac{C_f \cdot A_m}{f_m} \sin(\omega_m\, t) \right) \right] \qquad 1.16$$

$$f(t) = f_a + C_f \cdot A_m \cos(\omega_m\, t) \qquad 1.17$$

The quantity $C_f \cdot A_m = \Delta f$ is called the frequency excursion (frequency deviation).

Therefore, the pulsation and phase excursion are written:

$$\varphi(t) = \omega_a\, t + \frac{C_f \cdot A_m}{f_m} \sin(\omega_m\, t) \Rightarrow \Delta\varphi = \frac{C_f \cdot A_m}{f_m} \qquad\qquad 1.18$$

$$\omega(t) = \omega_a + 2\pi\, C_f \cdot A_m \cos(\omega_m\, t) \Rightarrow \Delta\omega = 2\pi\, C_f \cdot A_m \qquad\qquad 1.19$$

The relation between the frequency excursion and phase one is written then:

$$\Delta\varphi = \frac{\Delta f}{f_m} \qquad\qquad 1.20$$

Usually, this term is called frequency modulation index $\beta_f = \Delta\varphi = \dfrac{\Delta f}{f_m}$. It is then possible to

rewrite the expression of the FM signal in the form below:

$$A(t) = A_a\left[\cos\left(\omega_a\, t + \beta_f \sin(\omega_m\, t)\right)\right] \qquad\qquad 1.21$$

It is essential to note that the FM index, contrarily to AM index, depends in the same time on the frequency and the amplitude of the modulating signal [12].

1-3-1-2) Time domain of FM signal:

To plot FM signal as a function of time, we choose a carrier with a frequency of $f_a = 10^3\, Hz$ and a modulating signal of frequency $f_m = 10^2\, Hz$. The graphs below represent the FM signal for different values of β_f.

➢ t=0:.00001:0.02; y=cos((2*pi*1000*t)+ β_f*sin(2*pi*100*t)); plot(t,y),grid

$A(t)$

Time [s]
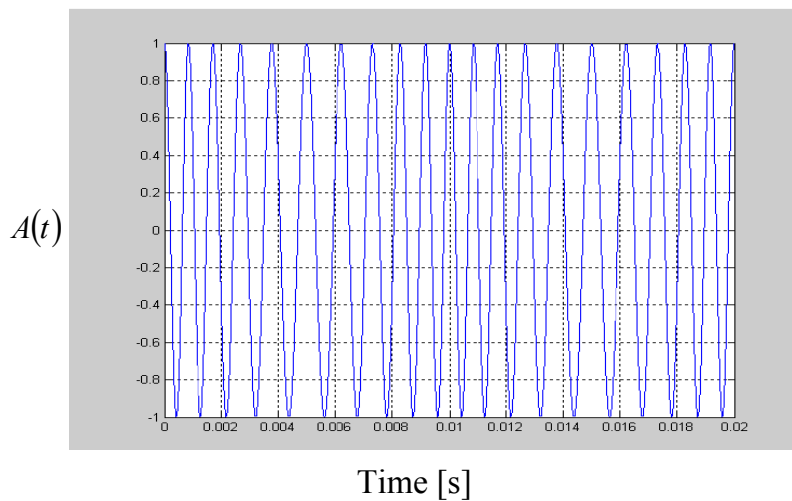
Figure 1.5: Time domain representation of FM signal for $\beta_f = 2$

14

Time [s]
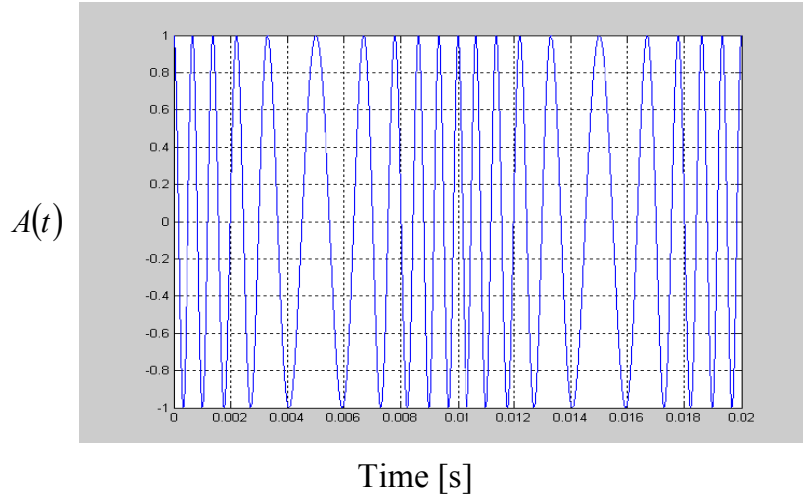
Figure 1.6: Time domain representation of FM signal for $\beta_f = 5$

Time [s]
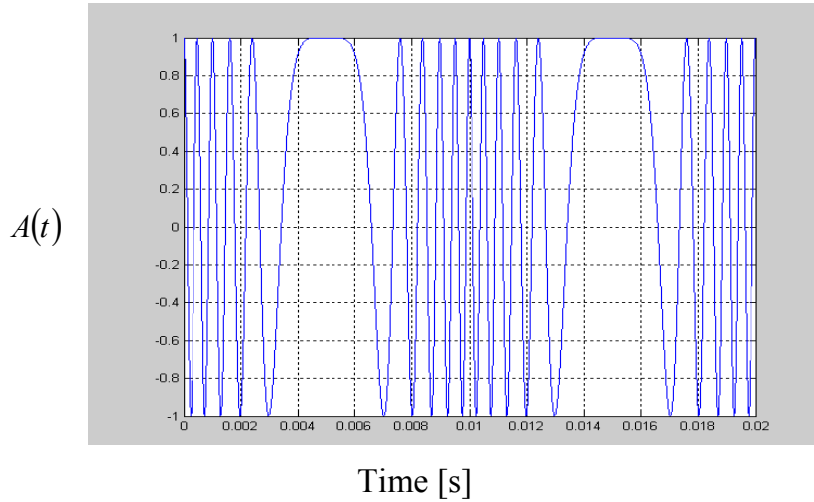
Figure 1.7: Time domain representation of FM signal for $\beta_f = 10$

From these figures, one can see that:

- If $\Delta f \ll f_a$, the FM signal appear as sinusoidal one because the instantaneous frequency becomes almost constant. Thus, whenever the frequency excursion approaches the carrier frequency, the frequency modulation becomes more representative.

- Experimentally, we can easily determine the FM index value from the signal curve, without knowing f_a , as follows:

We have: $\qquad\qquad f(t) = f_a + \Delta f \cdot \cos(\omega_m t)$

In the case where $\quad t = n' \cdot T_m \Rightarrow f(n' \cdot T_m) = f_{\max} = \Delta f + f_a$ $\qquad\qquad$ 1.22

15

And if $\quad\quad\quad\quad t = (n'+1/2)\cdot T_m \Rightarrow f((n'+1/2)\cdot T_m) = f_{min} = -\Delta f + f_a$ $\quad\quad\quad\quad$ 1.23

From (1.22) and (1.23) we can find:

$$\Delta f = \frac{f_{max} - f_{min}}{2}$$ $\quad\quad\quad\quad$ 1.24

Therefore, the value of FM index is: $\beta_f = \dfrac{f_{max} - f_{min}}{2 f_m}$

Where the value of f_{max} and f_{min} are extracted directly from the signal curve.

For instance, when we choose a carrier with a frequency of $f_a = 10\,MHz$, a modulating signal of frequency $f_m = 0.1\,Hz$ and $\beta_f = 5\cdot10^7$. The FM signal expression is written as follows:

$$A(t) = A_a \left[\cos\left(2\pi\ 10^7 t + 5\cdot10^7 \sin(2\pi\ 0.1t)\right)\right]$$

The instantaneous periods, of this signal $A(t)$, presented in the second column of the table (1.1) below are obtained theoretically using the MATLAB software, whereas the instantaneous periods of the third column are obtained experimentally using a memory oscilloscope (See chapter 4).

From this table, we can easily extract the values of T_{min} and T_{max} thus f_{max} and f_{min} .
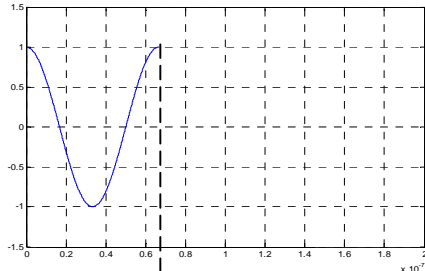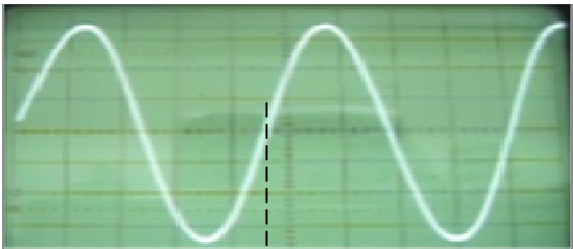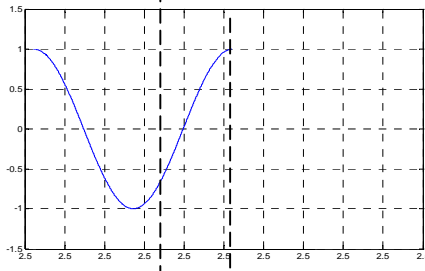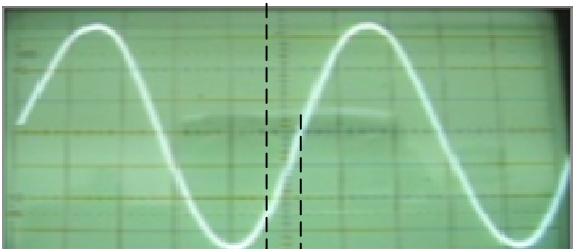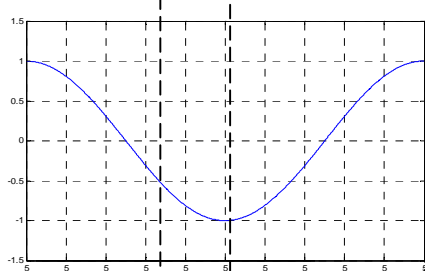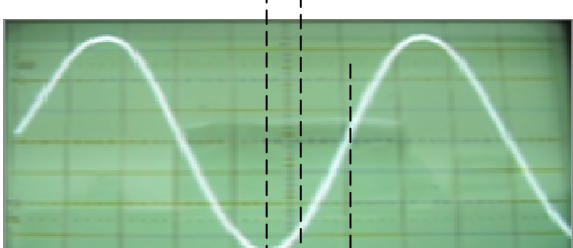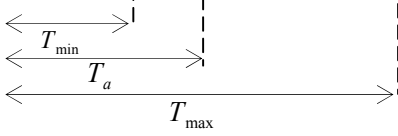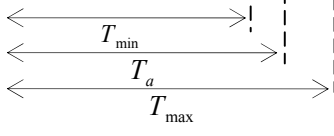
Time [s]	Instantaneous period obtained theoretically using MATLAB software	Instantaneous periods obtained experimentally using a memory oscilloscope
$0 \leq t \leq T_{min}$		
$2.5 \leq t \leq 2.5 + T_a$		
$5 \leq t \leq 5 + T_{max}$		
	T_{min} T_a T_{max}	T_{min} T_a T_{max}

Table 1.1: Instantaneous periods of FM signal.

<u>1-3-1-3) Frequency domain of FM signal:</u>

Using relationship number five derived from the Jacobi–Anger identity (Appendix 2), it is possible to put the equation (1.21) in the form [20]:

$$A(t) = A_a \left[\sum_{n=-\infty}^{+\infty} J_n(\beta_f) \cos(\omega_a t + n \omega_m t) \right] \qquad 1.25$$

$$\Rightarrow A(t) = A_a J_0(\beta_f) \cos(\omega_a t)$$
$$+ A_a J_1(\beta_f) \left[\cos(\omega_a t + \omega_m t) - \cos(\omega_a t - \omega_m t) \right]$$
$$+ A_a J_2(\beta_f) \left[\cos(\omega_a t + 2\omega_m t) + \cos(\omega_a t - 2\omega_m t) \right]$$
$$+ A_a J_3(\beta_f) \left[\cos(\omega_a t + 3\omega_m t) - \cos(\omega_a t - 3\omega_m t) \right] + ...$$

Where: J_n is the Bessel function of the first kind for integer orders n (Appendix 3).

Hence, the spectrum $\underline{A}(f)$ of signal $A(t)$ is written as follows:

$$\underline{A}(f) = TF[A(t)] = \frac{A_0}{2} J_0(\beta_f) \left[\delta(f - f_a) + \delta(f + f_a) \right]$$

$$+ \frac{A_a}{2} J_1(\beta_f) \left[\delta(f - (f_a + f_m)) + \delta(f + (f_a + f_m)) - \left[\delta(f - (f_a - f_m)) + \delta(f + (f_a - f_m)) \right] \right]$$

$$+ \frac{A_a}{2} J_2(\beta_f) \left[\delta(f - (f_a + 2f_m)) + \delta(f + (f_a + 2f_m)) + \left[\delta(f - (f_a - 2f_m)) + \delta(f + (f_a - 2f_m)) \right] \right] + ...$$

$$\Rightarrow \underline{A}(f) = \frac{A_a}{2} \sum_{n=-\infty}^{+\infty} J_n(\beta_f) \left[\delta(f - (f_a + nf_m)) + \delta(f + (f_a + nf_m)) \right] \qquad I.26$$

This shows two identical spectra, one for negative frequencies and the other for positive ones as indicated in figure (1.8). Each spectrum is composed of lateral lines infinity on each side of the carrier frequency f_a. The Bessel function $J_n(\beta_f)$ represents the line amplitude $(f_a + nf_m)$. Each two symmetrical lateral line have the same amplitude, so each spectrum is symmetrical with respect to the frequency f_a [20].

$$|\underline{A}(f)|$$

$$J_0(1) \qquad J_0(1)$$

$$J_1(1) \qquad J_1(1) \qquad J_1(1) \qquad J_1(1)$$

$$J_2(1) \qquad J_2(1) \quad J_2(1) \qquad J_2(1)$$

$-(f_a+2f_m) \quad -(f_a+f_m) \quad -f_a \quad -(f_a-f_m) \quad -(f_a-2f_m) \qquad f_a-2f_m \quad f_a-f_m \qquad f_a \qquad f_a+f_m \qquad f_a+2f_m$
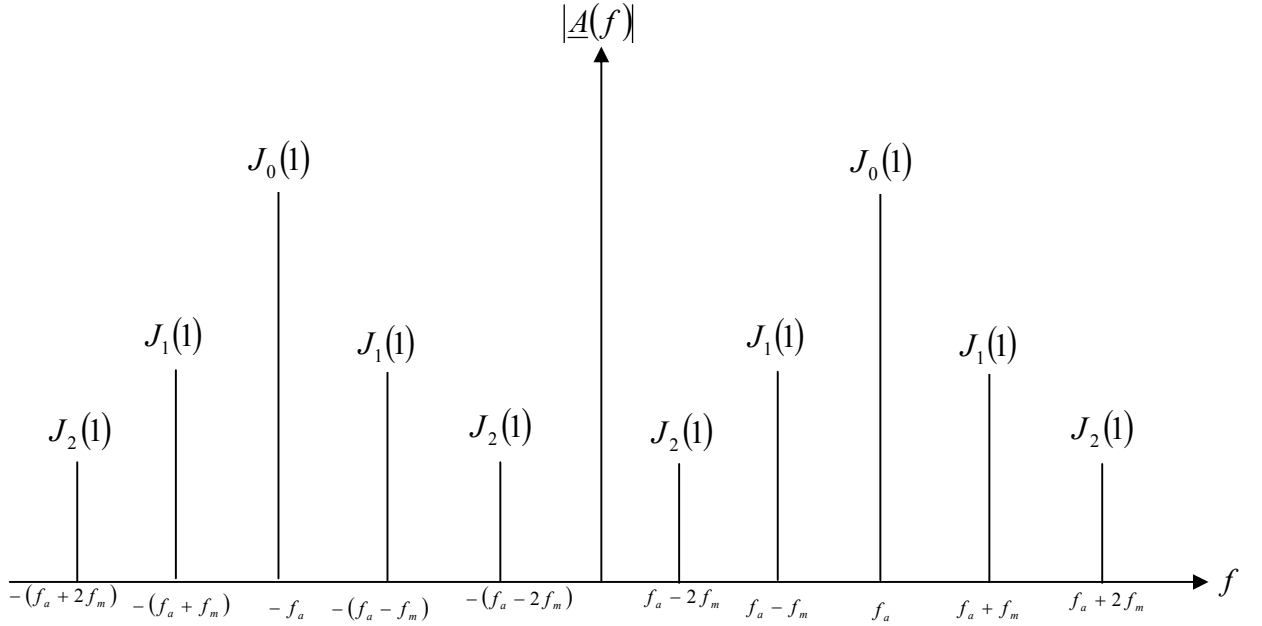
Figure 1.8: Frequency domain representation of FM signal $\beta_f = 1$ *et* $A_0 = 2$

Theoretically, the FM signal spectrum has components extending infinitely, although their amplitude decreases. In practice, only the N lines on both sides of f_a, in total 2N + 1, are taken into account when determining the bandwidth [12]. Using the Carson bandwidth rule which states that almost all lines that contribute 99% of the power of frequency modulated signal situate within the bandwidth given by:

$$BP_f = 2 N f_m = 2(\beta_f + 1) f_m \qquad\qquad\qquad \text{I.27}$$

It is important to note that the FM signal bandwidth is $(\beta_f + 1)$ times greater than that of the AM signal [20]:

$$BP_a = 2 \ f_m \qquad\qquad\qquad\qquad BP_f = 2(\beta_f + 1) f_m$$

Precisely:

In the case where: $\quad f_m << \Delta f \Rightarrow B_f >> 1 \Rightarrow BP_f = 2 B_f f_m = BP_a B_f$

And if: $\qquad\qquad\quad f_m >> \Delta f \Rightarrow B_f << 1 \Rightarrow BP_f = BP_a = 2 \ f_m$

As a result, FM systems are far better than AM ones; either in terms of its larger bandwidth or its higher immunity against random noise. This last permits to say there is virtually no interference picked up in the FM receiver.

1-3-2) Phase modulation:

1-3-2-1) Expression of phase modulated sinusoidal signal:

As we have already seen, phase modulation and frequency one are closely linked together, only in this case the information signal is encoded linearly in carrier phase as indicate these formulas:

$$A(t) = A_a \lfloor \cos(\omega_a t - C_p \cdot S(t)) \rfloor \qquad\qquad 1.28$$

Where C_p being the sensitivity of modulator.

The instantaneous phase and pulsation are given, respectively, by the following formulas:

$$\varphi(t) = \omega_a t - C_p \cdot S(t) \qquad\qquad 1.29$$

$$\omega(t) = \omega_a - C_p \frac{dS(t)}{dt} \qquad\qquad 1.30$$

In the case where $S(t)$ is cosinusoidal, the formula (1.28) becomes:

$$A(t) = A_a \lfloor \cos(\omega_a t - C_p \cdot A_m \cos(\omega_m t)) \rfloor \qquad\qquad 1.31$$

So, the instantaneous frequency is written as follows:

$$f(t) = f_a + C_p \cdot A_m \cdot f_m \sin(\omega_m t) \qquad\qquad 1.32$$

The quantity $C_p \cdot A_m \cdot f_m = \Delta f$ is called the frequency excursion (frequency deviation).

Therefore, the pulsation and phase excursion are written:

$$\varphi(t) = \omega_a t - C_p \cdot A_m \cos(\omega_m t) \Rightarrow \Delta\varphi = C_p \cdot A_m \qquad\qquad 1.33$$

$$\omega(t) = \omega_a + 2\pi C_p \cdot A_m \cdot f_m \sin(\omega_m t) \Rightarrow \Delta\omega = \omega_m \cdot C_p \cdot A_m \qquad\qquad 1.34$$

The combination of the two relationships allows us to extract the same relation obtained previously in frequency modulation:

$$\Delta\varphi = \frac{\Delta f}{f_m} \qquad\qquad 1.35$$

By analogy with frequency modulation, the phase modulation index is written:

$$\beta_p = \Delta\varphi = \frac{\Delta f}{f_m} \qquad\qquad 1.36$$

It should be noted that, contrary to what occurs for a FM signal, the PM index is independent from the modulating signal frequency.

It is then possible to rewrite the PM signal expression on the form below:

$$A(t) = A_a \lfloor \cos(\omega_a t - \beta_p \cos(\omega_m t)) \rfloor \qquad\qquad 1.37$$

The time and frequency domain of PM signal are identical to FM one.

The table below presents the main characteristics of FM and PM signals.

	modulation index	instantaneous phase	instantaneous frequency	$\Delta\varphi$	Δf
FM	$\beta_f = \dfrac{v_f A_m}{f_m}$	$\omega_a t + \beta_f \sin(\omega_m t)$	$f_a + \beta_f f_m \cos(\omega_m t)$	$\Delta\varphi = \beta_f$	$C_f A_m$
PM	$\beta_p = v_p A_m$	$\omega_a t - \beta_p \cos(\omega_m t)$	$f_a + \beta_p f_m \sin(\omega_m t)$	$\Delta\varphi = \beta_p$	$C_p A_m f_m$

Table 1.2: Comparison between FM and PM [12].

These electrical signals and others can be transformed, using a piezoelectric transducer, into ultrasonic waves. In the next chapter, we will see the propagation of these waves in elastic media and their influence on the optical characteristics of these last.

CHAPTER II

THE ULTRASOUND EFFECT ON REFRACTIVE INDEX

2-1) Introduction:

As stated in the previous chapter, some electrical signals can be transformed to ultrasonic waves using a piezoelectric transducer. In this chapter, we will study the effect of ultrasound propagation on refractive index of medium. This effect is discussed in detail; piezoelectric transducers are considered in section 2-3. The ultrasound propagation is the subject of section 2-5. This is followed by the presentation of the acousto-optic coefficients in isotropic and anisotropic media and their effect on the index ellipsoid when an ultrasonic wave is applied.

2-2) History and Definition:

Acoustics, the science of sound, started as far back as Pythagoras in the 6th century BC, who wrote on the mathematical properties of stringed instruments. Echolocation in bats was discovered by Lazzaro Spallanzaniin 1794, when he demonstrated that bats hunted and navigated by inaudible sound and not vision. Echolocation is the biological sonar used by several kinds of animals. Echolocating animals emit calls out to the environment and listen to the echoes of those calls that return from various objects near them. They use these echoes to locate and identify the objects. In 1893, Francis Galton invented the Galton whistle, an adjustable whistle is used to produce ultrasound and measure the hearing range of humans and other animals, demonstrating that many animals could hear sounds above the hearing range of humans. The first technological application of ultrasound was an attempt to detect submarines by Paul Langevin in 1917.

Ultrasound is mechanical waves, can only propagate in elastic media (gaseous, liquid or solid), with frequencies higher than the upper audible limit of human hearing. Ultrasound is no different from sound in its physical properties, except that humans cannot hear it. The upper audible limit varies from person to person and is approximately 20 KHz in healthy

adults. Children can hear some high-pitched sounds that older adults cannot hear, because in humans the upper limit pitch of hearing tends to decrease with age. The sounds have been classified compared to the reactions of the human ear. We distinguish: Infrasound, sound, ultrasound and hypersound as indicated in figure (2.1).

Infrasound	Sound	Ultrasound	Hypersound
0	20	20.10^3	10^9	$f_a\,(Hz)$
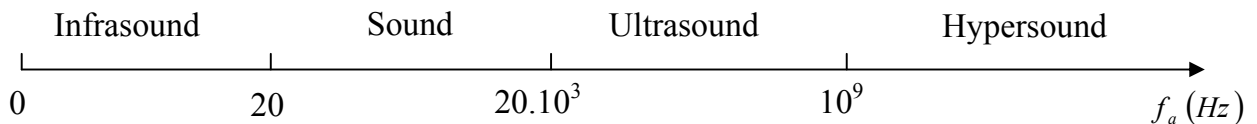
Figure 2.1: Acoustic waves spectrum

Not to be confused ultrasonic with Supersonic. At the beginning of the 20th century, the term "supersonic" was used as an adjective to describe sound whose frequency is above the range of normal human hearing. The modern term for this meaning is "ultrasonic" and the term of supersonic is limited to describe the objects speed that is between 1000-1500 km/h in dry air. Speed greater than five times the speed of sound is often referred to as hypersonic.

2-3) Transducers:

The ultrasonic wave production is done by transducers that convert mechanical, magnetic or electrical energy into ultrasonic energy [15].
Generally, the transducers are classified into three categories:
- Mechanical transducers.
- Magnetostrictive transducers.
- Piezoelectric transducers.

At first, all ultrasonic waves were produced by mechanical transducers. Afterwards, magnetostrictive transducers were used to generate them, where some materials change its size slightly when they are exposed to a magnetic field. The use of mechanical and magnetostrictive transducers remained limited due to the weak frequency and energy.

Nowadays, the term transducer typically refers to piezoelectric transducers, where the most of the commercial ultrasonic transducers are based on piezoelectric effect. These last are

23

discovered by the brothers Pierre Curie and Jacques Curie in 1880, but only in the 1950s manufacturers begun to use the piezoelectric effect in industrial sensing applications. Since then, this principle has been increasingly used, and has become technology with excellent reliability.

- The piezoelectric effect is based on the piezoelectric crystals properties, where these last change size and shape crystals when a voltage is applied. Alternating current voltage makes them oscillate at the same frequency which permits to produce ultrasonic wave [41]. This mechanism is known as inverse piezoelectric effect. Vice versa, the direct piezoelectric effect converts mechanical energy into electrical one as indicated in figure (2.2).
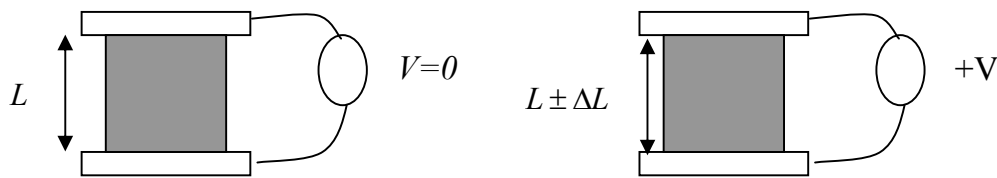
A) Inverse piezoelectric effect: an ultrasound is collected when a tension is applied.
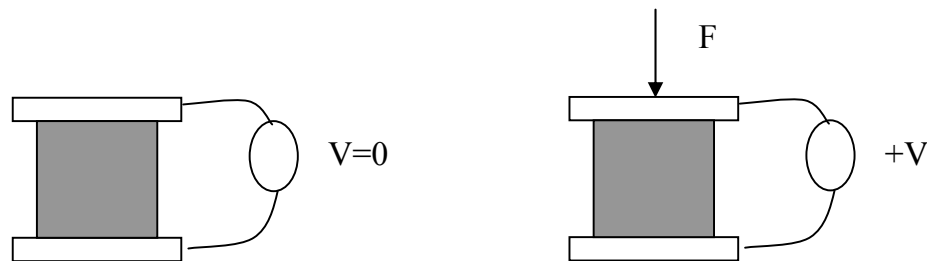
B) Direct piezoelectric effect: a tension is collected when a force is applied.

Figure 2.2: Inverse and direct effect representation [16].

Since piezoelectric materials generate a voltage when force is applied on them, they can also work as ultrasonic detectors. Thus, the piezoelectric transducers can be divided into three broad categories: transmitters, receivers and transceivers. Transmitters convert electrical signals into ultrasound, receivers convert ultrasound into electrical signals, and transceivers can both transmit and receive ultrasound.

When a piezoelectric material is placed in an electrical field of frequency f_E, its dimensions vary with the latter. This phenomenon makes it possible to generate ultrasonic waves of frequency ($f_a = f_E$) as indicated in figure (2.3).

Electrical field f_E $\longrightarrow$ | Piezoelectric material | $\longrightarrow$ Ultrasonic wave f_a
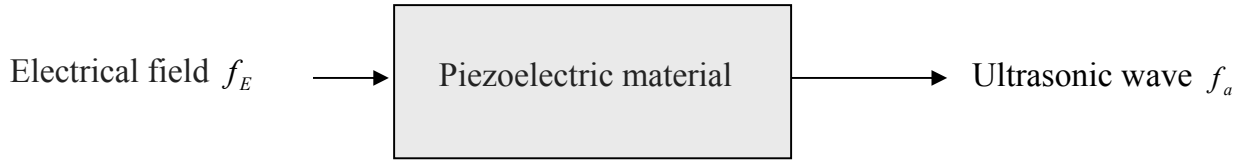
Figure 2.3: Piezoelectric transducer

In order to increase this deformation efficiency (the ultrasonic waves intensity), the excitation frequency f_E must be equal to the mechanical resonance one f_r of the piezoelectric material which is given by the following expression [18]:

$$f_r = \frac{V}{2L} \hspace{3cm} 2.1$$

Where:

   V : Ultrasonic velocity in the piezoelectric material.

   L: The piezoelectric material thickness.

The piezoelectricity phenomenon appears generally in crystals devoid of symmetry center (noncentrosymmetric). Indeed, of the 32 crystal classes (Appendix 6), 21 are noncentrosymmetric, and of these, 20 exhibit direct piezoelectricity (the 21st is the cubic class 432) [16]. This division is an elementary consideration in crystallography and this information is widely tabulated in [19]. These piezoelectric crystals lose this property when the temperature exceeds the Curie temperature T_{C_E}. In this case, we say that the crystal is found in a Para-electrical or non-polar state [16].

2-4) Ultrasounds Applications:

Ultrasound is used in many different fields:

- Industrially, ultrasound is frequently used in the nondestructive testing of products and structures. It is used also to detect invisible flaws and to measure the thickness of objects. For

example, by measuring the time between sending a signal and receiving an echo, the distance of an object can be calculated.

- Ultrasound is widely used in systems which evaluate targets by interpreting the reflected signals. For instance, a common use of ultrasound is in underwater finding; this use is also called Sonar. An ultrasonic pulse is generated in a particular direction. If there is an object in the path of this pulse, part or all of the pulse will be reflected back to the transmitter as an echo. By measuring the difference in time between the pulse being transmitted and the echo being received, it is possible to determine the distance.

- It also used in cars as parking sensors to aid the driver.

- A common ultrasound application is an automatic door opener, where an ultrasonic sensor detects a person's approach and opens the door.

- Ultrasound imaging or sonography is often used in medicine.

- Animals such as bats and porpoises use ultrasound for locating prey and obstacles (Echolocation), they can detect frequencies beyond 100 kHz, possibly up to 200 kHz.

2-5) Ultrasound propagation:

All material substances are comprised of atoms, which may be forced into vibratory motion about their equilibrium positions. When the medium particles are stressed in tension inferior its elastic limit, internal restoration forces arise that leads to the oscillatory motions of the medium particles. Ultrasound propagation is focused on particles that contain many atoms that move in unison to produce a mechanical wave which propagate in many modes [14].

2-5-1) Propagation modes:

In solids, Ultrasound waves can propagate in many modes that are based on the way the particles oscillate. Longitudinal and shear waves are the two modes of propagation most widely used in solids. The particle movement responsible for the propagation of longitudinal and shear waves is illustrated below:
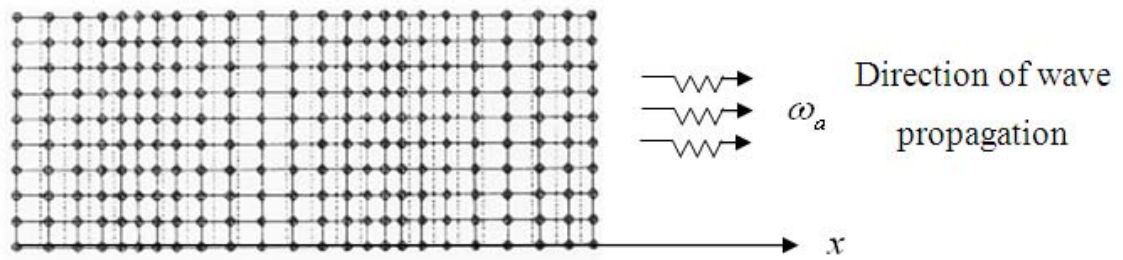
Figure 2.4: Longitudinal waves
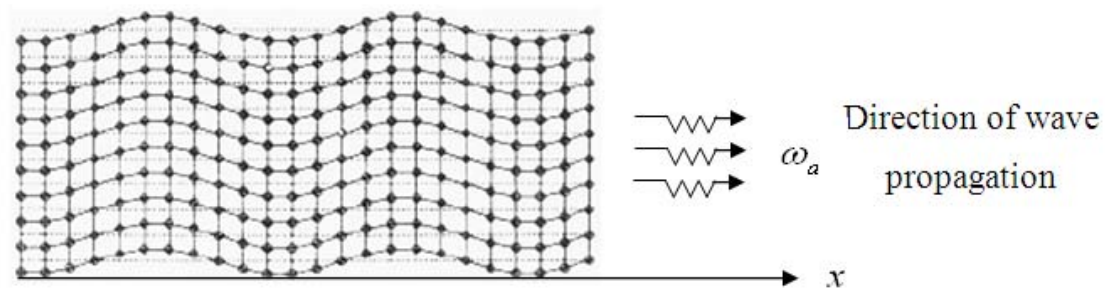
Figure 2.5: Shear waves.

In longitudinal waves, the oscillations occur in the direction of wave propagation. Since compressional and dilational forces are active in these waves, they are also called pressure or compressional waves. They are also sometimes called density waves because the particle density fluctuates as they move.

In the transverse or shear wave, the particles oscillate at a right angle or transverse to the direction of propagation. Shear waves require an acoustically solid material for effective propagation, and therefore, are not effectively propagated in materials such as liquids or gasses [14].

As mentioned previously, longitudinal and transverse waves are most often used in practical. However, at surfaces, various types of elliptical or complex vibrations of the particles make other waves possible. Some of these wave modes such as Rayleigh and Lamb waves are also useful.

The table below summarizes many, but not all, of the wave modes possible in solids.

Wave Types in Solids	Particle Vibrations
Longitudinal	Parallel to wave direction
Transverse (Shear)	Perpendicular to wave direction
Surface Wave - Rayleigh	Elliptical orbit
Plate Wave - Lamb	Complex vibration
Plate Wave - Love	Complex vibration

Table 2.1: Wave modes possible in solids [14]

Longitudinal and transverse waves were discussed on the previous page, so let's touch on surface and plate waves here.

Surface waves travel the surface of a relatively thick solid material penetrating to a depth of one wavelength. Surface waves combine both a longitudinal and transverse motion to create an elliptic orbit motion. Surface waves are generated when a longitudinal wave intersects a surface near the second critical angle and they travel at a speed close to the shear wave one (see section 2.6.3). Plate waves are similar to surface ones except they can only be generated in materials a few wavelengths thick. Lamb waves are complex vibratory ones that propagate parallel to the surface [18].

2-5-2) Position, velocity and pressure of particles in material:

In the previous section, it was pointed out that sound waves propagate due to the vibrations or oscillatory motions of particles within a material. An ultrasonic wave may be visualized as an infinite number of oscillating masses or particles connected by means of elastic springs. Each individual particle is influenced by the motion of its nearest neighbor and its restoring forces. This restoring forces is described by Hooke's Law [14].

Hooke's Law, when used along with Newton's Second Law can explain an ultrasound propagation. Newton's Second Law says that the force applied to a particle will be balanced by the particle's mass and its acceleration. Mathematically, let's consider a sinusoidal plane ultrasonic wave propagating in the direction x. The particles of the medium vibrate around an

equilibrium position with the same frequency of ultrasonic wave. The differential equation that describes this vibration is [17]:

$$\frac{\partial^2 X(x.t)}{\partial t^2} = V^2 \frac{\partial^2 X(x.t)}{\partial x^2}$$ 2.2

Where:

$X(x.t)$: Particle position of according to time and space.

x : Propagation direction of ultrasonic wave.

V : Ultrasonic wave velocity.

The solution of this differential equation is given by the following formula:

$$X(x.t) = X_0 . \sin(\omega_a t - k_a x)$$ 2.3

Where:

X_0 : The vibration amplitude.

$k_a = \dfrac{2\pi}{\lambda_a}$: Ultrasonic wave vector.

$\omega_a = 2\pi f_a$: Ultrasonic wave pulsation.

From equation (2.3), we remark that all the points situated at the same abscissa x are in the same vibratory state; they are called in phase and constitute a wave surface which is in this case plane [18].

The particle velocity is then given by:

$$X'(x,t) = \frac{dX(x,t)}{dt} = X_0 \, \omega_a \cos(\omega_a t - k_a x)$$ 2.4

The ultrasonic pressure variation in a given point is related to the particle velocity in the medium by equation [15]:

$$\Delta p(x,t) = \rho_0 \, V \, X'(x,t).$$ 2.5

The ratio of the pressure to the velocity at a given point is then equal to the product of the initial density of the medium by the wave velocity, this ratio is constant [15]:

$$\frac{\Delta p(x,t)}{X'(x,t)} = \rho_0 \, V$$ 2.6

This equation is often called the Ohm law, in acoustics, and the preceding ratio is called the acoustic impedance Z of the medium [15].

Therefore equation (2.6) becomes:

$$\Delta p(x,t) = Z\, X_0\, \omega_a \cos(\omega_a t - k_a x) \qquad\qquad 2.7$$

Acoustic impedance is important in the determination of transmission and reflection coefficients at the boundary of two materials having different acoustic impedances, as it will be indicated in section (2.6.2).

2-5-3) Ultrasound velocity:

Within a given material, ultrasound always travels at the same speed no matter how much force is applied when other variables, such as temperature, are held constant. By replacing equation (2.3) in equation (2.2), we obtain:

$$\lambda_a = \frac{V}{f_a} \qquad\qquad 2.8$$

Among the properties of ultrasonic waves are wavelength, frequency and velocity. The wavelength λ_a is directly proportional to the wave velocity and inversely proportional to the wave frequency f_a. As can be noted by previous equation, a change in frequency will result in a change in wavelength and the velocity remains constant in the same material.

Of course, in different materials, ultrasound does travel at different speeds. This is because ultrasound speed depends on the initial density ρ_0 and the elastic constants C (Appendix 4), both are different for different materials. The general relationship between the ultrasound speed, density and elastic constants is given by the following equation:

$$V = \sqrt{\frac{C}{\rho_0}} \qquad\qquad 2.9$$

This equation may take a number of different forms depending on the type of wave (longitudinal or shear). The typical elastic constants of a material include (Appendix 4):

- The Modulus of Elasticity (Young's modulus) E.

- The Modulus of rigidity (Shear modulus) G.

- The Bulk Modulus K.

- Poisson's Ratio σ.

30

- The Lamé parameters: Lamé's first parameter G_1

Lamé's second parameter $G_2 = G$

When calculating the velocity of a longitudinal wave, Young's Modulus and Poisson's Ratio are commonly used. When calculating the velocity of a shear wave, the Lamé parameters are used.

It must also be mentioned that the elastic constants C in the above equation are the same for all directions within isotropic material. However, most materials are anisotropic and the elastic constants differ with each direction [17].

2-5-4) Ultrasound propagation in gases and liquids:

Ultrasound propagates in gases and liquids in the form of longitudinal waves [15]. The differential equation which describes the particles vibration is written as follows:

$$\frac{\partial^2 X}{\partial t^2} = \frac{K}{\rho_0} \frac{\partial^2 X}{\partial x^2}$$

2.10

Where:

K : Is the Bulk Modulus.

From equations (2.2) and (2.10), we deduce that the longitudinal velocity of the ultrasonic wave is:

$$V_L = \sqrt{\frac{K}{\rho_0}}$$

2.11

The ultrasound speed within a material is a function of the material properties and is independent from the ultrasound amplitude.

❖ In the case of gases, the density varies as a function of temperature, so that:

$$\rho_T = \frac{\rho_0}{1 + \alpha T}$$

2.12

α : The coefficient of volumetric expansion

Therefore the relation (2.11) becomes:

$$V_L = \sqrt{(1 + \alpha T)\frac{K}{\rho_0}} \qquad\qquad 2.13$$

In dry air (0% humidity) the previous formula becomes as follows:

$$V_L = 331.3\sqrt{1 + \frac{T}{273.15}}$$

It can be deduced from equation (2.13) that the ultrasonic velocity in the gases varies proportionally with the square root of the temperature as indicated in table (2.2) and in figure (2.6) [22].

Temperature T (°C)	Velocity $\left(m/_s\right)$	Density $\left(kg/_{m^3}\right)$
35	351.88	1.1455
30	349.02	1.1644
25	346.13	1.1839
20	343.21	1.2041
15	340.27	1.2250
10	337.31	1.2466
5	334.32	1.2690
0	331.30	1.2922
−5	328.25	1.3163
−10	325.18	1.3413
−15	322.07	1.3673
−20	318.94	1.3943

Table 2.2: Effect of temperature on ultrasound speed in dry air
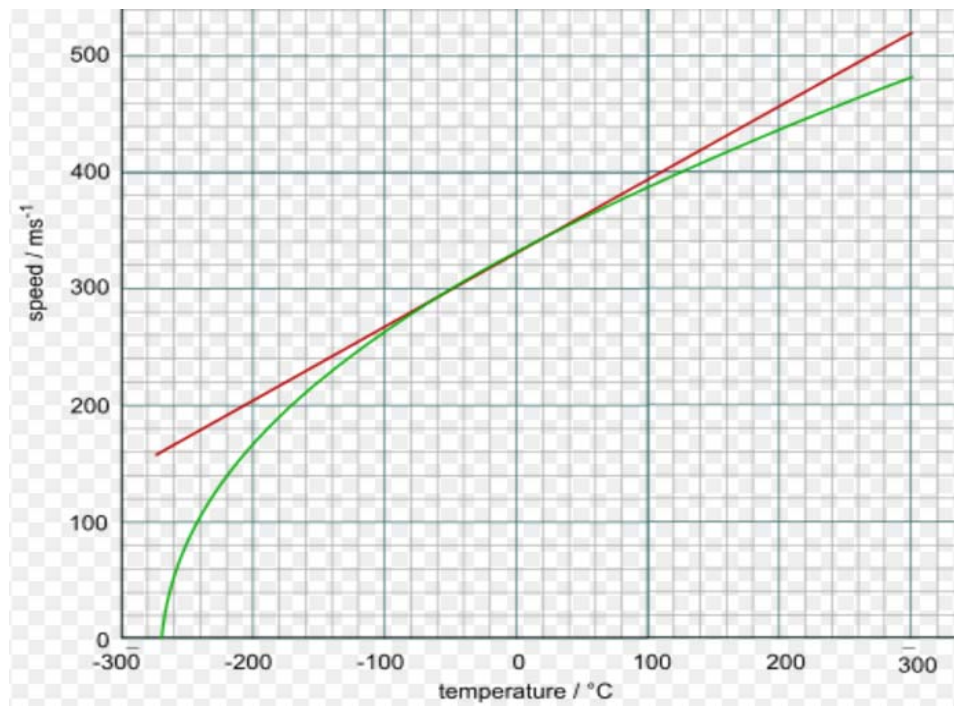
Figure 2.6: Speed of sound in dry air vs. temperature.

The table below gives the ultrasonond velocity, density, and acoustic impedance of a few gases at 0 °C [15].

Gas	Velocity $\left(m/s\right)$	Density $\left(kg/m^3\right)$	Impedance $\left(kg/m^2 s\right)$
Hydroiodic acid	157	5.7	900
Chlorine (CL_2)	206	3.2	660
Carbon dioxide (CO_2)	258	2.0	520
Hydrochloric acid (CLH)	296	1.64	485
Air	331	1.3	430
Helium	970	0.18	174
Hydrogen (H_2)	1,260	0.088	110
Argon	319	1.781	568
Nitrogen	334	1.251	418
Ethylene	317	1.26	400
Methane	430	0.717	308
Neon	435	0.9	392
Oxygen	316	1.429	452

Table 2.3: Ultrasound velocity, density and acoustic impedance of some gases

❖ In all liquids, except water, the ultrasound velocity is decreasing as a function of temperature. In water, however, the ultrasound velocity increases with temperature to reach a maximum at about 80 °C [15] as indicated in figure (2.7).
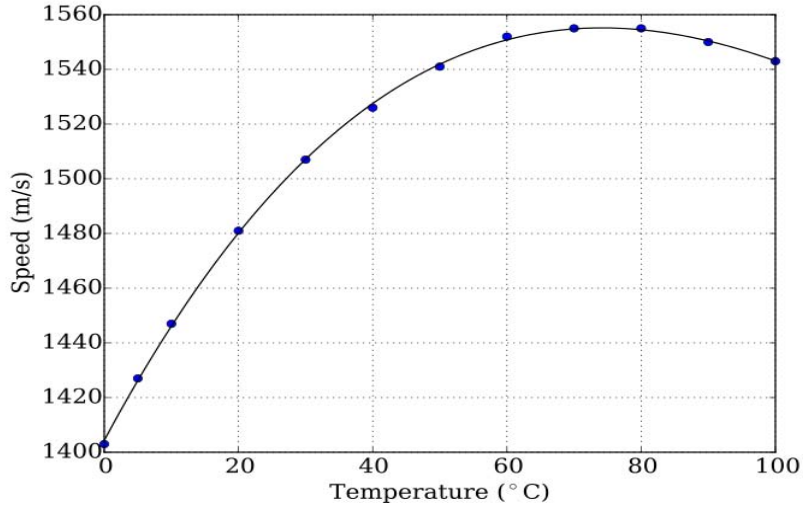
Figure 2.7: Ultrasound speed in water vs. temperature

Table (2.4) gives the ultrasonic velocity, density, and acoustic impedance of some liquids.

Liquid	Temperature °C	Velocity $\left(m/_s\right)$	Density $\left(kg/_{m^3}\right)*10^3$	Impedance $\left(kg/_{m^2 s}\right)*10^6$
Chloroform (CH$_3$ CL)	20	1,000	1.49	1.49
Metal alcohol (CH$_3$ OH)	20	1,120	0.79	0.89
Carbon sulphide (CS$_2$)	20	1,160	1.26	1.46
Ethyl alcohol (C$_2$H$_5$OH)	20	1,180	0.79	0.935
Petroleum (C$_7$H$_8$)	15	1,330	0.70	0.931
Water	17	1,430	1	1.43
Sea water	17	1,510	1.03	1.56
Mercury	20	1,450	13.6	19.7
Glycerine	20	1,920	1.26	2.42
Benzene	20	1,320	0.879	1.16
Ethanol	20	1,170	0.789	0.934

Table 2.4: Ultrasound velocity, density and acoustic impedance of some liquids [15]

2-5-5) Ultrasound propagation in solids:

The ultrasound propagation in gases and liquids is limited in longitudinal waves, since these media cannot withstand shear stresses. In solids, however not only the compressive forces but also the shear forces. This is why, alongside longitudinal waves, transverse waves can propagate.

The differential equations which describe the particles vibration in both longitudinal and transverse directions are written as follows [15, 18]:

$$\frac{\partial^2 X_1}{\partial t^2} = \frac{G_1 + 2G_2}{\rho} \frac{\partial^2 X_1}{\partial x^2} \qquad\qquad 2.14$$

$$\frac{\partial^2 X_2}{\partial t^2} = \frac{G_2}{\rho} \frac{\partial^2 X_2}{\partial x^2}. \qquad\qquad 2.15$$

Where:

X_1 et X_2: Particles motion in two directions.

G_1 et G_2: The Lamé parameters.

$$G_1 = \frac{E.\sigma}{(1+\sigma)(1-2\sigma)}$$

$$G_2 = \frac{E}{2(1+\sigma)}.$$

σ : Poisson's Ratio.

E: The Elasticity Modulus (Young's modulus).

From equations (2.2, 2.14 and 2.15), we can deduce that the longitudinal and transverse ultrasonic wave velocities are:

$$V_L = \sqrt{\frac{G_1 + 2G_2}{\rho}} = \sqrt{\frac{E.(1-\sigma)}{(1+\sigma)(1-2\sigma)\rho}} \qquad\qquad 2.16$$

$$V_T = \sqrt{\frac{G_2}{\rho}} = \sqrt{\frac{E}{2\rho(1+\sigma)}}. \qquad\qquad 2.17$$

Where:

V_L : Longitudinal velocity.

V_T : Transverse velocity.

It should be noted that the longitudinal velocity is always greater than the transverse one.

$$V_L = V_T \sqrt{\frac{2(1-\sigma)}{(1-2\sigma)}}$$

2.18

Table (2.5) gives the ultrasonic velocity, density, and acoustic impedance of some solids.

Solids	Velocity V_L $\left(\frac{m}{s}\right)$	Density $\left(\frac{kg}{m^3}\right)*10^3$	Impedance $\left(\frac{kg}{m^2 s}\right)*10^6$
Steel	5,900	7.8	46.02
Aluminum	6,260	2.7	16.90
Silver	3,600	10.5	38.00
Copper	4,700	8.9	41.80
Nickel	5,630	8.8	49.50
Cast iron	4,600	7.2	33.12
Brass	3,830	8.5	32.55
Magnesium	5,800	1.7	9.86
Gold	3,240	19.3	62.5
Bone	4,000	1.9	7.60
Lead	2,160	11.4	24.62
Quartz	5,720	2.65	14.4
Tungsten	5,460	19.1	104.2
Uranium	3,370	18.7	63.09
Glass (crown)	5,660	2.5	14.15
Zinc	4,170	7.1	29.2

Table 2.5: Ultrasonic velocity, density and acoustic impedance of some solids

From these tables, one can deduce that: the ultrasound speed varies from substance to substance. Ultrasound travels most slowly in gases, it travels faster in liquids and faster still in solids. For example, ultrasound travels at 331 m/s in air, it travels at 1,430 m/s in water (4.3 times as fast as in air) and at 5,120 m/s in iron. Exceptionally, in stiff material such as diamond, ultrasound travels at 12,000 m/s which is consider the maximum speed that ultrasound can reach it [22]. It is of interest to note that the velocity of surface waves, which are guided by the medium boundaries, is given by [15]:

$$V_s = \frac{0.87 + 1.12\sigma}{1+\sigma} \sqrt{\frac{G_2}{\rho_0}}$$

2.19

2-6) Characteristics of ultrasonic wave propagation:

When we studied the propagation of ultrasonic waves in the different elastic media, we did not take into account the attenuation phenomenon on the one hand and on the other the reflection and refraction phenomenon which appear at the boundaries of two media.

2-6-1) Ultrasonic waves attenuation:

When ultrasound travels through a liquid, its intensity diminishes with distance. In idealized materials, ultrasound amplitude remains constant. The differential equation describing the plane ultrasonic wave propagation in this medium is:

$$\frac{\partial^2 \Theta}{\partial t^2} = V^2 \frac{\partial^2 \Theta}{\partial x^2}$$
                    2.20

Where:

Θ : The potential energy of the ultrasonic wave.

Natural materials, however, all produce an effect which further weakens the ultrasound. This further weakening results from scattering and absorption. Scattering is the reflection of the ultrasound in directions other than its original propagation direction. Absorption is the conversion of the ultrasound energy to other forms of energy (heat). The combined effect of scattering and absorption is called attenuation. Ultrasonic attenuation is the decay rate of the wave as it propagates through material [22].

If we take into account the ultrasonic wave attenuation, we can then demonstrate that the preceding equation becomes:

$$\frac{\partial^2 \Theta}{\partial t^2} = V^2 \frac{\partial^2 \Theta}{\partial x^2} + \frac{3(\eta + \eta')}{4\rho} \frac{\partial^3 \Theta}{\partial x^2 \partial t}$$
                    2.21

Where:

η, η' : Kinetic and mass viscosities respectively.

The amplitude change of a decaying plane wave can be expressed as:

$$\Theta = \Theta_0 \exp\left(i \omega_a t - \alpha x\right)$$
                    2.22

In this expression Θ_0 is the unattenuated amplitude of the propagating wave at some location. The amplitude Θ is the reduced amplitude after the wave has traveled a distance x from that initial location. The quantity α is the attenuation coefficient of the wave traveling in the x-direction which is presented by the following relationship:

$$\alpha = \frac{2}{3} \frac{(\eta + \eta')\omega_a^2}{\rho V^3}$$ 2.23

Really, the absorption coefficient values α are not precise and it is Kirchhoff, who first, showed that we must take into account the energy losses due to the transmission of heat in the medium. Under these conditions, the absorption coefficient is then given by:

$$\alpha = \frac{1}{2} \frac{\omega_a^2}{\rho V^3} \left[\frac{4}{3}(\eta + \eta') + k'\frac{\gamma - 1}{C_p} \right]$$ 2.24

Or:

    k' : Heat conductivity of the medium.

    C_p : Heat at constant pressure.

Therefore, the ultrasonic intensity expression as a function of distance is given by:

$$I_a = I_{a0} \exp - 2\alpha x.$$ 2.25

- In viscous liquids, such as glycerine, absorption is mainly determined by the viscosity coefficient η, but in less viscous liquids such as benzene, the viscosity coefficient η' is the most important. In the case of water, it is necessary to take into account both η and η'.

- It is of interest to note that the attenuation is generally proportional to the square of ultrasound frequency that means acoustic losses are much higher in liquids than in solids. So, the improved efficiency can only be realized at relatively low frequencies. For water $f_a < 50\,MHz$ [33].

The table (2.6) gives the absorption coefficient values for some media.

Medium	$\alpha(dB/m)$
Steel	5-50
Aluminum	1-5
Water	1
Cast iron	20-200
Grease	100-500
Brass	50-200
Muscle	200-500
Bone	5000-20000
Skin	500-2000
Plexiglass	500

Table 2.6: Absorption coefficient for longitudinal waves $\left(f_a = 2MHz\right)$ [18]

- It should be noted that the quoted values of attenuation are often given for a single frequency, or an attenuation value averaged over many frequencies may be given. Thus, quoted values of attenuation only give a rough indication of the attenuation and should not be automatically trusted. Generally, a reliable value of attenuation can only be obtained by determining the attenuation experimentally for the particular material being used [14].

2-6-2) Reflection and transmission of ultrasonic wave:

Ultrasonic waves are reflected at boundaries where there is a difference in acoustic impedances of the materials. This difference in Z is commonly referred to as the impedance mismatch. The greater the impedance mismatch, the greater the percentage of energy that will be reflected at the interface.

Let's consider an ultrasonic wave passes through an interface between two materials at an oblique angle θ_i, as indicated in figure (2.8). These materials have different acoustic

impedances Z_1 and Z_2, so the incident ultrasonic wave is partially reflected and partially transmitted. This also occurs with light, which is why objects seen across an interface appear to be shifted relative to where they really are.

In order to determine the propagation direction of reflected and transmitted waves, it is enough to use the geometric laws similar to those of the light "Snell's law". We can demonstrate the equality between the ratio of material velocities V_1 and V_2 and the one of the sine's of incident θ_i and refracted θ_t angles. The below formula presents this equality:

$$\frac{\sin\theta_i}{\sin\theta_t} = \frac{V_1}{V_2}$$
<div align="right">2.26</div>

On the contrary, the reflected wave is propagating at the same angle as the incident one because the two waves are traveling in the same material, and hence have the same velocities.
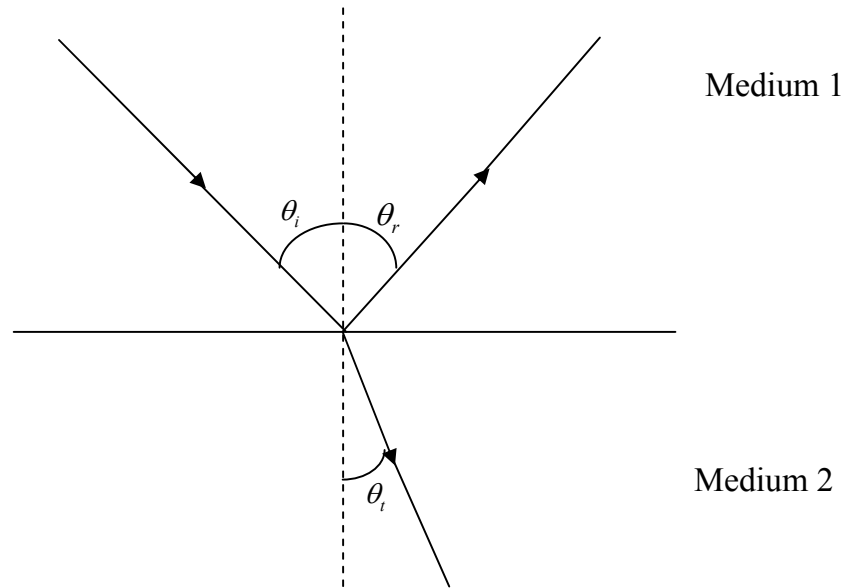
Figure 2.8: Reflection and transmission of ultrasonic wave at an interface

The amount of reflected and transmitted waves is determined using the same collusion principle of two balls which states that: the particle velocity $X'(x,t)$ and particle pressure $p(x,t)$ must be continuous across the boundary.

If the indices i, r and t refer to the incident, reflected and transmitted waves respectively, the reflection R and the transmission T coefficients are given by:

$$R = \left(\frac{Z_2 \cos \theta_1 - Z_1 \cos \theta_2}{Z_2 \cos \theta_1 + Z_1 \cos \theta_2} \right)^2 \qquad\qquad 2.27$$

$$T = \frac{4 Z_1 Z_2 \cos \theta_1}{\left(Z_2 \cos \theta_1 + Z_1 \cos \theta_2 \right)^2} \qquad\qquad 2.28$$

Where:

θ_i, θ_r and θ_t : Incident, reflected and transmitted angle respectively.

Z_1, Z_2 : Designate respectively the acoustic impedances of media 1 and 2.

In normal incidence, the previous expressions become:

$$R = \left(\frac{Z_1 - Z_2}{Z_2 + Z_1} \right)^2 \qquad\qquad 2.29$$

$$T = \frac{4 Z_1 Z_2}{\left(Z_2 + Z_1 \right)^2} \qquad\qquad 2.30$$

From these two equations, we can deduce that:

- When the acoustic impedances on both sides of the boundary are known, the fraction of the incident wave intensity that is reflected or transmitted can be calculated. Multiplying the reflection coefficient by 100 yields the amount of reflected energy as a percentage of the original energy.

- The amount of reflected energy plus the transmitted one must equal the total amount of incident energy, so the transmission coefficient can be also calculated by simply subtracting the reflection coefficient from one.

- The reflection and transmission coefficients are often expressed in decibels (dB) to allow for large changes in signal strength to be more easily compared. To convert the intensity or power of the wave to dB units, take the log of the reflection or transmission coefficient and multiply this value times 20.

- It is obvious that the reflection factor depends only on the impedance mismatch $Z_1 - Z_2$. This leads us to say that, in almost all cases of ultrasound transmission from a liquid or a solid to a gas or vice versa, produces a complete reflection due to the impedance mismatch. Conversely,

the ultrasound transmission from a solid to a liquid is more favorable since the impedance Z_1 becomes comparable to the impedance Z_2.

2-6-3) Mode conversion:

In the previous section, it was pointed out that when ultrasonic waves pass through an interface between materials having different acoustic velocities, refraction takes place at the interface. In the case when the two materials are solids, one form of wave can be transformed into another form. For example, when a longitudinal wave hits an interface at an angle θ, some of the energy can cause particle movement in the transverse direction to start a shear wave as presented in figure (2.9). Hence, mode conversion occurs when a wave encounters an interface between solids of different acoustic impedances and the incident angle is not normal to the interface.
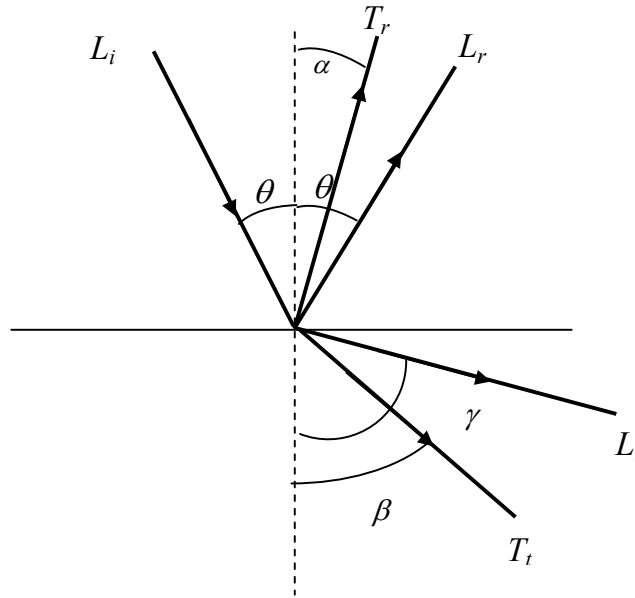
Figure 2.9: Mode conversion [15]

From this figure, one can observe that if the two media are solids, a longitudinal incident wave will be reflected and refracted at the boundary to give in each medium a longitudinal and a transverse wave.

What happens practically is that the shear wave T_t is not refracted as much as the longitudinal wave L_t. This occurs because shear waves travel slower than longitudinal ones as we have

already shown in equation (2.18). Therefore, the velocity difference between the incident longitudinal wave and the shear one is not as great as it is between the incident and refracted longitudinal waves. In reflection, we notice that the longitudinal wave L_r is reflected inside the material. The reflected shear T_r wave is reflected at a smaller angle than the reflected longitudinal wave. This is also due to the fact that the shear velocity is less than the longitudinal velocity within a given material.

Theoretically, these two cases can be explained by the equation (2.26) which remains true for shear waves as well as longitudinal ones. Hence the final formula is written as follows:

$$\frac{\sin\theta}{V_{Li}} = \frac{\sin\theta}{V_{Lr}} = \frac{\sin\alpha}{V_{Tr}} = \frac{\sin\beta}{V_{Tt}} = \frac{\sin\gamma}{V_{Lt}}$$

2.31

When a longitudinal wave moves from a slower to a faster material, there is an incident angle that makes the refraction angle, of longitudinal wave L_t, equals 90°. This is known as the first critical angle which can be found by putting $\gamma = 90^o$. So the first critical angle is equal to:

$$\sin\theta_{cL} = \frac{V_{Li}}{V_{Lt}}$$

2.32

At this angle of incidence the transverse wave T_t propagates in the second medium, conversely much of the acoustic energy presented by longitudinal wave travels along the interface and decays exponentially. This wave is sometime referred to as a creep wave and it is not very useful because it decays exponentially [14].

Beyond the first critical angle, only the shear wave propagates into the second material. For this reason, most transducers use a shear wave so that the signal is not complicated by having two waves present. In many cases, there is also an incident angle that makes the refraction angle for the shear wave equals 90°. This is known as the second critical angle which can be found by putting $\beta = 90^o$. So the second critical angle is equal to:

$$\sin\theta_{cT} = \frac{V_{Li}}{V_{Tt}}$$

2.33

Slightly beyond the second critical angle, surface waves will be generated [14].

2-7) Relationship between the ultrasound propagation and the optical characteristics of the medium:

Before developing the relationship between the ultrasonic wave propagation and the refractive index of the medium, we introduce here some notions on the permittivity and the electric displacement field.

2-7-1) The permittivity:

The permittivity, usually denoted by ε, describes the amount of charge needed to generate one unit of electric flux in a particular medium. More specifically, a charge will yield more electric flux in a medium with low permittivity than in a medium with high permittivity. Thus, permittivity is the measure of a material's ability to resist an electric field, not its ability to permit it as the name 'permittivity' might seem to suggest [35].

The permittivity study is not easy. In general, permittivity is not a constant; it can vary with the frequency of the applied field, temperature, position and other parameters. In a nonlinear medium, the permittivity can depend on the strength of the electric field. Permittivity can present by tensor or value (anisotropic or isotropic medium) as well as it can take complex or real values (Conducting or dielectric medium) [35].

The permittivity general expression is [36-38]:

$$\varepsilon = \varepsilon_0 \cdot \varepsilon_r = \varepsilon_0 \cdot (1 + \aleph) \qquad\qquad 2.34$$

Where:

ε_r : The relative permittivity tensor which represents the dimensionless quantity.

$\aleph$: The electric susceptibility tensor.

ε_0 : The vacuum permittivity equals $\dfrac{10^{-9}}{36\pi} \dfrac{F}{m}$ or $\dfrac{C^2}{N\,m^2}$ which represents the lowest possible permittivity $\aleph = 0$.

The relative permittivity of linear, homogeneous and anisotropic medium is represented by a second rank tensor. However, it is of interest to note that, due to the tensor theory complexity such as the high number of terms of some tensor, the Einstein summation convention and other, we prefer to use the matrix form which is more practical and more simple. The permittivity matrix is given as follows [30]:

$$\begin{pmatrix} \varepsilon_{11} & \varepsilon_{12} & \varepsilon_{13} \\ \varepsilon_{21} & \varepsilon_{22} & \varepsilon_{23} \\ \varepsilon_{31} & \varepsilon_{32} & \varepsilon_{33} \end{pmatrix} \qquad\qquad 2.35$$

In general case, permittivity has 9 independent elements ε_{ij}. However, we can choose a new set of axes when the matrix can be always diagonal. Accordingly, the preceding matrix simplifies to [31]:

$$\begin{pmatrix} \varepsilon_{11} & 0 & 0 \\ 0 & \varepsilon_{22} & 0 \\ 0 & 0 & \varepsilon_{33} \end{pmatrix} \qquad\qquad 2.36$$

The new coordinate axes are called the principal ones. Since, all of our analysis will be carried out in this system and the original coordinates cannot take place here. Accordingly, the anisotropic media can be classified as follows [30]:

Media	Permittivity	refractive Indices
Isotropic media $\varepsilon_{11} = \varepsilon_{22} = \varepsilon_{33} = n^2$	$\begin{pmatrix} \varepsilon_{11} & 0 & 0 \\ 0 & \varepsilon_{11} & 0 \\ 0 & 0 & \varepsilon_{11} \end{pmatrix}$	$n^2 \begin{pmatrix} 1 & 0 & 0 \\ 0 & 1 & 0 \\ 0 & 0 & 1 \end{pmatrix}$
Uniaxial media $\varepsilon_{11} = \varepsilon_{22} = n_0^2 \neq \varepsilon_{33} = n_e^2$ n_0 : Ordinary refractive index n_e : Extraordinary refractive index.	$\begin{pmatrix} \varepsilon_{11} & 0 & 0 \\ 0 & \varepsilon_{11} & 0 \\ 0 & 0 & \varepsilon_{33} \end{pmatrix}$	$\begin{pmatrix} n_0^2 & 0 & 0 \\ 0 & n_0^2 & 0 \\ 0 & 0 & n_e^2 \end{pmatrix}$

Biaxial media $\varepsilon_{11} \neq \varepsilon_{22} \neq \varepsilon_{33}$	$\begin{pmatrix} \varepsilon_{11} & 0 & 0 \\ 0 & \varepsilon_{22} & 0 \\ 0 & 0 & \varepsilon_{33} \end{pmatrix}$	$\begin{pmatrix} n_{11}^2 & 0 & 0 \\ 0 & n_{22}^2 & 0 \\ 0 & 0 & n_{33}^2 \end{pmatrix}$

Table 2.7: Anisotropic media classification

2-7-2) The relationship between the electric displacement vector and electric field vector:

In 1865, Maxwell unified and expanded the laws of Faraday, Ampere, Gauss and Poisson into a set of equations now known as Maxwell's equations. They express the relations between temporal and spatial variations of electric and magnetic fields. These equations are written as follows:

$$\overrightarrow{rot} \, \vec{E} = -\frac{\partial \vec{B}}{\partial t} \qquad\qquad 2.37$$

$$\overrightarrow{rot} \, \vec{H} = \vec{J} + \frac{\partial \vec{D}}{\partial t} \qquad\qquad 2.38$$

$$div\vec{D} = \rho \qquad\qquad 2.39$$

$$div\vec{B} = 0 \qquad\qquad 2.40$$

Where:

$\vec{B}$: Magnetic induction (displacement) vector $V.s/m^2$.

$\vec{H}$: Magnetic field vector A/m.

$\vec{D}$: Electric induction (displacement) vector $A.s/m^2$.

$\vec{E}$: Electric field vector V/m.

ρ : Free charge density C/m^3.

$\vec{J} = \sigma \vec{E}$: Vector of current density A/m^2.

The first equation is generally known as Faraday's Law. The second one, excluding the term $(\partial \vec{D}/\partial t)$, is known as Ampere's law. The two last equations are known as Gauss's law and

46

Poisson's equation, respectively. Maxwell modified Ampere's law by including the displacement term and showed that electric and magnetic fields are intimately connected and inseparable, thus the study beginning of electromagnetic waves.

In conjunction with the above four equations, we need the so-called constitutive equations which written in the case when the medium is linear and homogeneous as follows [31]:

$$\vec{D} = \varepsilon \vec{E} = \varepsilon_0 \varepsilon_r \vec{E} \qquad\qquad 2.41$$

$$\vec{B} = \mu \vec{H} = \mu_0 \mu_r \vec{H} \qquad\qquad 2.42$$

$$\vec{J} = \sigma \vec{E} \qquad\qquad 2.43$$

Where:

μ_r : Is the relative permeability tensor which represents the dimensionless quantity.

σ : Is the conductivity tensor $A/(V.m)$

μ_0 : Is the vacuum permeability equals $4.\pi.10^{-7} \dfrac{V\,s}{A\,m}$ or $\dfrac{wb}{A\,m}$

In order to determine the relation between $\vec{D}$ and $\vec{E}$ in non-magnetic and anisotropic medium, we consider a plane monochromatic wave of frequency ω and wave vector $\vec{k}$ propagates in an anisotropic medium characterized by a tensor ε. The electric field vector associated with this wave is then expressed, using the complex notation, by:

$$\vec{E} = \vec{E}_0 \cdot \exp i\left(-\omega\, t + \vec{k}\, \vec{r} \right)$$

The other components of the electromagnetic vectors $\vec{D}$, $\vec{B}$ and $\vec{H}$ naturally present the same spatio-temporal dependence. In this medium, where the magnetic induction vector and the magnetic field one are collinear, Maxwell's equations become:

$$\vec{rot}\, \vec{E} = -\mu \frac{\partial \vec{H}}{\partial t} \qquad\qquad 2.44$$

$$\vec{rot}\, \vec{H} = \frac{\partial \vec{D}}{\partial t} \qquad\qquad 2.45$$

$$div\,\vec{D} = 0 \qquad\qquad 2.46$$

$$div\,\vec{H} = 0 \qquad\qquad 2.47$$

Using the differential operator (Appendix 5), we can rewrite the previous equation as follows:

$$\vec{k} \wedge \vec{E} = \mu\omega\vec{H} \qquad\qquad 2.48$$

$$\vec{k} \wedge \vec{H} = -\omega\vec{D} \qquad\qquad 2.49$$

$$\vec{k} \cdot \vec{D} = 0 \qquad\qquad 2.50$$

$$\vec{k} \cdot \vec{H} = 0 \qquad\qquad 2.51$$

From equations (2.48 and 2.49), we can observe that: $\vec{E} \perp \vec{H}$ and $\vec{k} \perp \vec{H} \perp \vec{D}$.

This last perpendicular can be confirmed using the two equations (2.50 and 2.51). In addition, we remark that the vectors $\vec{k}$, $\vec{D}$ and $\vec{E}$ are coplanar, they all lie the same plane as presented in figure (2.10) [31]:
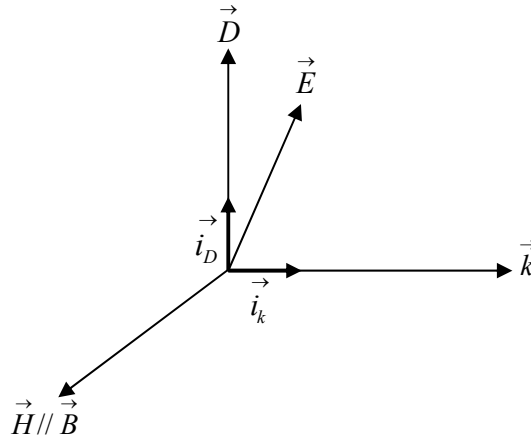
Figure 2.10: Vectorial representation of different components in anisotropic medium

To determine the relation between $\vec{D}$ and $\vec{E}$, it is necessary and sufficient to combine the two formulas (2.48 and 2.49), we find finally:

$$\begin{cases} \dfrac{n}{C}\left(\vec{i_k} \wedge \vec{H}\right) = -\vec{D} \\[2mm] \dfrac{n}{C}\left(\vec{i_k} \wedge \vec{E}\right) = \mu\vec{H} \end{cases} \Rightarrow \vec{D} = -\frac{n^2}{C^2\mu}\left(\vec{i_k} \wedge \left(\vec{i_k} \wedge \vec{E}\right)\right)$$

Using the vector identity $\vec{A} \wedge \left(\vec{B} \wedge \vec{C} \right) = \vec{B} \left(\vec{A} \cdot \vec{C} \right) - \vec{C} \left(\vec{A} \cdot \vec{B} \right)$, we get:

$$\vec{D} = \frac{n^2}{C^2 \mu} \left[\vec{E} - \vec{i_k} \left(\vec{i_k} \cdot \vec{E} \right) \right] = \frac{n^2}{C^2 \mu} \vec{E_D}$$

2.52

Where $\vec{E_D}$ is the component of the electric field parallel to $\vec{i_D}$.

By replacing the equation (2.52) in (2.41), we can find after a long development an equation which is called Fresnel's equation. This latter enables us to determine the various possible refractive indices using the index ellipsoid.

2.8) The electro-optic and the acousto-optic effect on the index ellipsoid:

In this section, we discuss the effect of the applied electric field on the index ellipsoid in crystal. This is followed by the effect of ultrasound propagation.

2.8.1) The electro-optic effect:

The application of an electric field changes the dielectric tensor of a material, however small. The electro-optic effect is in general defined by the change in the refractive index rather than the change in the dielectric constant because of the usefulness of the index ellipsoid method in solving problems. Thus the change in the index ellipsoid, due to an applied electric field, is written as follows [31]:

$$\Delta \left[\frac{1}{n_i^2} \right] = r_{ij} \cdot E_j + R_{ik} \cdot E_k^{(2)}$$

2.53

Where:

r_{ij} : The Pockels electro-optic coefficients of rectangular matrix (6,3).

R_{ik} : The Kerr electro-optic coefficients of square matrix (6,6).

i and k : Indices vary from 1 to 6.

j : Index varies from 1 to 3.

E_j : The electric field components.

49

$E_k^{(2)}$: The two components product of the electric field. $E_1^{(2)} = E_x \cdot E_x$, $E_4^{(2)} = E_x \cdot E_y$ ….

This matrix formula can develop to the following form:

$$
\begin{pmatrix} \Delta(1/n_1^2) \\ \Delta(1/n_2^2) \\ \Delta(1/n_3^2) \\ \Delta(1/n_4^2) \\ \Delta(1/n_5^2) \\ \Delta(1/n_6^2) \end{pmatrix} = \begin{pmatrix} r_{11} & r_{12} & r_{13} \\ r_{21} & r_{22} & r_{23} \\ r_{31} & r_{32} & r_{33} \\ r_{41} & r_{42} & r_{43} \\ r_{51} & r_{52} & r_{53} \\ r_{61} & r_{62} & r_{63} \end{pmatrix} \begin{pmatrix} E_1 \\ E_2 \\ E_3 \end{pmatrix} + \begin{pmatrix} R_{11} & R_{12} & R_{13} & R_{14} & R_{15} & R_{16} \\ R_{21} & R_{22} & R_{23} & R_{24} & R_{25} & R_{26} \\ R_{31} & R_{32} & R_{33} & R_{34} & R_{35} & R_{36} \\ R_{41} & R_{42} & R_{43} & R_{44} & R_{45} & R_{46} \\ R_{51} & R_{52} & R_{53} & R_{54} & R_{55} & R_{56} \\ R_{61} & R_{62} & R_{63} & R_{64} & R_{65} & R_{66} \end{pmatrix} \begin{pmatrix} E_1^{(2)} \\ E_2^{(2)} \\ E_3^{(2)} \\ E_4^{(2)} \\ E_5^{(2)} \\ E_6^{(2)} \end{pmatrix} \qquad 2.54
$$

- The terms r_{ij} and R_{ik} are called respectively the linear electro-optic matrix coefficients characterizing the Pockels effect and the quadratic electro-optic matrix coefficients characterizing the Kerr effect.

- The Pockels effect doesn't exist in centrosymmetric media, which possess a symmetry center, because the Pockels coefficients go to zero $(r_{ij} = 0)$ such as glasses, liquids and in general isotropic media. Conversely, all piezoelectric materials lack symmetry center and in this case the Pockels effect takes place. Concerning the Kerr effect, all materials are endowed with it. The explicit form of the linear and the quadratic electro-optic matrices are given in (Appendix 6) for the seven crystal systems [30].

- The magnitude order of the linear electro-optic matrix coefficients r_{ij} is $(10^{-10} \ to \ 10^{-12} \ m.V^{-1})$, they can be positive or negative and they vary according to the wavelength of light. As regards the magnitude order of the quadratic electro-optic matrix coefficients R_{ik} ranging from (10^{-15}) to $(10^{-20} \ m^2.V^{-2})$ [30].

- In the Kerr cell, we can use as a medium; lithium niobate ($LiNbO_3$), ammonium dihydrogen phosphate (ADP) and so on which are uniaxial media. In addition, liquids which are initially isotropic can become uniaxial anisotropic by using this cell.

2.8.2) The acousto-optic or elasto-optic Effect:

A material deforms if subjected to an elastic stress field. The local density of the latter is modified and consequently its optical properties are also modified. The acousto-optic effect involves the first order changes in the optical properties of medium due to elastic strain [32]. In a manner analogous to that introduced in the case of electro-optic effect, the different variations of the index ellipsoid coefficients are given by six-component column vector (6,1). The latter is expressed as a function of the square photo-elastic matrix and the column vector of strain as indicated below [30]:

$$\Delta\left[\frac{1}{n_i^2}\right] = p_{ij} \cdot S_j \qquad\qquad 2.55$$

Where:

p_{ij} : The photo-elastic coefficients of square matrix (6,6).

i and j : Indices vary from 1 to 6.

S_j : The strain components.

This matrix formula can develop to the following form:

$$\begin{pmatrix} \Delta(1/n_1^2) \\ \Delta(1/n_2^2) \\ \Delta(1/n_3^2) \\ \Delta(1/n_4^2) \\ \Delta(1/n_5^2) \\ \Delta(1/n_6^2) \end{pmatrix} = \begin{pmatrix} p_{11} & p_{12} & p_{13} & p_{14} & p_{15} & p_{16} \\ p_{21} & p_{22} & p_{23} & p_{24} & p_{25} & p_{26} \\ p_{31} & p_{32} & p_{33} & p_{34} & p_{35} & p_{36} \\ p_{41} & p_{42} & p_{43} & p_{44} & p_{45} & p_{46} \\ p_{51} & p_{52} & p_{53} & p_{54} & p_{55} & p_{56} \\ p_{61} & p_{62} & p_{63} & p_{64} & p_{65} & p_{66} \end{pmatrix} \begin{pmatrix} S_1 \\ S_2 \\ S_3 \\ S_4 \\ S_5 \\ S_6 \end{pmatrix} \qquad 2.56$$

- It should be noted that the matrix p is depended on a fourth rank piezoelectric tensor and an elastic tensor by the Hooke law, of course, if we remain in the elastic domain.

- The terms of the matrix p are dimensionless quantity and their magnitude order is typically 10^{-1}, we say often that the deformation of the index ellipsoid $\Delta(1/n_1^2)$ is equal to one tenth of the material strain. The magnitude order of the piezoelectric tensor terms is $10^{-12} m^2.N^{-1}$. The

explicit form of the photo-elastic coefficients is given in (Appendix 7) for the seven crystal systems as well as the isotropic media.

- If we assume that the stress is applied only in one direction x, the first component variation of the refractive index, which is in the same direction, is given by the following formula:

$$\Delta\left(\frac{1}{n_1^2}\right) = p_{11}\, S_1$$

$$\Rightarrow \frac{1}{n_1^2} - \frac{1}{n_0^2} = p_{11}\, S_1$$

And as the amplitude of S_1 is very small, we can write then:

$$\Rightarrow \frac{(n_1 - n_0)(n_1 + n_0)}{n_1^2\, n_0^2} = p_{11}\, S_1$$

$$\Rightarrow n_1 = n_0 + \frac{n_0^3}{2}\, p_{11}\, S_1 \qquad\qquad 2.57$$

2.8.3) Some applications of acousto-optic effect:

Among the most significant effects involving the photo-elasticity of materials, we cite: the strain measurement inside a material by calculating the induced birefringence. The creation of dynamic phase grating using acoustic waves which allows modifying the amplitude, frequency and propagation direction of an incident wave. The latter is the subject of our thesis. Other applications use this active phase grating as; Correlators, Spectrum analyzers and heterodyne interferometers that go far beyond the thesis scope and the reader should consult other references.

a) The strain measurement inside a material by calculating the induced birefringence:

Let us consider an isotropic silica block placed under uniform stress in the direction Ox. The medium undergoes only one strain S_1. The index variation, considering the silica photo-elastic matrix mentioned in (Appendix 7), is given as follows.

$$
\begin{pmatrix}
\Delta(1/n_1^2) \\
\Delta(1/n_2^2) \\
\Delta(1/n_3^2) \\
\Delta(1/n_4^2) \\
\Delta(1/n_5^2) \\
\Delta(1/n_6^2)
\end{pmatrix}
=
\begin{pmatrix}
p_{11} & p_{12} & p_{12} & 0 & 0 & 0 \\
p_{12} & p_{11} & p_{12} & 0 & 0 & 0 \\
p_{12} & p_{12} & p_{11} & 0 & 0 & 0 \\
0 & 0 & 0 & p_{44} & 0 & 0 \\
0 & 0 & 0 & 0 & p_{44} & 0 \\
0 & 0 & 0 & 0 & 0 & p_{44}
\end{pmatrix}
\begin{pmatrix}
S_1 \\
0 \\
0 \\
0 \\
0 \\
0
\end{pmatrix}
\qquad 2.58
$$

Thus, the index variations are written:

$$
\Rightarrow
\begin{cases}
n_1 = n_0 + \dfrac{n_0^3}{2} p_{11}\, S_1 \\[2mm]
n_2 = n_3 = n_0 + \dfrac{n_0^3}{2} p_{12}\, S_1
\end{cases}
$$

Therefore, the medium becomes uniaxial anisotropic and the birefringence is proportional to the strain, which enables us to measure the stress inside the materials.

b) The creation of dynamic phase grating:

Another domain of application, which is the subject of our thesis, is the use of this photo-elasticity to diffract light. Indeed, the ultrasonic sinusoidal wave propagation in the x direction, in water, causes a spatio-temporal variation of its refractive index with the same rhythm of the ultrasonic wave describing by equation (2.59). This variation gives rise to a dynamic phase grating of pitch equal to the acoustic wavelength λ_a.

Considering the photo-elastic matrix of water mentioned in (Appendix 7) and using the same previous analysis, we demonstrate that the refractive index is no longer constant but it varies sinusoidally as a function of time and space as indicated by the following formula:

$$
n(x,\, t) = n_0 + \frac{n_0^3}{2} p_{11}\, S_1 \sin(\omega_a t - k_a x)
$$

$$
\Rightarrow \Delta n(x,\, t) = n(x,\, t) - n_0 = \frac{n_0^3}{2} p_{11}\, S_1 \sin(\omega_a t - k_a x) \qquad 2.59
$$

Where:

$\quad n_0$: Average index of medium.

$\quad x$: Propagation direction of ultrasonic wave.

k_a : Ultrasonic wave vector.

ω_a : Ultrasonic wave pulsation.

$P_{11} = 0.31$: The photo-elastic coefficient.

The variation amplitude of index is generally too weak 10^{-5} and it is written as follows:

$$\Delta n_0 = \frac{n_0^3}{2} p_{11} S_1 \qquad\qquad 2.60$$

The conservation principle of kinetic energy of the ultrasonic wave permits to write [15 p: 3]:

$$I_a = \frac{1}{2} \rho_0 V^3 S_1^2. \qquad\qquad 2.61$$

Where:

I_a : Ultrasonic wave intensity.

By combining the two equations (2.60-2.61), we obtain:

$$\Delta n_0 = \frac{n_0^3}{2} p_e \sqrt{\frac{2 I_a}{\rho_0 V^3}}$$

$$\Rightarrow \Delta n_0 = \frac{n_0^3 p_e}{\sqrt{\rho_0 V^3}} \sqrt{\frac{I_a}{2}}$$

Putting:

$$M_2 = \frac{n_0^6 p_e^2}{\rho_0 V^3} \qquad\qquad 2.62$$

$$\Rightarrow \Delta n_0 = \sqrt{M_2 \frac{I_a}{2}} \qquad\qquad 2.63$$

M_2 : Is called the figure of merit. It determines the inherent efficiency of material regardless of the interaction geometry. As equation (2.62) shows, high efficiency materials must have high merit coefficient, precisely a high refractive index and a low acoustic velocity [29].

We replace the previous equation in equation (2.59), we get:

$$n(t,x) = n_0 + \sqrt{M_2 \frac{I_a}{2}} \ \sin(\omega_a t - k_a x) \qquad\qquad 2.64$$

In the same manner, we can demonstrate that the refractive index variations in a medium perturbed by an AM and FM signal are:

AM signal [6]: $n(x,t) = n_0 + \Delta n_0 \left[\left[1 + \beta_a \cos(\omega_m t - k_m x) \right] \sin \left(\omega_a t - k_a x \right) \right]$ 2.65

FM signal: $n(x,t) = n_0 + \Delta n_0 \left[\sin \left(\omega_a t - k_a x + \beta_f \sin \left(\omega_m t - k_m x \right) \right) \right]$ 2.66

According to these relationships, we conclude that the ultrasonic wave propagation of intensity I_a in the elastic medium causes a spatio-temporal variation of its refractive index. This variation amplitude is proportional to the square root of the ultrasonic wave intensity.

In the next chapter, we will study the diffraction phenomenon which results from the interaction of light with these elastic media.

CHAPTER III

THEORETICAL STUDY OF ACOUSTO-OPTIC

INTERACTION

3-1) Introduction:

In the previous chapter, we have seen that the piezoelectric transducers were used to generate ultrasound which has the same frequency of electrical signal supply, also the ultrasonic wave propagation in elastic medium causes a spatiotemporal variation of its refractive index.

The interaction of this ultrasonic wave with electromagnetic one in this medium provokes the diffraction phenomenon. The latter depends on the ultrasonic wave shape. In this chapter, we will treat theoretically this diffraction phenomenon for three types of ultrasonic waves (sinusoidal, amplitude modulated and frequency modulated). The first diffraction has been explained by Raman and Nath whereas the second one was performed by Pancholy and Parthasarathy and explained mathematically by Mertens and Hereman. In the last diffraction, which presents our study, we will start from the diffraction relation to finally reach a very important relationship between the diffraction orders positions and the modulating signal.

3-2) Principle of acousto-optic interaction:

An electrical signal $A(t)$ emitted by a high frequency generator feeds a piezoelectric transducer, which is immersed in liquid medium. The transducer converts the electrical signal to an ultrasonic wave via piezoelectric effect. The output acoustic power delivered by the transducer depends on the mismatch between the acoustic impedance of the transducer and the liquid acoustic impedance as presented by the formula (2.29). The propagation of this ultrasonic wave in the medium creates dilation and compression regions according to the rhythm of the electrical signal. A compression causes an increase in the density of the medium [40], and therefore of its refractive index. This variation in the index transforms the medium which is initially homogeneous into an inhomogeneous medium.

In the case where the ultrasonic wave is periodic, the medium may be considered as a moving phase grating figure (3.1).
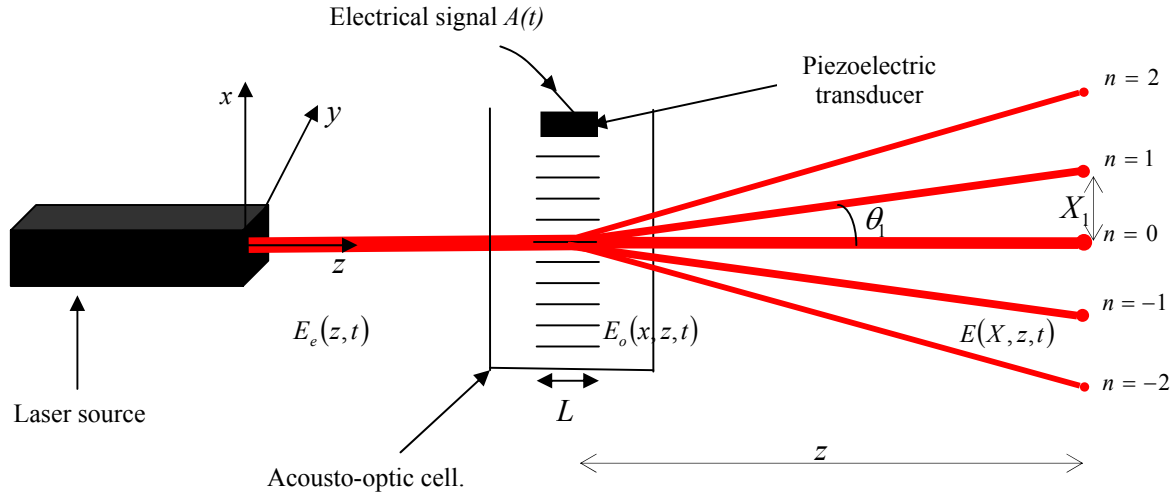
Figure 3.1: Acousto-optic interaction.

The interaction of a laser with this phase grating leads to the diffraction phenomenon. The diffraction spectrum is observed at a distance "z" from the AO cell.

3-3) Theoretical study of the acousto-optic interaction:

In order to explain this diffraction phenomenon we can follow two methods. The first one is based on the calculation of the spatial Fourier transform (FT) of the outgoing field $E_o(x,z,t)$ from the AO cell. This FT is written, in the case of the one-dimensional diffraction, as follows [23]:

$$E(X,z,t) = \int_{-\infty}^{\infty} E_o(x,z,t)\exp[-i\,2\pi\nu_x\,x]dx \qquad 3.1$$

Where $\nu_x = \dfrac{X}{\lambda_0 \cdot z}$ represents the spatial frequency in direction x

In the second method, we calculate the phase derivative of vibratory term of the output field $E_o(x,z,t)$ in relation to spatial coordinates in order to find the wave vectors, in the two directions, and in relation to time to find the luminous frequency.

57

Let's assume a plane monochromatic light wave of amplitude E_i hits perpendicularly the interaction medium. The complex light field immediately behind the AO cell is written [23-24]:

$$E_o(x,z,t) = T(x,t)\, E_e(z,t).$$
$$= T(x,t)\, E_i \exp i(\omega\, t + k_0\, z) \qquad 3.2$$

Where:

$T(x,t)$: The phase transformation.

ω : Luminous pulsation.

$k_0 = \dfrac{2\pi}{\lambda_0}$: Wave vector in vacuum.

λ_0 : Wave length in vacuum.

z : Propagation direction of luminous wave.

The phase transformation of a medium perturbed by an ultrasonic wave is given by the following formula:

$$T(x,t) = \exp - i\varphi(x,t)$$
$$T(x,t) = \exp - i \frac{2\pi}{\lambda_0}\, n(x,t)\, L \qquad 3.3$$

Where:

$n(t,x)$: The refractive index of the medium depends on time and space.

L: Interaction width.

By replacing equation (3.3) in equation (3.2), we obtain:

$$E_o(x,z,t) = E_i \exp - i\left(\frac{2\pi}{\lambda_0}\, n(x,t)\, L \right) \cdot \exp i(\omega\, t + k_0\, z) \qquad 3.4$$

This expression represents the distribution of the complex field immediately after the interaction medium. It is directly linked by the ultrasonic wave $n(x,t)$ which is proportional to the electrical signal $A(t)$.

3-3-1) Theoretical study of the acousto-optic interaction in a medium perturbed by a sinusoidal signal:

We have seen in chapter II, that the propagation of a sinusoidal ultrasonic wave in an elastic medium causes a spatiotemporal variation of its refractive index. This variation is given by equation (2.64):

$$n(x,t) = n_0 + \Delta n_0 \sin(\omega_a t - k_a x)$$

Where:

n_0 : Average index of medium.

Δn_0 : Variation amplitude of refractive index.

x : Propagation direction of ultrasonic wave.

k_a : Ultrasonic wave vector.

ω_a : Ultrasonic wave pulsation.

Therefore the field at the medium output, using the relation (3.4), is written [21, 29]:

$$E_o(x,z,t) = E_i \exp i(\omega t + k_0\, z) \exp i\left(-\frac{2\pi\, n_0 L}{\lambda_0}\right) \exp i\left(-\frac{2\pi\, \Delta n_0 L}{\lambda_0}\,\sin\left(\omega_a\, t - \frac{2\pi}{\lambda_a}x\right)\right) \qquad 3.5$$

A term of the form $\exp i\varepsilon \sin \xi$ can be developed in a series of the Bessel function of the first kind (Appendix 3) using the Jacobi relation (Appendix 2):

$$\exp -i(\varepsilon \sin \xi) = \sum_{n=-\infty}^{+\infty} J_n(\varepsilon)\exp -i(n\xi) \qquad 3.6$$

Where:

$$\varepsilon = \frac{2\pi\, \Delta n_0 L}{\lambda_0} \qquad and \qquad \xi = \left(\omega_a\, t - \frac{2\pi}{\lambda_a}x\right)$$

So the field at the medium output will be given by:

$$E_o(x,z,t) = E_i \exp i(\omega t + k_0 z)\exp i\left(-\frac{2\pi n_0 L}{\lambda_0}\right)\sum_{n=-\infty}^{+\infty}\exp i\, n\left(-\left(\omega_a t - \frac{2\pi}{\lambda_a}x\right)\right)J_n\left(\frac{2\pi\, L\, \Delta n_0}{\lambda_0}\right) \qquad 3.7$$

❖ The calculation of diffracted order angle using FT:

By replacing the equation (3.7) in equation (3.1), we obtain:

$$E(X,z,t)=E_i \cdot \exp i\left(-\frac{2\pi n_0 L}{\lambda_0}\right)\cdot \exp i(k_0 z)\sum_{n=-\infty}^{+\infty}\exp i(\omega t-n\omega_a t)J_n\left(\frac{2\pi L \Delta n_0}{\lambda_0}\right)$$

$$\int_{-\infty}^{+\infty}\exp\left[in\frac{2\pi}{\lambda_a}x\right]*\exp\left[-ik_0\left(\frac{X\cdot x}{z}\right)\right]dx$$

$$\Rightarrow E(X,z,t)=E_i \cdot \exp i\left(-\frac{2\pi n_0 L}{\lambda_0}\right)\cdot \exp i(k_0 z)\sum_{n=-\infty}^{+\infty}\exp i(\omega t-n\omega_a t)J_n\left(\frac{2\pi L \Delta n_0}{\lambda_0}\right)$$

$$\int_{-\infty}^{+\infty}\exp-i2\pi\left[\frac{X}{z\lambda_0}-\frac{n}{\lambda_a}\right]x \; dx$$

$$\Rightarrow E(X,z,t)=E_i \cdot \exp i\left(-\frac{2\pi n_0 L}{\lambda_0}\right)\cdot \exp i(k_0 z)\sum_{n=-\infty}^{+\infty}\exp i(\omega t-n\omega_a t)J_n\left(\frac{2\pi L \Delta n_0}{\lambda_0}\right)\delta\left(\frac{X}{\lambda_0 z}-\frac{n}{\lambda_a}\right) \qquad 3.8$$

Where $\delta(\Psi)$ is the Dirac function (Appendix 1).

So each diffracted order angle is written as follows:

$$\tan\theta_n=\frac{X}{z}=\frac{n\,\lambda_0}{\lambda_a} \qquad\qquad 3.9$$

❖ The calculation of diffracted order angle using the wave vector definition:

From the equation (3.7), we can deduce that the diffracted order field is given by the following equation:

$$E_n(x,z,t)=E_i\exp i(\omega t+k_0 z)\exp i\left(-\frac{2\pi n_0 L}{\lambda_0}\right)\cdot \exp in\left(-\left(\omega_a t-\frac{2\pi}{\lambda_a}x\right)\right)\cdot J_n\left(\frac{2\pi L \Delta n_0}{\lambda_0}\right) \qquad 3.10$$

The resultant wave vector $\vec{k_n}$, represented in figure (3.2), is obtained by deriving the vibratory term with respect to spatial coordinates:

$$k_x=\frac{\partial\varphi(x,z,t)}{\partial x}=\frac{\partial((\omega-n\omega_a)t+n\,k_a\,x+k_0 z)}{\partial x}=n\,k_a \qquad 3.11$$

$$k_z=\frac{\partial\varphi(x,z,t)}{\partial z}=\frac{\partial((\omega-n\omega_a)t+n\,k_a\,x+k_0 z)}{\partial z}=k_0 \qquad 3.12$$

$$\Rightarrow \vec{k_n}=k_x\,\vec{i_x}+k_z\,\vec{i_z}=n\,k_a\,\vec{i_x}+k_0\,\vec{i_z} \qquad 3.13$$
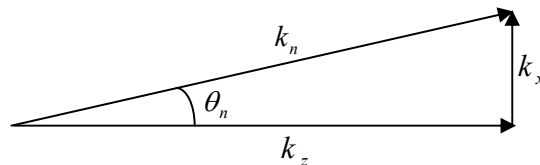
Figure 3.2: The wave vector of the outgoing field $E_n(x,z,t)$ from the AO cell when the ultrasonic wave is sinusoidal.

Hence, the propagation direction is given by the following equation:

$$\tan\theta_n = \frac{n\,k_a}{k_0} = \frac{n\,\lambda_0}{\lambda_a}$$

And luminous frequency is obtained by deriving the vibratory term in relation to time:

$$\omega_n = \frac{\partial\varphi(x,z,t)}{\partial t} = \frac{\partial\left((\omega - n\omega_a)t + n\,k_a\,x - k_0\,z\right)}{\partial t} = \omega - n\omega_a$$

From the previous discussion, we conclude:

1) Different diffraction orders will appear as indicated in figure (3.3) which will propagate in the directions given by the below relation:

$$\sin\theta_n \approx \tan\theta_n = \frac{n\,\lambda_0}{\lambda_a} \qquad\qquad 3.14$$

2) The luminous frequency ω_n of the diffracted order n is shifted with respect to the initial frequency ω of the incident light:

$$\omega_n = \omega - n\omega_a \qquad\qquad 3.15$$
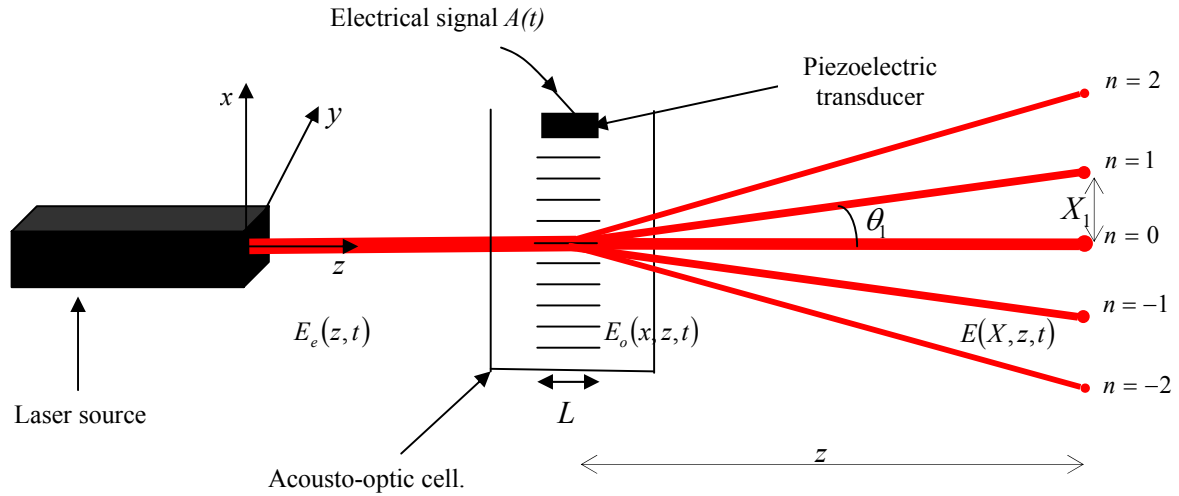
Figure 3.3: Representation of the light diffraction by a sinusoidal ultrasonic wave.

3) The diffracted order intensity is given as follows:

$$\Rightarrow I_n = I_i J_n^{\,2}\left(\frac{2\pi\,L\,\Delta n_0}{\lambda_0}\right) \qquad\qquad 3.16$$

3-3-2) Theoretical study of the acousto-optic interaction in a medium perturbed by amplitude modulated signal:

The propagation of an amplitude modulated ultrasonic wave in an elastic medium causes a spatiotemporal variation of its refractive index. This variation is given by the formula [6]:

$$n(x,t) = n_0 + \Delta n_0 \left[\left[1 + \beta_a \cos(\omega_m t - k_m x) \right] \sin(\omega_a t - k_a x) \right] \qquad 3.17$$

Where:

ω_a, ω_m : Pulsation of carrier and modulating wave respectively.

k_a, k_m : Wave vector of carrier and modulating wave respectively.

β_a : The amplitude modulation index.

We can rewrite the previous equation on the following form:

$$n(x,t) = n_0 + \Delta n_0 \left[\left[1 + \beta_a \cos\left(2\pi\left(f_m t - \frac{x}{\lambda_m} \right) \right) \right] \sin\left(2\pi\left(f_a t - \frac{x}{\lambda_a} \right) \right) \right]$$

$$\Rightarrow n(x,t) = n_0 + \Delta n_0 \sin\left(2\pi\left(f_a t - \frac{x}{\lambda_a} \right) \right) + \Delta n_0 \, \beta_a \cos\left(2\pi\left(f_m t - \frac{x}{\lambda_m} \right) \right) \sin\left(2\pi\left(f_a t - \frac{x}{\lambda_a} \right) \right) \qquad 3.18$$

Putting:

$$\mu_1 = \Delta n_0 \qquad 3.19$$

$$\mu_2 = \Delta n_0 \, \beta_a \qquad 3.20$$

$$\Rightarrow n(x,t) = n_0 + \mu_1 \sin\left(2\pi\left(f_a t - \frac{x}{\lambda_a} \right) \right) + \mu_2 \cos\left(2\pi\left(f_m t - \frac{x}{\lambda_m} \right) \right) \sin\left(2\pi\left(f_a t - \frac{x}{\lambda_a} \right) \right)$$

The phase is then written as follows:

$$\varphi(x,t) = \frac{2\pi}{\lambda_0} L \left[n_0 + \mu_1 \sin\left(2\pi\left(f_a t - \frac{x}{\lambda_a} \right) \right) \right]$$

$$+ \frac{2\pi}{\lambda_0} L \, \mu_2 \cos\left(2\pi\left(f_m t - \frac{x}{\lambda_m} \right) \right) \sin\left(2\pi\left(f_a t - \frac{x}{\lambda_a} \right) \right)$$

$$\Rightarrow \varphi(x,t) = \frac{2\pi}{\lambda_0} L n_0 + \mu_1 \frac{2\pi}{\lambda_0} L \sin\left(2\pi\left(f_a t - \frac{x}{\lambda_a} \right) \right)$$

$$+ \mu_2 \frac{2\pi}{\lambda_0} L \cos\left(2\pi\left(f_m t - \frac{x}{\lambda_m} \right) \right) \sin\left(2\pi\left(f_a t - \frac{x}{\lambda_a} \right) \right)$$

$$\Rightarrow \varphi(x,t) = \frac{2\pi}{\lambda_0} L\, n_0 + \mu_1 \frac{2\pi}{\lambda_0} L\, \sin\left(2\pi\left(f_a t - \frac{x}{\lambda_a}\right)\right)$$

$$+ \mu_2 \frac{\pi}{\lambda_0} L\, \sin\left(2\pi\left(f_a t - \frac{x}{\lambda_a}\right) + 2\pi\left(f_m t - \frac{x}{\lambda_m}\right)\right)$$

$$+ \mu_2 \frac{\pi}{\lambda_0} L\, \sin\left(2\pi\left(f_a t - \frac{x}{\lambda_a}\right) - 2\pi\left(f_m t - \frac{x}{\lambda_m}\right)\right)$$

3.21

Therefore the field at the medium output, using the relation (3.4), is written [32]:

$$E_o(x,z,t) = E_i \exp i(\omega t + k_0\, z) \cdot \exp i\left(-\frac{2\pi n_0 L}{\lambda_0}\right) \cdot \exp i\left[-\frac{2\pi \mu_1 L}{\lambda_0}\, \sin\left(2\pi\left(f_a t - \frac{x}{\lambda_a}\right)\right)\right]$$

$$\cdot \exp i\left[-\frac{\pi \mu_2 L}{\lambda_0}\, \sin\left(2\pi\left(f_a t - \frac{x}{\lambda_a}\right) + 2\pi\left(f_m t - \frac{x}{\lambda_m}\right)\right)\right]$$

3.22

$$\cdot \exp i\left[-\frac{\pi \mu_2 L}{\lambda_0}\, \sin\left(2\pi\left(f_a t - \frac{x}{\lambda_a}\right) - 2\pi\left(f_m t - \frac{x}{\lambda_m}\right)\right)\right]$$

Using the Jacobi relation, the previous formula becomes:

$$E_o(x,z,t) = E_i \exp i(\omega t + k_0\, z) \cdot \exp\left(-i 2\pi \frac{n_0}{\lambda_0} L\right)\left[\sum_{g=-\infty}^{\infty} \exp\left(-i\, g\, 2\pi\left(f_a\, t - \frac{x}{\lambda_a}\right)\right) J_g\left(\frac{2\pi L \mu_1}{\lambda_0}\right)\right]$$

$$\left[\sum_{q=-\infty}^{\infty} \exp\left(-i\, q\, 2\pi\left(f_a\, t + f_m\, t - \frac{x}{\lambda_a} - \frac{x}{\lambda_m}\right)\right) J_q\left(\frac{\pi L \mu_2}{\lambda_0}\right)\right]$$

$$\left[\sum_{p=-\infty}^{\infty} \exp\left(-i\, p\, 2\pi\left(f_a\, t - f_m\, t - \frac{x}{\lambda_a} + \frac{x}{\lambda_m}\right)\right) J_p\left(\frac{\pi L \mu_2}{\lambda_0}\right)\right]$$

Putting:

$$\begin{cases} \alpha = i\, 2\pi\left(f_a t - \dfrac{x}{\lambda_a}\right) \\[2mm] \beta = i\, 2\pi\left(f_a t + f_m t - \dfrac{x}{\lambda_a} - \dfrac{x}{\lambda_m}\right) \\[2mm] \gamma = i\, 2\pi\left(f_a t - f_m t - \dfrac{x}{\lambda_a} + \dfrac{x}{\lambda_m}\right) \end{cases} \quad \text{And} \quad \begin{cases} V_1 = \dfrac{2\pi L \mu_1}{\lambda_0} \\[3mm] V_2 = \dfrac{2\pi L \mu_2}{\lambda_0} \end{cases}$$

$$\Rightarrow E_o(x,z,t) = E_i \exp i(\omega t + k_0 z) \cdot \exp\left(-i\, 2\pi \frac{n_0}{\lambda_0} L\right)\left[\sum_{g=-\infty}^{\infty} \exp(-g\,\alpha)\, J_g(V_1)\right]$$

$$\left[\sum_{q=-\infty}^{\infty} \exp(-q\,\beta)\, J_q\left(\frac{V_2}{2}\right)\right]\left[\sum_{p=-\infty}^{\infty} \exp(-p\,\gamma)\, J_p\left(\frac{V_2}{2}\right)\right]$$

$$\Rightarrow E_o(x,z,t) = E_i \exp i(\omega t + k_0 z) \cdot \exp\left(-i\, 2\pi \frac{n_0}{\lambda_0} L\right)$$

$$\left[\sum_{g,q,p=-\infty}^{\infty} \exp(-g\,\alpha - q\,\beta - p\,\gamma)\, J_g(V_1) J_q\left(\frac{V_2}{2}\right) J_p\left(\frac{V_2}{2}\right)\right]$$

3.23

So the field at the medium output can be written as follows:

$$E_o(x,z,t) = E_i \exp i(\omega t + k_0 z)\cdot \exp\left(-i\, 2\pi \frac{n_0}{\lambda_0} L\right)\cdot \sum_{g,q,q=-\infty}^{+\infty}\left[J_g(V_1)\, J_q\left(\frac{V_2}{2}\right)\, J_p\left(\frac{V_2}{2}\right)\right]$$

$$\exp -i\, 2\pi\left((q+g+p)f_a\, t + (q-p)f_m\, t - (q+g+p)\frac{x}{\lambda_a} + (p-q)\frac{x}{\lambda_m}\right)$$

3.24

❖ The calculation of diffracted order angle using FT:

By replacing the equation (3.24) in equation (3.1), we obtain:

$$E(X,z,t) = E_i \cdot \exp i\left(-\frac{2\pi n_0 L}{\lambda_0}\right)\cdot \exp i(k_0 z)\cdot \exp i\, 2\pi\left[f\, t - (q+g+p)f_a\, t - (q-p)f_m\, t\right]$$

$$\sum_{g,q,q=-\infty}^{+\infty}\left[J_g(V_1)\, J_q\left(\frac{V_2}{2}\right)\, J_p\left(\frac{V_2}{2}\right)\right]\int_{-\infty}^{+\infty} \exp -i\, 2\pi\left(-(q+g+p)\frac{x}{\lambda_a} + (p-q)\frac{x}{\lambda_m}\right)\exp\left[-i k_0\left(\frac{X\cdot x}{z}\right)\right]\, dx$$

$$\Rightarrow E(X,z,t) = E_i \cdot \exp i\left(-\frac{2\pi n_0 L}{\lambda_0}\right)\cdot \exp i(k_0 z)\cdot \exp i\, 2\pi\left[f\, t - (q+g+p)f_a\, t - (q-p)f_m\, t\right]$$

$$\cdot \sum_{g,q,q=-\infty}^{+\infty}\left[J_g(V_1)\, J_q\left(\frac{V_2}{2}\right)\, J_p\left(\frac{V_2}{2}\right)\right]\int_{-\infty}^{+\infty} \exp -i\, 2\pi\left(-\frac{(q+g+p)}{\lambda_a} + \frac{(p-q)}{\lambda_m} + \frac{X}{\lambda_0 z}\right)x\, dx$$

$$\Rightarrow E(X,z,t) = E_i \cdot \exp i\left(-\frac{2\pi n_0 L}{\lambda_0}\right)\cdot \exp i(k_0 z)\cdot \exp i\, 2\pi\left[f\, t - (q+g+p)f_a\, t - (q-p)f_m\, t\right]$$

$$\cdot \sum_{g,q,q=-\infty}^{+\infty}\left[J_g(V_1)\, J_q\left(\frac{V_2}{2}\right)\, J_p\left(\frac{V_2}{2}\right)\right]\delta\left(\frac{X}{\lambda_0 z} - \frac{(q+g+p)}{\lambda_a} - \frac{(q-p)}{\lambda_m}\right)$$

3.25

From this equation, we can deduce that the diffracted order angle is written as follows:

$$\tan\theta_{n,r} = \frac{X}{z} = \left[n\frac{1}{\lambda_a} + r\frac{1}{\lambda_m} \right]\lambda_0 \qquad\qquad 3.26$$

Where:

$$n = (g + q + p) \quad et \quad r = (q - p) \qquad\qquad 3.27$$

Hence, for each pair (n, r) there is a diffraction angle.

From the two previous equations, we can deduce:

$$q = \frac{(n + r - g)}{2} \quad et \quad p = \frac{(n - r - g)}{2}$$

And as the values of (p, q) are integers, that means if $(n \pm r)$ is even (g) is even too and if $(n \pm r)$ is odd (g) is also odd.

So each diffracted order angle is written as follows:

$$\tan\theta_{n,r} = \left[n\frac{1}{\lambda_a} + r\frac{1}{\lambda_m} \right]\lambda_0 \qquad\qquad 3.28$$

❖ The calculation of diffracted order angle using the wave vector definition:

From the equation (3.24) and using (3.27) we can deduce that the field of each diffracted order is given by the following equation:

$$E_{n,r}(x,z,t) = E_i \cdot \exp i\left(-\frac{2\pi n_0 L}{\lambda_0} \right) \cdot \exp i(k_0 z) \cdot \exp i\, 2\pi \left[f\, t - n f_a\, t - r f_m\, t \right]$$
$$\cdot \left[\sum_{g=-\infty}^{\infty} J_g(V_1) J_{\frac{n-r-g}{2}}\!\left(\frac{V_2}{2}\right) J_{\frac{n+r-g}{2}}\!\left(\frac{V_2}{2}\right) \right] \cdot \exp i\, 2\pi \left(n\frac{x}{\lambda_a} + r\frac{x}{\lambda_m} \right) \qquad 3.29$$

The resultant wave vector $\vec{k}_{m_1, m_2}$, represented in figure (3.4) is obtained by deriving the vibratory term in relation to spatial coordinates:

$$k_x = \frac{\partial \varphi(x,z,t)}{\partial x} = \frac{\partial \left[(\omega t + k_0\, z - n\,\omega_a\, t - r\,\omega_m\, t + nk_a x + rk_m x)\right]}{\partial x} \qquad 3.30$$
$$= n k_a + r\, k_m$$

$$k_z = \frac{\partial \varphi(x,z,t)}{\partial z} = \frac{\partial \left[(\omega t + k_0\, z - n\,\omega_a\, t - r\,\omega_m\, t + nk_a x + rk_m x)\right]}{\partial z} = k_0 \qquad 3.31$$

$$\Rightarrow \vec{k}_{n,r} = k_x\, \vec{i_x} + k_z\, \vec{i_z} = (n k_a + r k_m)\vec{i_x} + k_0\, \vec{i_z} \qquad\qquad 3.32$$
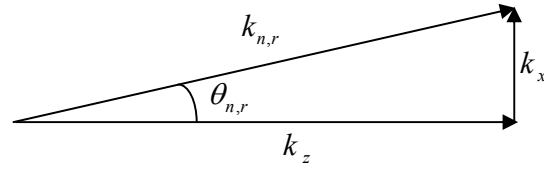
Figure 3.4: The wave vector of the outgoing field $E_n(x,z,t)$ from the AO cell

when the ultrasonic wave is amplitude modulated.

Hence, the propagation direction is given by the following equation:

$$\tan\theta_{n,r} = \left[n\frac{1}{\lambda_a} + r\frac{1}{\lambda_m} \right]\lambda_0$$

And luminous frequency is obtained by deriving the vibratory term in relation to time:

$$\omega_{n,r} = \frac{\partial\varphi(x,z,t)}{\partial t} = \frac{\partial\left[(\omega t + k_0 z - n\omega_a t - r\omega_m t + nk_a x + rk_m x)\right]}{\partial t}$$

$$= \omega - n\omega_a t - r\omega_m t$$

From the previous discussion, we conclude:

1) Different diffraction orders will appear as indicated in figure (3.5) which will propagate in the directions given by the below relation:

$$\sin\theta_{n,r} \approx \tan\theta_{n,r} = \left[n\frac{1}{\lambda_a} + r\frac{1}{\lambda_m} \right]\lambda_0 \qquad\qquad 3.33$$

2) The luminous frequency ω_n of the diffracted order (n,r) is shifted with respect to the initial frequency ω of the incident light:

$$\omega_{n,r} = \omega - n\omega_a t - r\omega_m t \qquad\qquad 3.34$$

66

Figure 3.5: Representation of the light diffraction by an amplitude modulated

sinusoidal ultrasonic wave.

Hereby the formulas (3.33) and (3.34) one can observe that the diffraction spectrum consists of:

- Principal diffracted orders obtained when $n = 0, \pm 1, \pm 2,...$ and $r = 0$ having the same directions as in the case where the ultrasonic wave is not modulated.

- Satellite diffracted orders obtained for each value of n with $r = \pm 1, \pm 2,...$

Likewise, from the formula (3.29) we can distinguish between two symmetry properties in this diffraction:

- The symmetry property of satellite diffracted orders with respect to the corresponding principal diffracted order n which is obtained by changing (r) into $(-r)$ in equation (3.29). We can see immediately that $E_{n,r} = E_{n,-r}$. This signif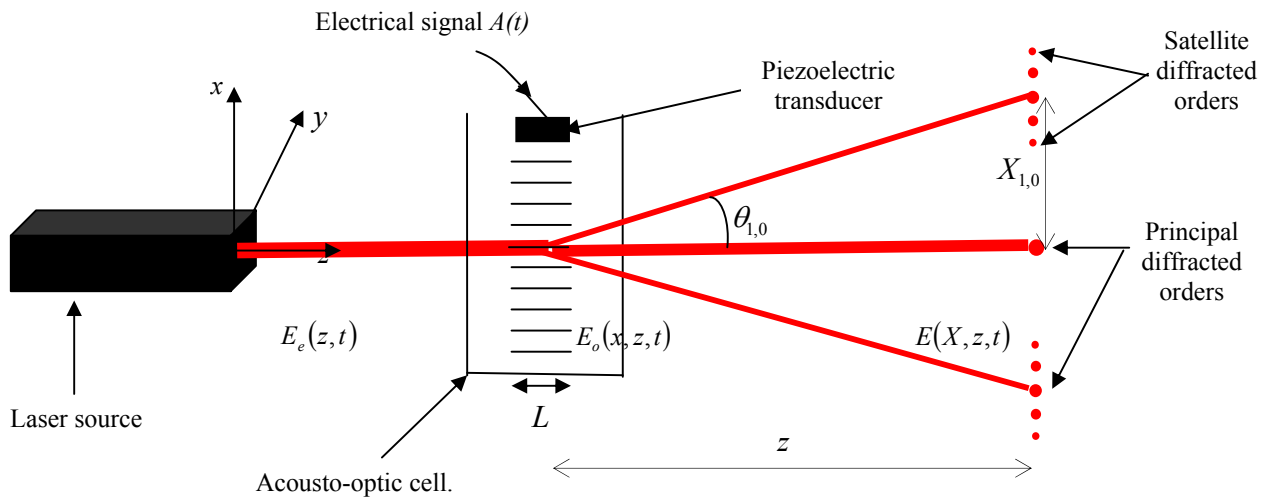ies that the intensity of satellite diffracted orders is symmetrical with respect to the corresponding principal diffracted order.

- The symmetry property of diffracted orders with respect to the non diffracted order ($n=0$) which is obtained by changing (n) into $(-n)$ and (r) into $(-r)$ in equation (3.29). By taking into account the Bessel function priority, we can find after some elementary calculations that $E_{n,r} = E_{-n,-r}$. So the whole diffraction is symmetrical with respect to the non diffracted order.

3-3-3) Theoretical study of the acousto-optic interaction in a medium perturbed by a frequency modulated signal:

The propagation of a frequency modulated ultrasonic wave in an elastic medium causes a spatiotemporal variation of its refractive index. This variation is given by the formula:

$$n(x,t) = n_0 + \Delta n_0 \lfloor \sin(\omega_a t - k_a x + \beta_f \sin(\omega_m t - k_m x)) \rfloor \qquad 3.35$$

Where:

ω_a, ω_m: Pulsation of carrier and modulating wave respectively.

k_a, k_m : Wave vector of carrier and modulating wave respectively.

β_f: The frequency modulation index.

The phase is then written as follows:

$$\varphi(x,t) = \frac{2\pi}{\lambda_0} L \left[n_0 + \Delta n_0 \left[\sin(\omega_a t - k_a x + \beta_f \sin(\omega_m t - k_m x)) \right] \right] \qquad 3.36$$

67

Therefore the field at the medium output, using the relation (3.2), is written [32]:

$$E_o(x,z,t) = E_i \exp i(\omega t + k_0 z) \exp\left(-i\frac{2\pi}{\lambda_0} L n_0\right)$$

$$\exp\left(-i\frac{2\pi}{\lambda_0} L \Delta n_0 \left[\sin\left(\omega_a t - k_a x + \beta_f \sin\left(\omega_m t - k_m x\right)\right)\right]\right)$$

Using the Jacobi relation, the previous formula becomes:

$$E_o(x,z,t) = E_i \exp\left(-i\frac{2\pi}{\lambda_0} L n_0\right) \exp i(\omega t + k_0 z)$$

$$\sum_{n=-\infty}^{+\infty} \exp\left[-i n \left(\omega_a t - k_a x + \beta_f \sin\left(\omega_m t - k_m x\right)\right)\right] J_n\left(\frac{2\pi}{\lambda_0} L \Delta n_0\right)$$

3.37

❖ The calculation of diffracted order angle using FT:

By replacing the equation (3.37) in equation (3.1), we obtain:

$$E(X,z,t) = E_i \cdot \exp i\left(-\frac{2\pi n_0 L}{\lambda_0}\right) \cdot \exp i(k_0 z) \sum_{n=-\infty}^{+\infty} \exp i(\omega t - n\omega_a t) J_n\left(\frac{2\pi L \Delta n_0}{\lambda_0}\right)$$

$$\int_{-\infty}^{+\infty} \exp - i n \left(-k_a x + \beta_f \sin\left(\omega_m t - k_m x\right)\right) \cdot \exp\left[-i k_0\left(\frac{X \cdot x}{z}\right)\right] dx$$

$$\Rightarrow E(X,z,t) = E_i \cdot \exp i\left(-\frac{2\pi n_0 L}{\lambda_0}\right) \cdot \exp i(k_0 z) \sum_{n=-\infty}^{+\infty} \exp i(\omega t - n\omega_a t) J_n\left(\frac{2\pi L \Delta n_0}{\lambda_0}\right)$$

$$\int_{-\infty}^{+\infty} \exp - i\left(\left(k_0 \frac{X}{z} - n k_a\right) x + n\beta_f\left[\sin\left(\omega_m t\right)\cos\left(k_m x\right) - \sin\left(k_m x\right)\cos\left(\omega_m t\right)\right]\right) dx$$

Under some conditions [42-43], we can suppose that: $\begin{cases} \cos\left(k_m x\right) \approx 1 \\ \sin\left(k_m x\right) \approx k_m x \end{cases}$

Hence, the previous integral becomes:

$$E(X,z,t) = E_i \cdot \exp i\left(-\frac{2\pi n_0 L}{\lambda_0}\right) \cdot \exp i(k_0 z) \sum_{n=-\infty}^{+\infty} \exp i(\omega t - n\omega_a t) J_n\left(\frac{2\pi L \Delta n_0}{\lambda_0}\right)$$

$$\int_{-\infty}^{+\infty} \exp - i\left(\left(k_0 \frac{X}{z} - n k_a\right) x + n\beta_f\left[\sin\left(\omega_m t\right) - k_m x \cos\left(\omega_m t\right)\right]\right) dx$$

$$\Rightarrow E(X,z,t) = E_i \cdot \exp i\left(-\frac{2\pi n_0 L}{\lambda_0}\right) \cdot \exp i(k_0 z) \sum_{n=-\infty}^{+\infty} \exp i(\omega t - n\omega_a t) J_n\left(\frac{2\pi L \Delta n_0}{\lambda_0}\right)$$

$$\exp - i n\beta_f\left[\sin\left(\omega_m t\right)\right] \cdot \int_{-\infty}^{+\infty} \exp - i\left(\left(k_0 \frac{X}{z} - n k_a\right) x - n\beta_f k_m x \cos\left(\omega_m t\right)\right) dx$$

$$\Rightarrow E(X,z,t) = E_i \cdot \exp i\left(-\frac{2\pi\, n_0 L}{\lambda_0}\right) \cdot \exp i(k_0 z) \sum_{n=-\infty}^{+\infty} \exp i(\omega t - n\omega_a t)\, J_n\left(\frac{2\pi\, L\, \Delta n_0}{\lambda_0}\right)$$

$$\exp{-i\,n\beta_f}\left[\sin(\omega_m t)\right] \cdot \int_{-\infty}^{+\infty} \exp{-i\,2\pi}\left(\frac{X}{\lambda_0 z} - \frac{n}{\lambda_a} - \frac{n\beta_f}{\lambda_m}\cos(\omega_m t)\right) x\ dx$$

$$\Rightarrow E(X,z,t) = E_i \cdot \exp i\left(-\frac{2\pi\, n_0 L}{\lambda_0}\right) \cdot \exp i(k_0 z) \sum_{n=-\infty}^{+\infty} \exp i(\omega t - n\omega_a t)\, J_n\left(\frac{2\pi\, L\, \Delta n_0}{\lambda_0}\right)$$

$$\exp{-i\,n\beta_f}\left[\sin(\omega_m t)\right] \cdot \delta\left(\frac{X}{\lambda_0 z} - \frac{n}{\lambda_a} - \frac{n\beta_f}{\lambda_m}\cos(\omega_m t)\right) \qquad 3.38$$

So each diffracted order angle is written as follows:

$$\tan \theta_n(t) = \frac{X_n(t)}{z} = \frac{n\,\lambda_0}{\lambda_a} + n\frac{\lambda_0 \beta_f}{\lambda_m}\cos(\omega_m t) \qquad 3.39$$

❖ The calculation of the diffracted order angle using the wave vector definition:

From the equation (3.37), we can deduce that the diffracted order field is given by the following equation:

$$E_n(x,z,t) = E_i \exp\left(-i\frac{2\pi}{\lambda_0}L\,n_0\right)\exp i(\omega t + k_0 z)$$

$$\exp\left[-i\,n\left(\omega_a t - k_a x + \beta_f \sin(\omega_m t - k_m x)\right)\right] J_n\left(\frac{2\pi}{\lambda_0}L\,\Delta n_0\right) \qquad 3.40$$

The resultant wave vector $\vec{k}_n(t)$, represented in figure (3.6), is obtained by deriving the vibratory term in relation to spatial coordinates:

$$k_z = \frac{\partial \varphi(x,t)}{\partial z} = \frac{\partial\left(\left(\omega t + k_0 z\right) - n\left(\omega_a t - k_a x + \beta_f \sin(\omega_m t - k_m x)\right)\right)}{\partial z} = k_0 \qquad 3.41$$

$$k_x(t) = \frac{\partial \varphi(x,t)}{\partial x} = \frac{\partial\left(\left(\omega t + k_0 z\right) - n\left(\omega_a t - k_a x + \beta_f \sin(\omega_m t - k_m x)\right)\right)}{\partial x}$$
$$= n\left(k_a + \beta_f\, k_m \cos(\omega_m t - k_m x)\right) \qquad 3.42$$

Since the $(k_m x)$ value is very small compared to $(\omega_m t)$, the wave vector $\vec{k}_n(t)$ can be written as follows:

$$\vec{k}_n(t) = k_x(t)\vec{i}_x + k_z \vec{i}_z = n\left(k_a + \beta_f\, k_m \cos(\omega_m t)\right)\vec{i}_x + k_0 \vec{i}_z \qquad 3.43$$
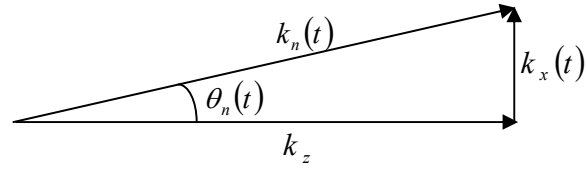
Figure 3.6: The wave vector of the outgoing field $E_n(x,z,t)$ from the AO cell

when the ultrasonic wave is frequency modulated.

Hence, the propagation direction is given by the following equation:

$$\tan \theta_n(t) = \frac{X_n(t)}{z} = \frac{n \lambda_0}{\lambda_a} + n \frac{\lambda_0 \beta_f}{\lambda_m} \cos(\omega_m t)$$

And luminous frequency is obtained by deriving the vibratory term in relation to time:

$$\omega_n(t) = \frac{\partial \varphi(x,t)}{\partial t} = \frac{\partial\big((\omega t + k_0 z) - n(\omega_a t - k_a x + \beta_f \sin(\omega_m t - k_m x))\big)}{\partial t}$$

$$= \omega - n\omega_a - n \beta_f \omega_m \cos(\omega_m t)$$

From the previous discussion, we conclude:

1) A very important relationship that describes the diffracted order deflection as function of time:

$$\sin \theta_n(t) \approx \tan \theta_n(t) = \frac{n \lambda_0}{\lambda_a} + n \frac{\lambda_0 \beta_f}{\lambda_m} \cos(\omega_m t)$$

$$\Rightarrow \sin \theta_n(t) = \frac{X_n(t)}{z} = \frac{X_{n\,med} + \Delta X_n \cos(\omega_m t)}{z} = \theta_{n\,med} + \Delta \theta_n \cos(\omega_m t) \qquad 3.44$$

Where $\Delta \theta_n$ is the angular excursion and $\theta_n(t)$ represents the diffraction angles for n=0,±1, ± 2, ±3…. as indicated in figure (3.7).
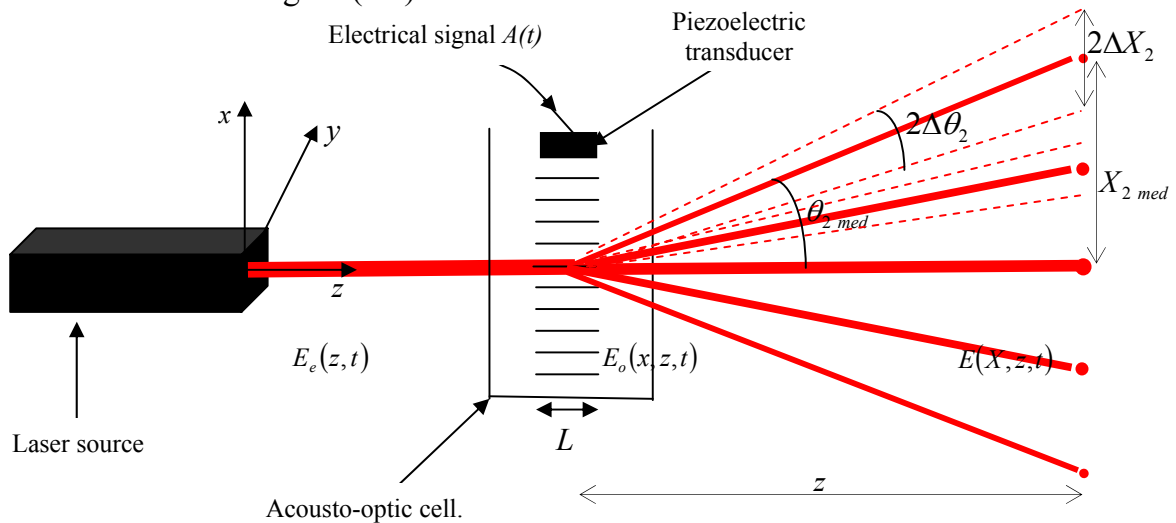
Figure 3.7: Representation of the light diffraction by a frequency modulated

ultrasonic wave.

70

2) This equation contains two parts; a constant part $\theta_{n\,med}$ which represents the angle of nth diffracted order without modulation as shown in figure (3.8-a) and the second one, which depends on time, describes theoretically the diffracted orders deflection around a central position $\theta_{n\,med}$ of the scanned area as presented in figure (3.8-b).
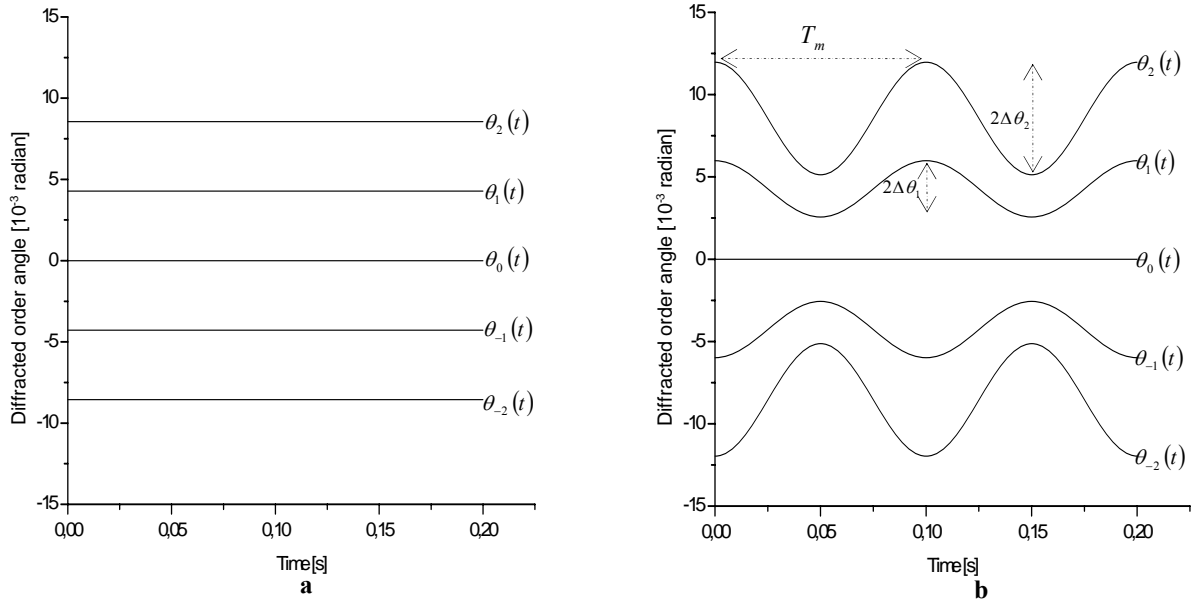
Figure 3.8: Diffracted orders angles for n=0, ±1, ± 2 as a function of time for two cases:
(a) Ultrasonic wave without modulation ($\Delta f = 0$) (b) Ultrasonic wave is frequency modulated ($\Delta f \neq 0$)

3) It is obvious, from figure (3.8-b), that the diffracted orders positions vary in sinusoidal manner with time, where $(T_m = 1/f_m)$ represents the period of the modulating signal as presented in equation (1.2).

4) The angular excursion of each diffracted order $\Delta\theta_n$ depends on two parameters; the diffracted order number n and the frequency excursion Δf as indicated in the following relationship:

$$\Delta\theta_n = n \cdot \frac{\Delta f \cdot \lambda_0}{V} \qquad\qquad 3.45$$

Furthermore, the angular excursion of the nth diffracted order is n times the first diffracted order one, as presented by the following relationship:

71

$$\Delta\theta_n = n \cdot \frac{\Delta f \cdot \lambda_0}{V} = n \cdot \Delta\theta_1$$

We note that, the same formula has been obtained by the reference [37] for the case of Tellurium Dioxide TeO_2 (anisotropic material) taken as an interaction medium.

5) The mathematical expression of β_f is given by the following formula (1.20):

$$\beta_f = \frac{\Delta f}{f_m}$$

Combining this theoretical formula and the relationship given by equation (3.45), the frequency modulation index can be rewritten as follows [44-45]:

$$\beta_f = \frac{\Delta f}{f_m} = \frac{\Delta\theta_n \cdot f_a}{\theta_{n\,med} \cdot f_m} \qquad\qquad 3.46$$

This last relationship indicates that is possible to obtain β_f experimentally by a simple measurement of $\Delta\theta_n$ and $\theta_{n\,med}$ (without modulation).

6) The luminous frequency ω_n of the diffracted order n is shifted with respect to the initial frequency ω of the incident light:

$$\omega_n(t) = \omega - n\omega_a - n\,\beta_f\,\omega_m \cos(\omega_m t) \qquad\qquad 3.47$$

7) The diffracted order intensity is given as follows:

$$I_n = I_i J_n^2\left(\frac{2\pi L\,\Delta n_0}{\lambda_0}\right) \qquad\qquad 3.48$$

8) Using the equation (3.44), the scanning velocity of each diffracted orders is written as follows:

$$X'_n(t) = \frac{dX_n(t)}{dt} = -n \cdot z \cdot \lambda_0 \frac{\Delta f \cdot \omega_m}{V} \sin(\omega_m t) = X'_{n\,max} \sin(\omega_m t) \qquad 3.49$$

It is clear from the obtained equation that the scanning velocity varies; linearly according to the frequency excursion as well as modulating signal frequency and sinusoidally according of time as indicated in figure (3.9). Furthermore, the equation below shows that the scanning maximal velocity of the nth diffracted order is n times of the first diffracted order one.

$$X'_{n\,max} = n \cdot X'_{1\,max} = n \cdot z \cdot \lambda_0 \frac{\Delta f \cdot \omega_m}{V} \qquad\qquad 3.50$$
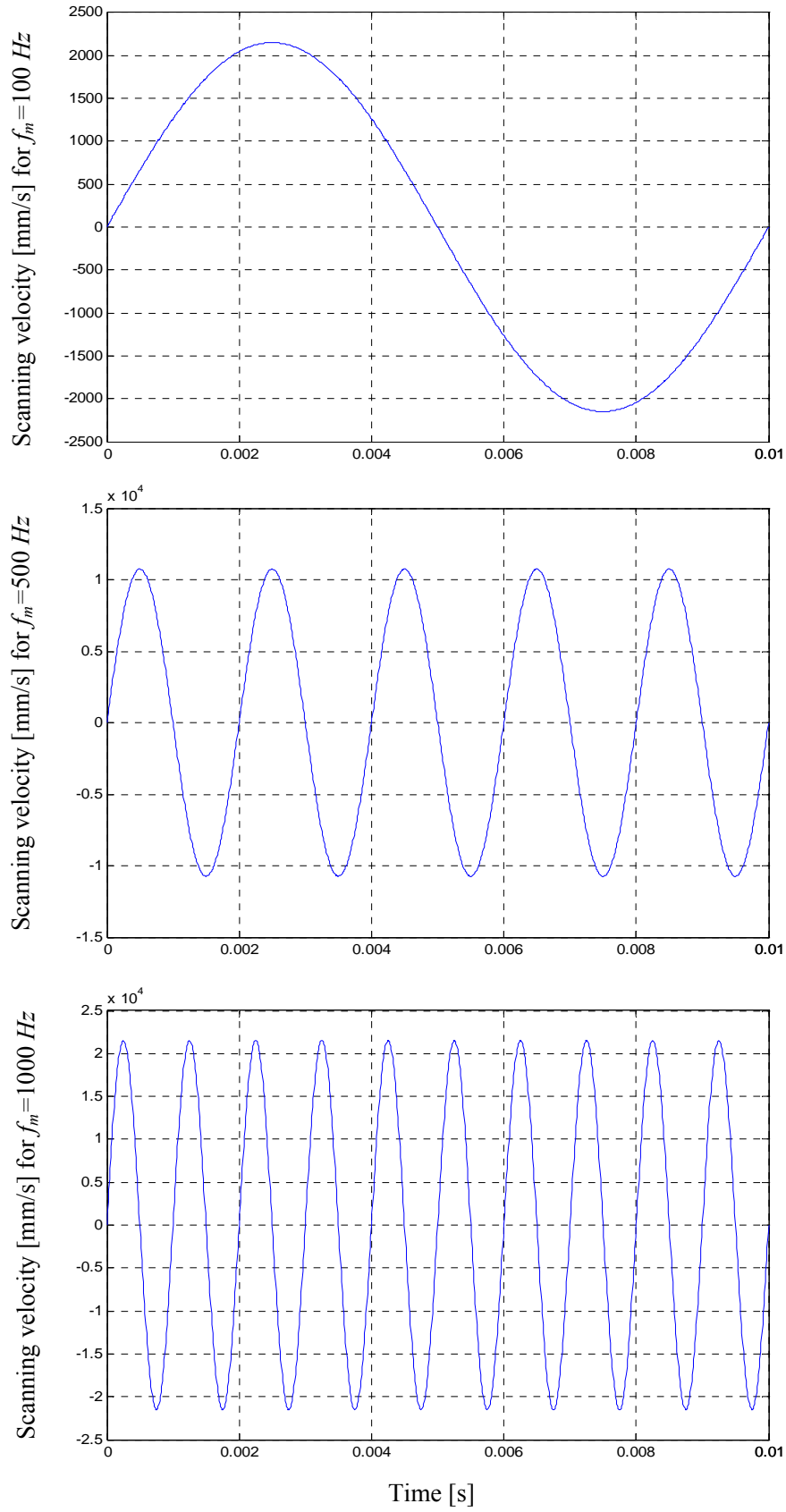
Figure 3.9: The scanning velocity variation as a function of time for different frequencies f_m.

9) To calculate the scanning velocity in each spatial position of diffracted order without knowing time it is enough to combine the two equations (3.44) and (3.49). The obtained formula is presented below:

$$\left(\frac{X_n(t) - X_{n\,med}}{\Delta X_n}\right)^2 + \left(\frac{X'_n(t)}{X'_{n\,max}}\right)^2 = 1 \qquad 3.51$$

This last relation presents ellipse equation which has; a center situated on abscissa axis and at a distance of $X_{n\,med}$ from the center of reference (0, 0) and two diameters: the first one locates on abscissa axis and its value is ΔX_n whereas the second is on ordinate axis and has value of $X'_{n\,max}$ as indicated in figure (3.10).
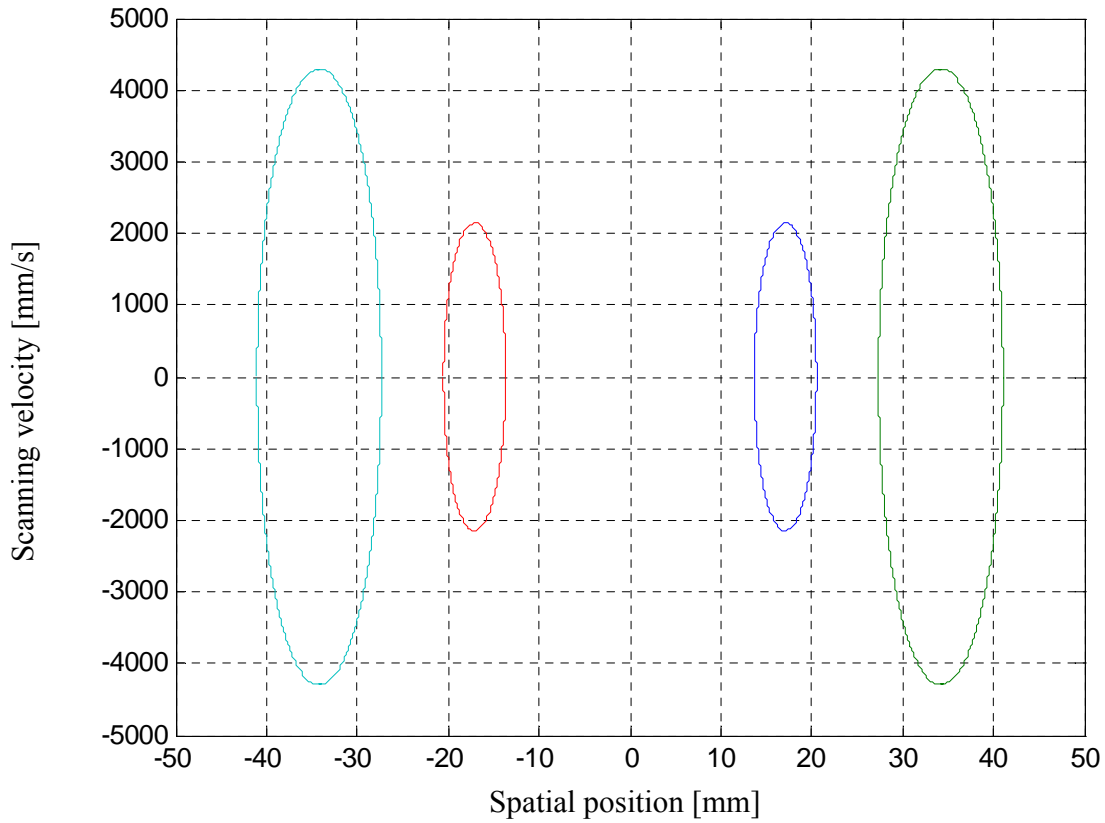
Figure 3.10: Scanning velocity variation according to spatial position for each diffracted order.

It is clear from the obtained figure that the scanning velocity varies elliptically as a function of spatial position, where it takes maximal value $X'_{n\,max}$ when diffracted order passes by central position of scanned area and reduces to zero at both extremities ($X_{n\,max}$, $X_{n\,min}$).

During this chapter, we have confirmed that the intensity and the position of the diffracted orders are constant when a sinusoidal ultrasonic wave is presented. Once this last is replaced by amplitude modulated ultrasonic wave; the diffraction orders position remains constant and also it was observed that besides these diffracted orders, the spectrum showed satellite diffracted orders. Meanwhile, our theoretical study of the light deflection by a frequency modulated ultrasonic wave was enabled us to establish a very important relationship between the diffraction orders positions and the modulating signal. This last relationship showed that; the scanning frequency is equal to the modulating signal frequency f_m and the angular excursion $\Delta\theta_n$ doesn't depend on the modulating signal frequency f_m. Furthermore, for the nth diffracted order, the angular excursion $\Delta\theta_n$ is n times the first diffracted order one.

In the next chapter, we will try to confirm experimentally all results obtained previously.

CHAPTER IV

EXPERIMENTAL STUDY OF THE LIGHT DEFLECTION

4-1) Introduction:

In preceding chapter, we have studied theoretically the diffraction phenomenon for three cases of ultrasonic waves (sinusoidal, amplitude modulated and frequency modulated) and we have succeeded in establishing a mathematical formula which allows us to determine; the diffracted order position as a function of time, the scanning frequency and the angular excursion.

In order to check the proposed theoretical development, a series of experiments will be performed in this chapter; the influence of the modulating signal frequency on the scanning frequency for each diffracted order is considered in section (4-3-1), the influence of the modulating signal frequency on the angular excursion of each diffracted order is the subject of section (4-3-2). This is followed by the presentation of the relationship between frequency excursion and angular excursion of the diffracted order.

4-2) Experimental setup:

Details of the experimental setup are given in Figure (4.1).

Figure 4.1: Experimental set-up

The experimental setup consists of:
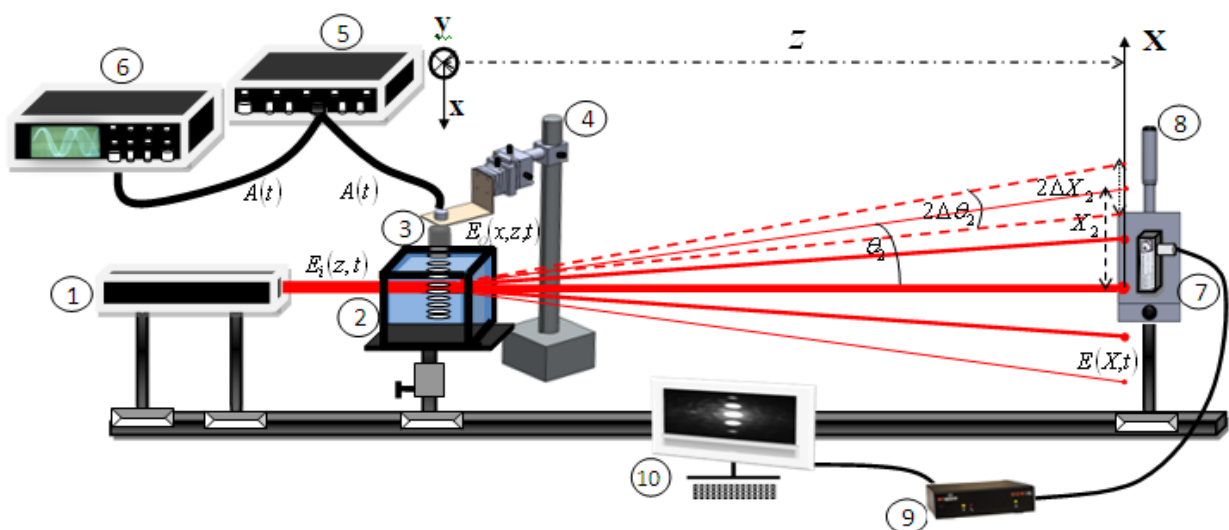
1-He-Ne laser source (output power 30mW at λ_0 =632.8nm) 2- Parallelepiped AO cell, 3- A circular piezoelectric transducer (Panametrics INC, with 19 mm in diameter and with f_r=10MHz as a resonance frequency)**,** 4- A transducer holder. 5- A frequency generator (FI 5500GA) with maximum frequency $f_{a\ max}$=25MHz, U_{max}=20 V and a modulation frequency $f_{m\ max}$ =20kHz, 6- An oscilloscope (Philips) with a maximum detectable frequency f_{max} =80MHz, 7- An ultrafast photodiode (UPh) with a detection specter ranging from λ=170 to 1100 nm, 8- A UPh holder, 9- An acquisition card, 10- A Computer, 11- A CCD Camera with resolution 1034x779 pixel and a pixel size equals 4.65 umx4.65 um), 12- Screen.

The presented optical arrangement allows us to study the acousto-optical interaction using a frequency modulated acoustical signal. An He-Ne laser beam illuminates in the z direction a progressive ultrasonic wave inside a parallelepiped AO cell made of transparent glass and filled with distilled water. A frequency modulated (FM) ultrasonic wave is generated by a piezoelectric circular transducer made of $LiNbO_3$ and driven by a variable frequency generator, where the carrier signal is sinusoidal and presents a high frequency f_a equals 10MHz and a maximum amplitude U equals 20Vpp. The modulating signal in turn, presents a variable frequency f_m .We assume, like Raman and Nath that ultrasound can act as a pure phase grating. Vibrations of the piezoelectric transducer caused variations of the refractive

index of the medium inside the AO cell. Hence, so the distribution of the refractive index is expressed by equation (2.66).

Having left the AO cell, the intensity of the diffracted light in the far field can be observed at a position z equals 4m, as shown in figure (4.1). The acquisition card which is connected to the computer and to the ultrafast photodetector (UPh), as shown in figure (4.1-A) allows us to obtain the scanning frequency of each diffracted order. Whereas its scanning excursion is recorded by a CCD camera as illustrated in figure (4.1-B). The obtained figures of the electrical signals and their respective deflected orders are presented in table (4.1) for different modulating frequencies.
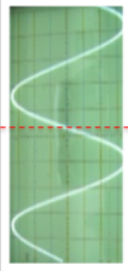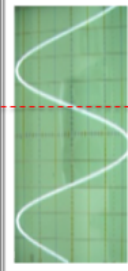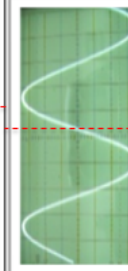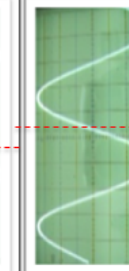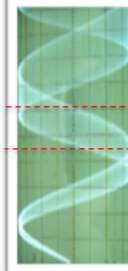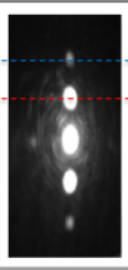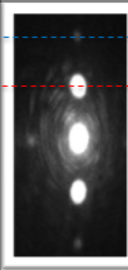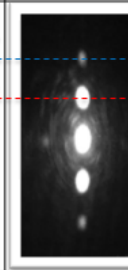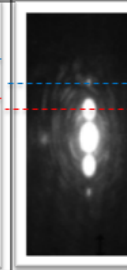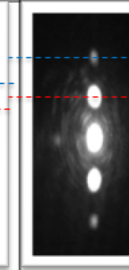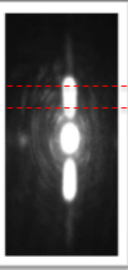
Modulating signal	Low frequency $f_m = 0.1\ Hz$					Moderate frequency $f_m = 100\ Hz$	
	$t = 0\ s$	$t = 2.5\ s$	$t = 5\ s$	$t = 7.5\ s$	$t = 10\ s$		$t(s)$
FM electrical signal recorded by a memory oscilloscope						$2\,\Delta\,T$	$2\,\Delta\,T$
	$t = 0\ s$	$t = 2.5\ s$	$t = 5\ s$	$t = 7.5\ s$	$t = 10\ s$		$t(s)$
Diffracted orders scanning recorded by a CCD camera						$2\,\Delta X_2$ $2\,\Delta X_1$	$2\,\Delta X_1$

Table 4.1: Presentation of FM electrical signals and their corresponding diffracted orders scanning for low and moderate frequencies f_m

From the obtained images, one can observe that the increase of the modulating signal frequency leads to a faster variation of the instantaneous period, as well as the diffracted orders scanning frequency. This can be displayed on the spectral plane by a luminous band.

4-3) Results and discussion

In order to check the proposed theoretical development, a series of experiments have been conducted: the first one consists of observing the influence of a modulating signal frequency f_m on the scanning frequency f_S for each diffracted order, the second consists of observing the influence of the modulating signal frequency f_m and the frequency excursion Δf on the diffracted order angular excursion $\Delta \theta_n$.

The perpendicularity between the ultrasound field and the light beam must be kept at an exact value during the experiment. For this, two goniometers, with an angular resolution of 12', are placed in two perpendicular directions (y and z) to monitor the angular position of the piezoelectric transducer. The perpendicularity is checked at maximum diffraction efficiency. In addition, the UPh is mounted on a holder with two dimensionally moving benches with a step of 10 μm, along x and y directions.

4-3-1) Influence of the modulating signal frequency on the scanning frequency for each diffracted order [46]:

The experimental setup shown in figure (4.1) is carried out in order to observe the effect of the modulating signal frequency f_m on the scanning frequency f_S for each diffracted order ($n= \pm 1$, ± 2).

First, we start the experiment by feeding the transducer with an electrical signal without modulation. The UPh is located at a distance z equals 4m from the parallelepiped AO cell and exactly on the diffracted order position. Then, the previous electrical signal is frequency modulated with a frequency excursion of Δf=2MHz and a modulating signal of f_m=100Hz. The refractive index inside the AO cell takes consequently the form given by equation (2.66). Each

diffracted order will deflect around its central position $\theta_{n\ med}$. The obtained signal of the first diffracted order intensity, recorded by the UPh, is presented in figure (4.2).

Time [s]
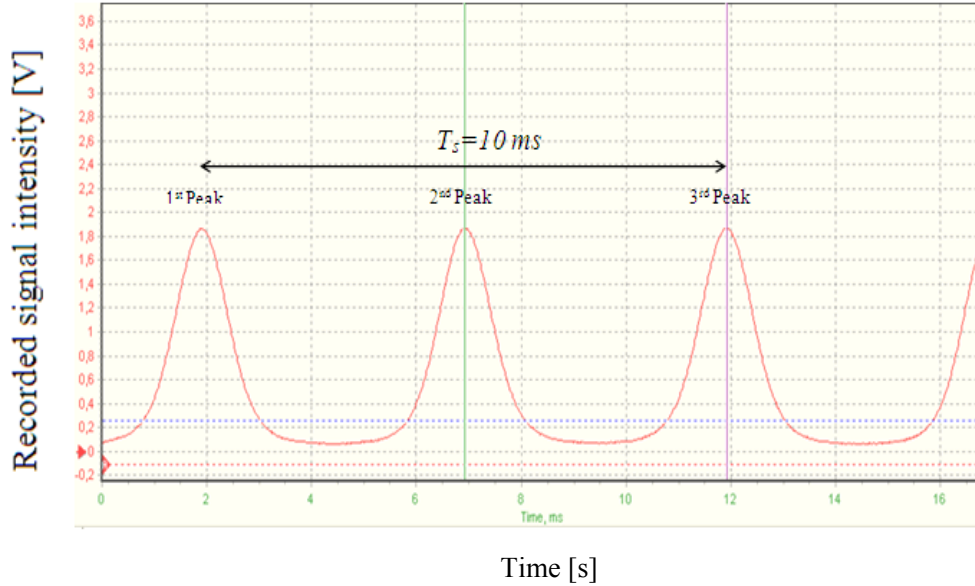
Figure 4.2: Recorded signal intensity of the first diffracted order vs time when the UPh is situated in central position of the scanned area.

What happens practically is that the diffraction order oscillates around a central position with a given period $T_S = 1/f_s$. When the UPh is placed in the central position of the scanned area, it would detect three peaks for two sweeps of the excursion range. The first peak represents the intensity of the first diffracted order when it passes through the central position of the angular excursion in +X direction. Equally, the second peak is the intensity of the same diffracted order but when it returns back to the central position in the opposite direction. The third peak is similar to the first situation. The measurement of time between the first and the third peak corresponds to the scanning period ($T_S = 10\,ms$).

In order to check the exact scanning frequency value of first diffracted order, many measurements have been conducted for different frequencies f_m and for each frequency three UPh positions on X axis have been chosen: the highest reached position of the deflected order (θ_{1max}), the lowest (θ_{1min}), and the medium (θ_{1med}) one. The table (4.2) presents the obtained values.

The modulating signal frequency of the generator f_m [Hz]	Measured scanning frequency f_S [Hz]		
	θ_{1max}	θ_{1min}	θ_{1med}
0.10	0.098	0.097	0.099
1.00	0.970	1.050	1.000
10	9.888	10.010	9.780
100	105.000	103.500	100.000
1 000	1,000.000	1,040.000	1,040.000

Table 4.2: The scanning frequency values f_s of the first diffracted order for different positions of the UPh.

It is clear from the obtained results that the scanning frequency is very close to the modulating signal one f_m and the relative difference between the two frequencies varies from 0 to 5%. We note that the same results were recorded for the remaining diffracted orders.

To explain theoretically the obtained results, it is sufficient to consider equation (3.44). A double excursion $2(\theta_{n\,max} - \theta_{n\,min})$, takes place for time t=1/f_m. This means that, theoretically, the scanning frequency is exactly equal to the modulating signal frequency, which is observed experimentally in table (4.2).

In order to clarify what happens when the UPh moves from position to another, we propose to see these recorded signals by acquisition card:
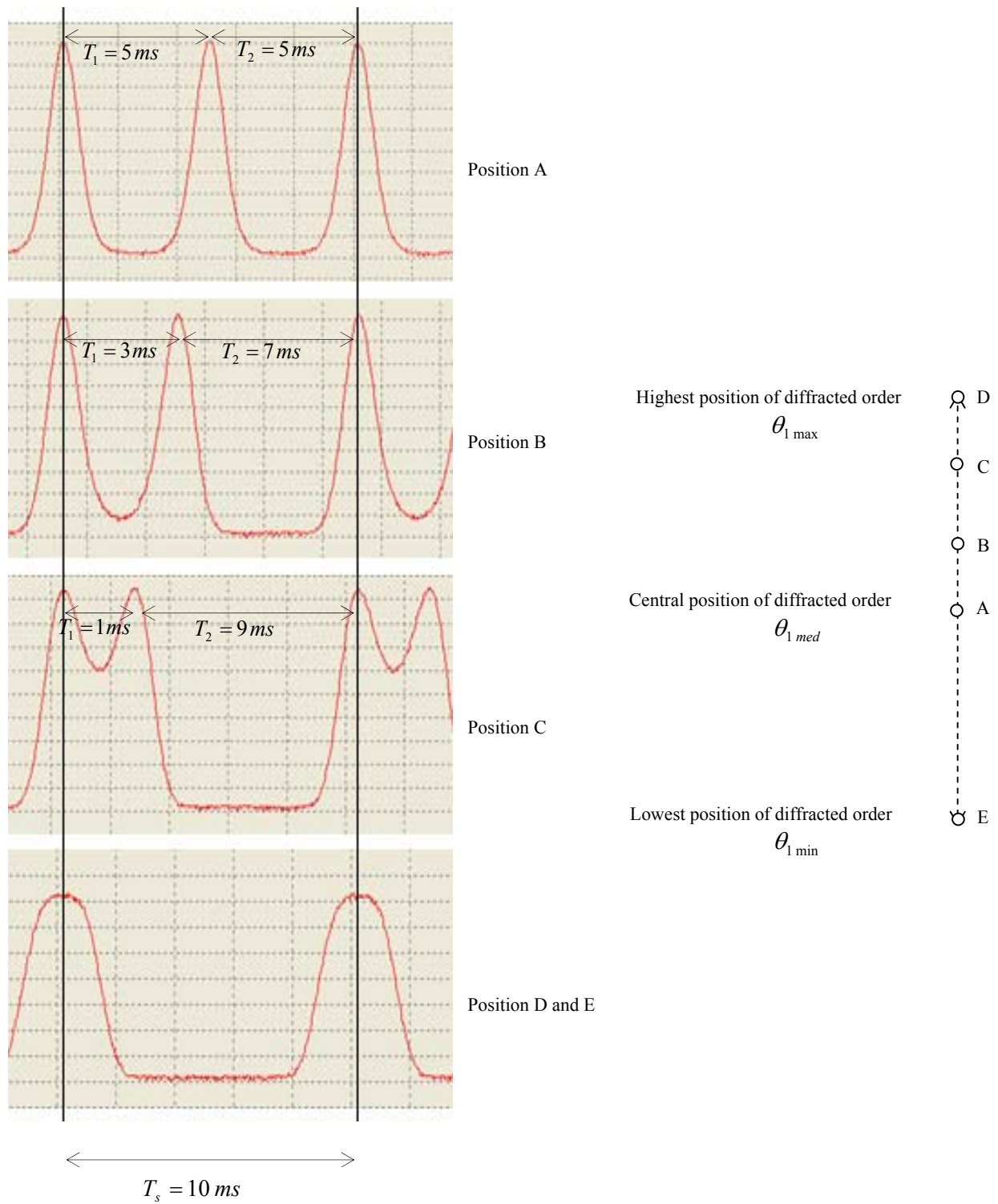
Figure 4.3: Recorded signals intensity of the first diffracted order vs time for different positions of UPh.

4-3-2) Influence of the modulating signal frequency on the angular excursion of the diffracted order [46]:

This experiment has been conducted in order to observe the influence of the modulating signal frequency f_m on the angular excursion $\Delta\theta_n$. For this purpose the same electrical signal without modulation, previously used, has been employed to measure the medium angle θ_{1med} using a micro displacement of the UPh holder. This last has shown that the value of this angle is to the order of ($4.25 \ 10^{-3}$ rd). Then, we choose $\Delta f = 2$MHz and measure the maximum and the minimum reached angles of the first diffracted order θ_{1max} and θ_{1min} respectively, for different values of f_m. The diffracted light intensity was used as a tool to define the exact limits of the deflected area. The table (4.3) and the figure (4.4) illustrate the obtained average values of the deflected angles with their standard deviations.

Generator frequency [*Hz*]	1st angular measurement [rd .10^{-3}]	2nd angular measurement [rd .10^{-3}]	Average values [rd .10^{-3}]	Standard deviation [rd .10^{-3}]	Angular excursion [rd .10^{-3}]
f_m	$\theta_{1\,max}$	$\theta_{1\,max}$	$\overline{\theta}_{1\,max}$	Sd_{1max}	$\Delta\theta_1 = \overline{\theta}_{1max} - \theta_{1med}$
0.1	5.115	5.103	5.109	0.0084	0.859
1	5.125	5.115	5.12	0.0070	0.870
10	5.118	5.108	5.113	0.0070	0.863
100	5.12	5.11	5.115	0.0070	0.865
1000	5.115	5.113	5.114	0.0014	0.864

Generator frequency [*Hz*]	1st angular measurement [rd .10^{-3}]	2nd angular measurement [rd .10^{-3}]	Average values [rd .10^{-3}]	Standard deviation [rd .10^{-3}]	Angular excursion [rd .10^{-3}]
f_m	$\theta_{1\,min}$	$\theta_{1\,min}$	$\overline{\theta}_{1\,min}$	Sd_{1min}	$\Delta\theta_1 = \theta_{1med} - \overline{\theta}_{1min}$
0.1	3.39	3.39	3.39	0	0.860
1	3.39	3.403	3.3965	0.0091	0.854
10	3.388	3.403	3.3955	0.0106	0.855
100	3.385	3.393	3.389	0.0056	0.861
1000	3.385	3.398	3.3915	0.0091	0.859

Table 4.3: Presentation of the angular excursion $\Delta\theta_1$, the maximal and the minimal angle of the first diffracted order for $\Delta f = 2$MHz and different values of f_m

Figure 4.4: The angular excursion $\Delta\theta_n$, the maximum and minimum deflected angles of the first diffracted order according to f_m.

It should be noted that the theoretical curves are plotted using equation (3.44) for an acoustic velocity V equals 1488m/s. To generalize previous results, the same experiment was done for the remaining diffracted orders as indicated in figure (4.5).
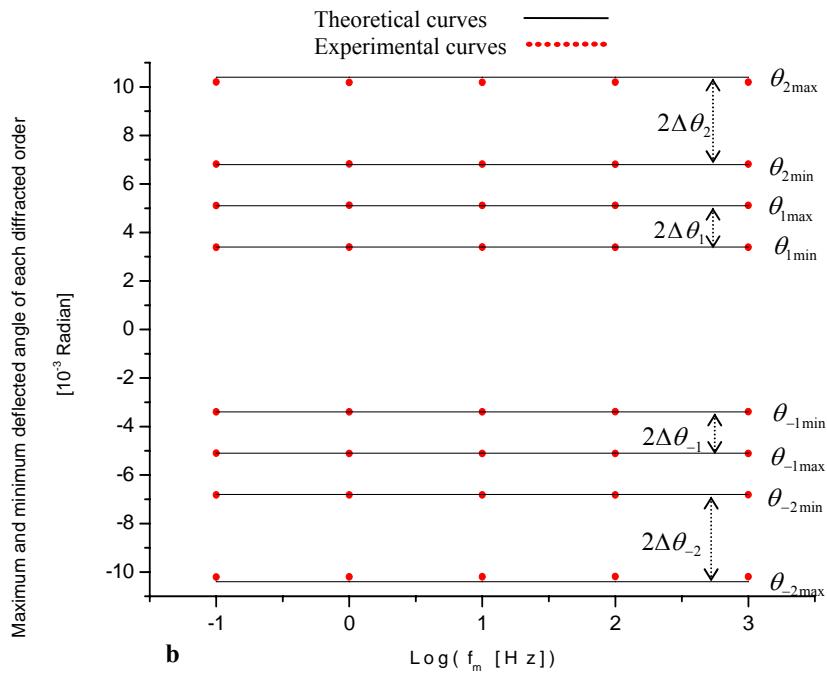
Figure 4.5: The angular excursion $\Delta\theta_n$, the maximum and minimum deflected angles of each diffracted order according to f_m.

From the obtained curves presented in figures (4.4) and (4.5), one can observe that the experimental results are very close to theoretical ones. In addition, the maximum and the minimum deflection angles are symmetrical to a central position θ_{1med} of the diffraction order. Moreover, the angular excursion doesn't depend on the variation of the modulating signal frequency. Furthermore, the angular excursion of the 2nd diffracted order is 2 times the first diffracted order one, as presented by the following relationship:

$$\Delta\theta_n = n\left(\lambda_0\,\Delta f\,/V\right) = n\cdot\Delta\theta_1$$

4-3-3) Influence of frequency excursion on the angular excursion of the diffracted order [46]:

To conduct this experiment, the same previous optical arrangement was undertaken, except in this case the modulating frequency f_m is constant (f_m= 100Hz) and the frequency excursion Δf varies by a step of 0.5MHz. The angular excursion of the first diffracted order is measured for each value of Δf as indicated in table (4.4) and in figure (4.6).

Frequency excursion [MHz]	Average values [rd .10^{-3}]	Standard deviation [rd .10^{-3}]	Average values [rd .10^{-3}]	Standard deviation [rd .10^{-3}]	Angular excursion [rd .10^{-3}]
Δf	$\overline{\theta}_{1\,max}$	$Sd_{1\,max}$	$\overline{\theta}_{1\,min}$	$Sd_{1\,min}$	$2\cdot\Delta\theta_1$
0	4.250	0	4.25	0	0.000
0.5	4.464	0.05	4.063	0.07	0.401
1	4.689	0.05	3.828	0.09	0.861
1.5	4.919	0.055	3.648	0.05	1.271
2	5.065	0.007	3.378	0.009	1.687
2.5	5.319	0.043	3.175	0.04	2.144
3	5.513	0.035	3	0.05	2.513
3.5	5.691	0.004	2.75	0.008	2.941
4	5.909	0.029	2.57	0.025	3.339
4.5	6.144	0.0155	2.335	0.018	3.809
5	6.356	0.026	2.138	0.029	4.218
5.5	6.513	0.010	1.925	0.01	4.588
6	6.765	0.021	1.713	0.007	5.052
6.5	6.981	0.026	1.5	0.04	5.481
7	7.266	0.023	1.255	0.05	6.011

Table 4.4: Presentation of the angular excursion $\Delta\theta_1$, the maximal and the minimal angle of the first diffracted order for f_m =100MHz and different values of Δf.   **85**
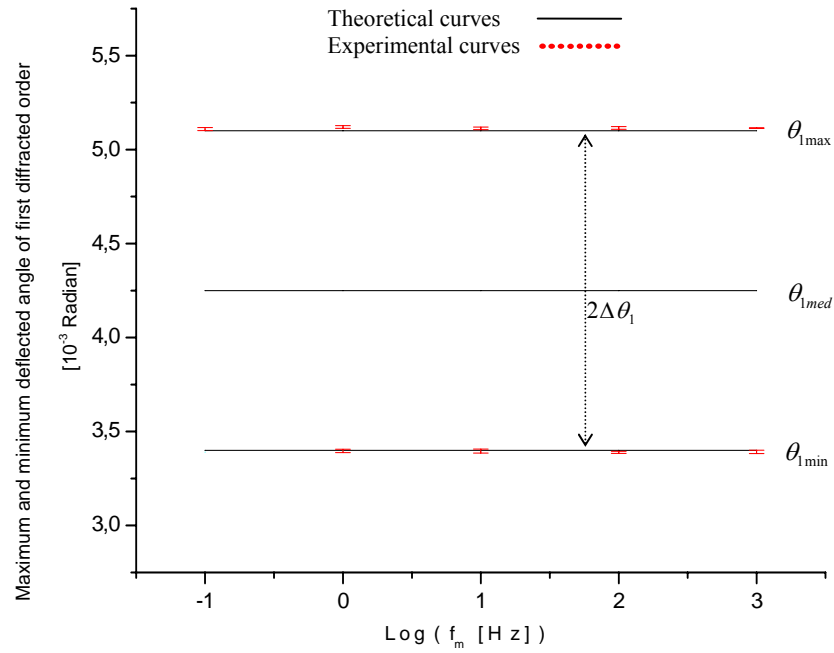
Figure 4.6: Angular excursion $\Delta\theta_n$, the maximum and minimum deflected angles of the

first diffracted order as a function of the frequency excursion Δf.

To generalize these results for the rest of the diffracted orders, the same experiment was undertaken. The obtained results are illustrated in figure (4.7)
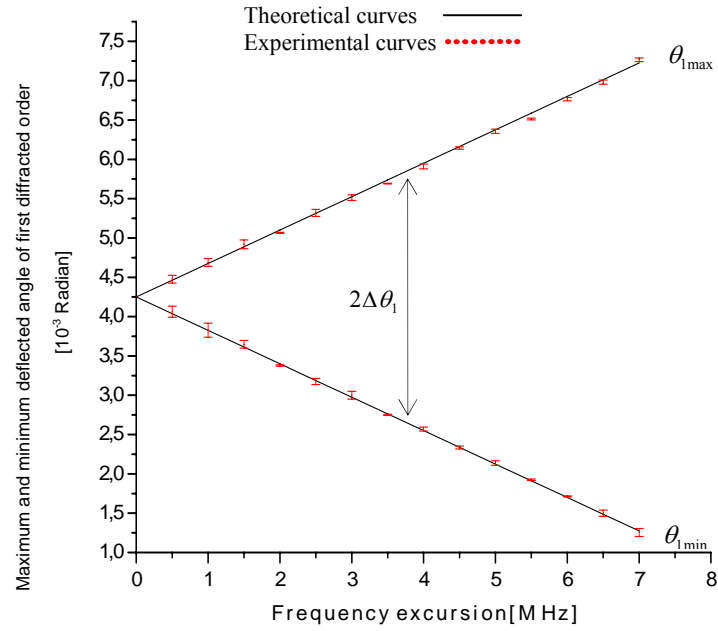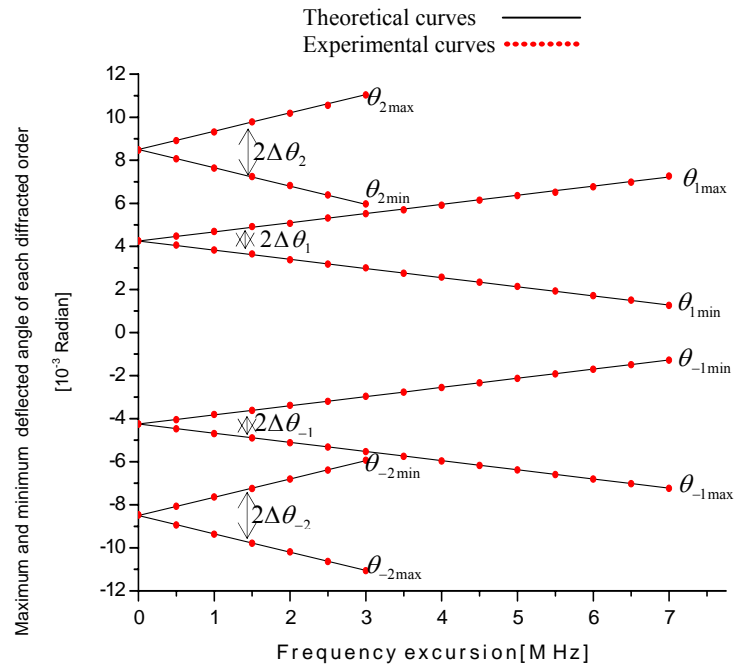

Figure 4.7: Angular excursion $\Delta\theta_n$, the maximum and minimum deflected angles of

each diffracted order as a function of the frequency excursion Δf.

86

The obtained curves show evidently a large concordance between theoretical and experimental results. In addition, a linear relationship is observed between Δf and $\Delta \theta_n$ of the diffracted orders, each pair of curves for the same diffracted order starts from a common point corresponding to $\Delta f = \Delta \theta_n = 0$ (diffraction orders without deflection). The obtained linearity is clearly justified mathematically using equation (3.45) where $\Delta \theta_n$ and Δf are linearly related.

4-3-4) Determination of the frequency modulation index using acousto-optic method:

In this experiment, a new method has been performed to determine with good accuracy a frequency modulation index β_f of an FM signal. This parameter is generally obtained using an electronic spectrum analyzer [11].

The relationship (3.46), mentioned in chapter 3, indicates that is possible to obtain β_f experimentally by a simple measurement of $\Delta \theta_n$ and $\theta_{n\ med}$ (without modulation). The following table presents the values of β_f obtained theoretically using the generator parameters Δf and f_m, and experimentally using the values of $\Delta \theta_n$ and θ_n taken from the previous experiment. The all results are summarized in figure (4.8).

Frequency excursion given by the generator Δf [MHz]	Modulation index given by the generator β_f	First diffracted order (+1)		Second diffracted order (+2)	
		Measured frequency excursion Δf [MHz]	Measured modulation index β_f	Measured frequency excursion Δf [MHz]	Measured modulation index β_f
0	0	0.000	0	0.000	0
0.5	5 000	0.504	5 035	0.514	5 145
1	10 000	1.033	10 329	0.986	9 864
1.5	15 000	1.574	15 741	1.540	15 398
2	20 000	1.918	19 176	2.013	20 130
2.5	25 000	2.515	25 153	2.448	24 484
3	30 000	2.972	29 718	3.012	30 124
3.5	35 000	3.391	33 906		
4	40 000	3.904	39 035		
4.5	45 000	4.456	44 565		
5	50 000	4.955	49 553		

5.5	55 000	5.325	53 247		
6	60 000	5.918	59 176		
6.5	65 000	6.426	64 259		
7	70 000	7.096	70 965		

Table 4.5: Experimental determination of the frequency modulation index
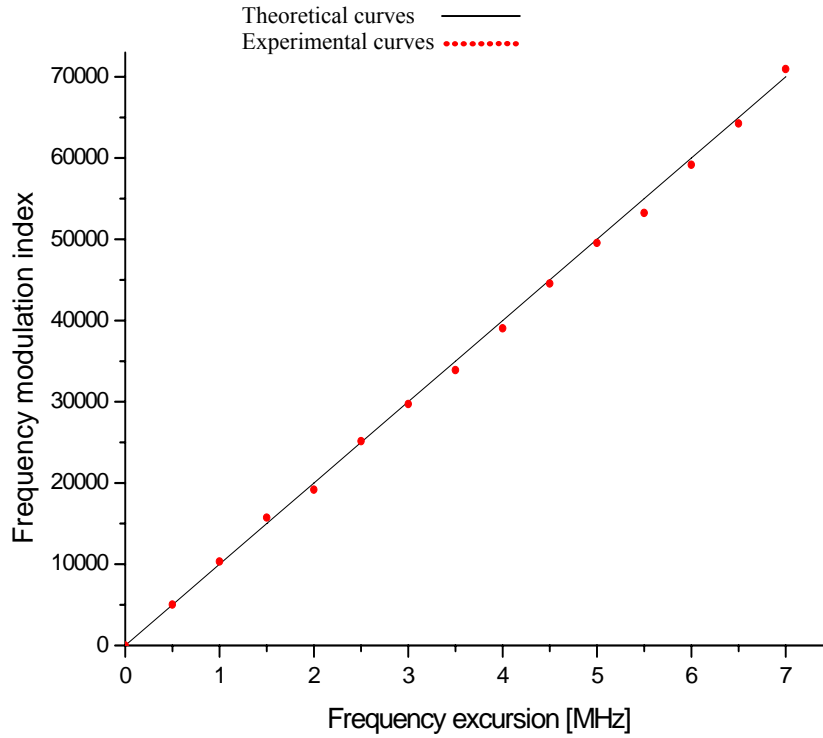
Figure 4.8: Frequency modulation index variation according to the frequency excursion Δf for the first diffracted order

It is clear from the obtained values, that the experimental results of the frequency modulating index are very close to the values given by the generator, the maximum relative error doesn't exceed 5%. It should be noted that the frequency modulation index can also be obtained using the 2nd diffraction order but the bandwidth of the piezoelectric transducer will limit this measurement.

Finally, we have demonstrated theoretically and shown experimentally the possibility of using the (AOD) to obtain the frequency modulation index β_f.

CONCLUSION

The acousto-optic phenomenon is based on three effects; the piezoelectric effect concerns the conversion of an electrical signal into acoustic one, the photoelastic effect has a direct relation with the elastic behavior of the medium and its optical parameters and ultimately the light-ultrasound interaction. This phenomenon is realized by sending a high frequency ultrasonic wave in an elastic medium using a piezoelectric transducer. The interaction of ultrasonic waves with light leads to the diffraction phenomenon. This latter depends on the ultrasonic wave shape (sinusoidal, amplitude modulated and frequency modulated).

In this work, we have theoretically studied all these cases of diffraction then we followed it by experimental study of the last one to confirm the theoretical development. The obtained results show that when ultrasonic wave is sinusoidal, each diffracted order position X_n varies linearly with ultrasound frequency f_a and its optical frequency ω_n shifts from the initial one ω by an amount $n\omega$. In case where the sinusoidal ultrasonic wave of high frequency f_a (carrier) is amplitude-modulated by another one of low frequency f_m (message), the principal diffracted orders have the same directions and optical frequencies as in the previous case whereas, the satellite diffracted orders are symmetrically distributed with respect to the corresponding principal diffracted order n, so the whole diffraction is symmetric with respect to the non diffracted order. It is of interest to note that the satellite diffracted orders are generally superimposed unless if the frequencies of the carrier f_a and message f_m are close to each other.

In the last case when the sinusoidal ultrasonic wave is frequency-modulated by another one, we have established a very important relationship between the diffraction orders positions and the modulating signal. This relationship shows that each diffraction order position $X_n(t)$ oscillates sinusoidally around a central position which represents the diffracted order position without modulation and the scanning frequency f_s is equal to the modulating frequency f_m. In addition, the angular excursion $\Delta\theta_n$ doesn't depend on the frequency modulation f_m and at the same time it has a linear relation with the frequency excursion Δf. Furthermore, the

angular excursion of the nth diffracted order is n times the first diffracted order one. As regards the scanning velocity, it varies linearly according to the frequency excursion as well as modulating signal frequency and sinusoidally according to time. Moreover, the scanning maximal velocity of the nth diffracted order is also n times of the first diffracted order one. Our ultimate goal is to demonstrate theoretically and calculate experimentally the frequency modulation index β using the (AOD).

By this work, we finally wish to open the doors for a better understanding of light deflection by an acousto-optic method. Several points may be the subjects for other theses such as:

- Measure experimentally the scanning velocity of the diffracted order in order to verify the formula already obtained.

-The theoretical development of the same work using Maxwell's differential equation.

-The study of diffracted order intensity.

All these works can contribute to confirm our theoretical and experimental study.

REFERENCES

[01] L. BRILLOUIN « Diffusion de la lumière et des rayons X par un corps transparent homogène influence de l'agitation thermique » annales de physique, Vol. 17, 88-122, 1922.

[02] P. DEBYE and F.W. SEARS « On the scattering of light by supersonic waves » National academy of science, Vol. 18, 409-414, 1932.

[03] R. LUCAS and P. BIQUARD « Propriétés optiques des milieux solides et liquides soumis aux vibrations élastiques ultrasonores » Jour. de physique, Vol. 3, 464-477, 1932.

[04] C.V. RAMAN and S.N.NATH « The diffraction of light by sound waves of high frequency» Part I: Proc. Indian Acad. Sci. 2A, 406-412, Sep. 1935. Part II: Proc. Indian Acad. Sci. 2A, 413-420, Oct. 1935

[05] C.V. RAMAN and S.N.NATH « The diffraction of light by high frequency sound waves» Part III: Proc. Indian Acad. Sci. 2A, 75-84, Jan.1936. Part IV: Proc. Indian Acad. Sci. 2A, 459-465, Fev.1936. Part V: Proc. Indian Acad. Sci. 2A, 119-125, May-1936.

[06] R. MERTENS « On the diffraction of light by an Amplitude modulated ultrasonic wave » Simon Stevin, Vol. 53, 111-120, 1979.

[07] W. HEREMAN « Diffraction of light by an amplitude-modulated ultrasonic wave at normal and oblique incidence of the light » Simon Stevin, Volume 54, 193-211, 1980.

[08] N. FRIEDMAN, A. KAPLAN and N. DAVIDSON « Acousto-optic scanning system with very fast nonlinear scans » OPTICS LETTERS, Vol.25, No. 24, 2000.

[09] A.KAPLAN, N. FRIEDMAN and N. DAVIDSON « Acousto-optic lens with very fast focus scanning » OPTICS LETTERS, Vol.26, No. 14, 2001.

[10] A.H. MACK, M.K. TRIAS, S.G.J. MOCHRIE « Precision optical trapping via a programmable direct-digital-synthesis-based controller for acousto-optic deflectors » Rev. Sci.80, 2009.

[11] J.C.KASTELIK, S.DUPONT, K.B.YUSHKOV, J.GAZALET « Frequency and angular bandwidth of acousto-optic deflectors with ultrasonic walk-off » Ultrasonics, Vol.53, 219–224, 2013.

REFERENCES

[12] A. DUPRET et A. FISHER « Cours de télécommunication » Paris, 1990.

[13] J.MAX et J.L. LACOUME « Méthodes et techniques de traitement du signal » Masson ,1996.

[14] B. A. AULD « Acoustic fields and waves in solids »Wiley-inter-science, New York, 1949.

[15] B. BROWN « ultrasons de haute intensité» Dunod, 1971.

[16] B. ZUG « Etude des pertes d'origine piézoélectrique dans les matériaux piézoélectriques et les transducteurs ultrasonores » PhD thesis, National Institute of Applied Sciences of Lyon, 1994.

[17] E. DIEULESAINT & D. ROYER « Ondes élastiques dans les solides » Paris.

[18] J. PERDIJON « L'échographie » Bordas, paris, 1981.

[19] J.F. NYE «Physical proprieties of crystals» Oxford, 1957.

[20] C. FRANCIS « Traitement des signaux et acquisition de données » Dunod, 2002.

[21] P.K. DAS and M.C DECUSATIS « acousto-optic signal processing: fundamentals and applications» Artech House, 1991.

[22] C. KITTEL « Introduction à la physique de l'état solide » Bordas, 1972.

[23] J.W.GOODMAN « Introduction to Fourier Optics » 7th Edition, McGRAW-HILL, 1996.

[24] A. BENCHEIKH, K. FERRIA « Gaussian laser beam tailoring using acousto-optic cell » Optics and Laser Technology; Vol.44, 806–809, 2011.

[25] M.R. SPIEGEL « Analyse vectorielle »NEW YORK, 1973.

[26] M.R. SPIEGEL « Analyse de Fourier » NEW YORK, 1973.

[27] B. MAURICE « Traitement numérique du signal »PARIS, 2002.

[28]M. CHOSSAT « Mathématiques de l'ingénieur »PARIS, 1977.

[29] A. GOUTZOULIS, R.P. DENNIS and V.K SERGI « Design and fabrication of acousto–optic devices» Marcel dekker, New York, 1994.

[30] S. HUARD « Polarisation de la lumière » Masson, Paris, 1993.

[31] K. D. PANKAJ « Optical signal processing » 1st edition, Springer, Berlin Heidelberg, 1991.

REFERENCES

[32] A. YARIV « Quantum electronics » 3rd edition, New York, 1987.

[33] K. ADRIAN, Acousto-optics, 2nd edition, Marcel Dekker, Now York, 1997.

[34] J.MAX « Traitement du signal et applications aux mesures physiques » Masson, 1987.

[35] M- BORN & E- WOLF « Principles of optics» 7^{éme} edition, 1999.

[36] M. BERTIN- J.P. FAROUX K. & J. RENAULT « Electromagnétisme» Paris, 1984.

[37] Z. TOFFANO «Optoélectronique, Composants photonique et fibre otique » ellipses, 2001.

[38] J-P- MATHIEU « Optique électromagnétique T1 » Jouve, 1965.

[39] L. KINSLER, A.R. FREY, A.B. COPPENS and, J.V. SANDERS « Fundamentals of acoustics » 3rd edition, John Wiley, 1982.

[40] R. N. Thurston « Wave Propagation in Fluids and Normal Solids » in Physical Acoustics, **1A,** Academic Press, New York, 1964.

[41] H. F. HASSAN, S. I. HASSAN and R. RAHIM « Acoustic Energy Harvesting Using Piezoelectric Generator for Low Frequency Sound Waves Energy Conversion » International Journal of Engineering and Technology, Vol.**5,** 6, 2014.

[42] A. Guessoum, N. Laouar & K. Ferria «Theoretical and experimental study of the light deflection by a frequency modulated ultrasonic wave» 10th international Conference School on Acousto-Optics and Applications, Gdansk-Sopot, Poland 12-15 May 2008.

[43] Amir Guessoum, Naamane Laouar & Kouider Ferria « Interaction of light with a perturbed medium by a frequency modulated ultrasonic wave » RAP **03,** 37-41, 2009.

[44] A. Guessoum, K. Ferria « Determine the modulation index of frequency by an acousto optic method» ICO, Novembre -2008-Sétif - Algeria.

[45] A. Guessoum, K. Ferria « Control of the displacement's speed of a photonic spot » The Third International seminar on laser and applications, May 14-16, 2010-Constantine - Algeria.

[46] Amir Guessoum, Naamane Laouar & Kouider Ferria «Theoretical and experimental study of the light deflection by a frequency modulated ultrasonic wave » Optics and laser technology **97**, 260-267, 2017.

Appendix 1: Dirac delta function [27-28]

The Dirac delta can be loosely thought of as a function which is zero everywhere except at the origin, where it is infinite. Thus, the graph of the delta function is usually thought of as following the whole x-axis and the positive y-axis. The integral over the entire real line is equal to one. As there is no function that has these properties, the computations that were done by the theoretical physicists appeared to mathematicians as nonsense, until the introduction of distributions by Laurent Schwartz, for formalizing and validating mathematically these computations. It is widely used in diffraction, signal processing, Laplace transform and probability.

The mathematical expression of this distribution is given by:

$$\delta(x) = \begin{cases} +\infty & x = 0 \\ 0 & x \neq 0 \end{cases}$$

Schematic representation of the Dirac delta function by a line surmounted by an arrow.

Some properties:

- $\int_{-\infty}^{+\infty} \delta(x)\,dx = 1$

- $\delta(x) = \int_{-\infty}^{+\infty} \exp(-j2\pi \cdot x) \cdot v \, dv$

- $\begin{cases} \int_{-\infty}^{+\infty} f(x)\delta(x)\,dx = f(0) \\ \int_{-\infty}^{+\infty} f(x)\delta(x - x_0)\,dx = f(x_0) \end{cases}$

- $f(x)\delta(x - x_0) = f(x - x_0)$

Appendix 2: Jacobi-Anger expansion [26-28]

In mathematics, the Jacobi–Anger expansion (or Jacobi–Anger identity) is an expansion of exponentials of trigonometric functions in the basis of their harmonics. This identity is named after the 19th-century mathematicians Carl Jacobi and Carl Theodor Anger.

The general identity is given by:

$$\exp(i\,z\sin(\alpha)) = \sum_{n=-\infty}^{+\infty} J_n(z)\,\exp(i\,n\alpha)$$

There are other forms derived from this identity, such as:

- $\exp(i\,z\cos(\alpha)) = \sum_{n=-\infty}^{+\infty} J_n(z)\,\exp(i\,n\alpha)(i)^n$

- $\exp(-i\,z\sin(\alpha)) = \sum_{n=-\infty}^{+\infty} J_n(z)\,\exp(-i\,n\alpha)$

- $\exp(-i\,z\sin(\alpha)) = \sum_{n=-\infty}^{+\infty} J_n(z)\,\exp(i\,n\alpha)(-1)^n$

- $\begin{cases} \cos(z\sin(\alpha)) = J_0(z) + 2\sum_{n=1}^{+\infty} J_{2n}(z)\,\cos(2n\alpha) \\ \sin(z\sin(\alpha)) = 2\sum_{n=0}^{+\infty} J_{2n+1}(z)\,\sin((2n+1)\alpha) \end{cases}$

- $\cos(\omega_a t + \beta_f\,\sin(\omega_m t)) = \sum_{n=-\infty}^{+\infty} J_n(\beta_f)\,\cos(\omega_a t + n\,\omega_m t)$

Appendix 3: Bessel functions [26-28]

Bessel functions, first defined by the mathematician Daniel Bernoulli and then generalized by Friedrich Bessel, are the solutions $y(x)$ of Bessel's differential equation [26]:

$$y'' + \frac{1}{x}y' + \left(1 - \left(\frac{n}{x}\right)^2\right)y = 0$$

Where:

n: Complex number

The differential equation solutions are:

1st case (n non-integer): $\qquad\qquad y(x) = A\,J_n(x) + B J_{-n}(x)$

2nd case (n integer): $\qquad\qquad y(x) = C_1\,J_n(x) + C_2\,Y_n(x)$

Where:

$J_n(x)$: Bessel functions of the first kind

$Y_n(x)$: Bessel functions of the second kind

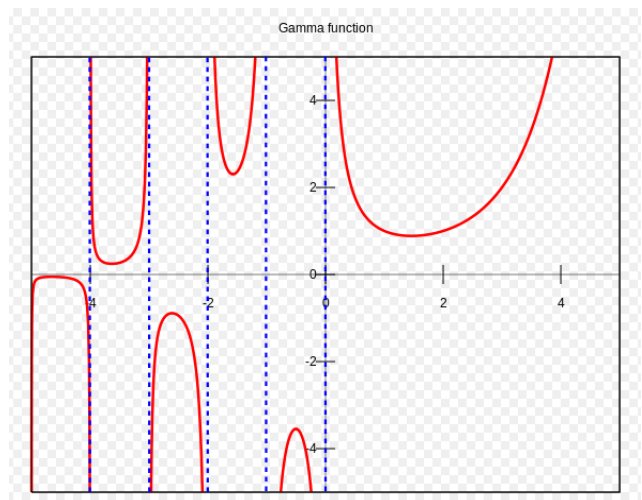<u>Bessel functions of the first kind</u>: It is defined as follows:

$$J_n(x) = \sum_{r=0}^{\infty} \frac{(-1)^r\,(x/2)^{n+2r}}{r!\,\Gamma(n+r+1)}$$

Where:

$\Gamma(\alpha)$: is the gamma function defined as follows:

$$\Gamma(\alpha) = \int_0^{+\infty} y^{n-1}\,e^{-y}\,dy \qquad \alpha \in R$$

From the graph [43 p 73], we can deduc

Gamma function

If $\alpha = 1,2,3....$the gamma function is called the factorial function $\Rightarrow \Gamma(\alpha) = (\alpha - 1)! < \infty$

If $\alpha = 0,-1,-2,-3,.... \Rightarrow \Gamma(\alpha) = \pm\infty$

If $\alpha \neq \begin{cases} 1,2,3.... \\ 0,-1,-2,-3,... \end{cases} \Rightarrow \Gamma(\alpha) < \infty$

Accordingly, if « n » is a positive integer we can simplify the Bessel function to:

$$J_n(x) = \sum_{r=0}^{\infty} \frac{(-1)^r (x/2)^{n+2r}}{r!(n+r)!}$$

$$\Rightarrow J_n(x) = \sum_{r=0}^{\infty} \frac{(-1)^r (x/2)^{n+2r}}{r!(n+r)!} = \frac{(-1)^0 (x/2)^n}{0!(n)!} + \frac{(-1)^1 (x/2)^{n+2}}{1!(n+1)!} + \frac{(-1)^2 (x/2)^{n+4}}{2!(n+2)!} + ...$$

$$\Rightarrow J_n(x) = \frac{(x/2)^n}{(n)!} - \frac{(x/2)^{n+2}}{(n+1)!} + \frac{(x/2)^{n+4}}{2!(n+2)!} + ...$$

The figure below presents the Bessel function of the first kind for integer orders $n = 1,2,3$:
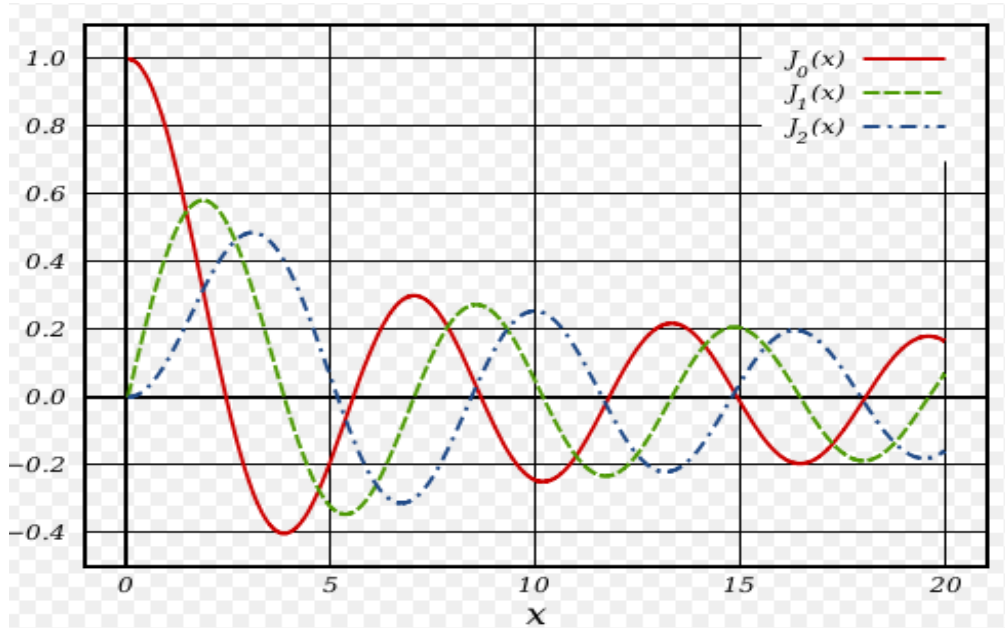
Figure 1: The Bessel function of the first kind for integer orders $n = 1,2,3$

In the case where « n » is a negative integer we can demonstrate that [43]:

$$J_{-n}(x) = (-1)^n J_n(x)$$

Bessel functions of the second kind:

$$Y_n(x) = \frac{J_n(x)\cos(n\pi) - J_{-n}(x)}{\sin(n\pi)} \quad n \neq 0,1,2,3...$$

$$Y_n(x) = \lim \frac{J_p(x)\cos(p\pi) - J_{-p}(x)}{\sin(p\pi)} \quad n = 0,1,2,3... \quad p \longrightarrow n$$

When « n » is an integer, as was similarly the case for the functions of the first kind, the following relationship is valid: $Y_{-n}(x) = (-1)^n Y_n(x)$
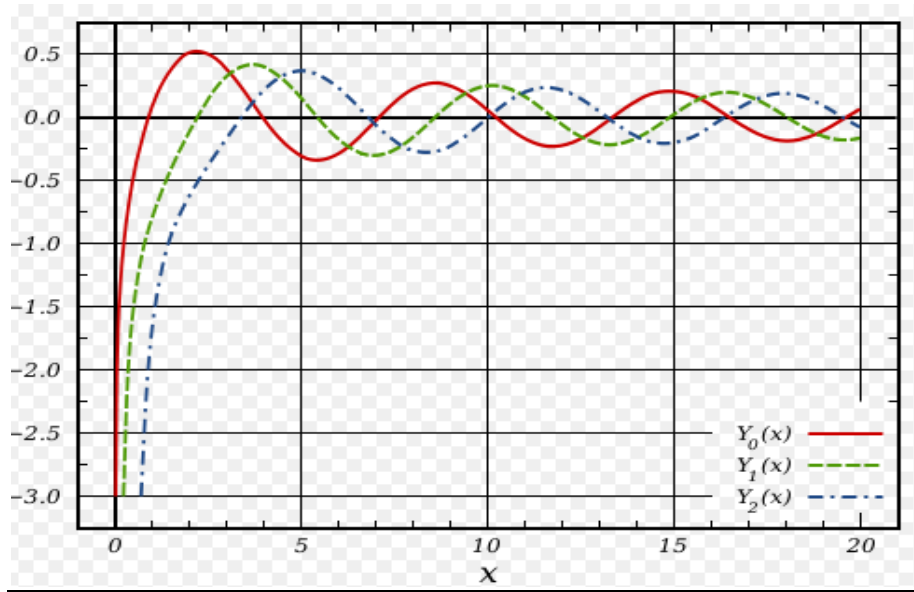
Figure 2: The Bessel function of the second kind for integer orders $n = 1,2,3$

Some properties of the Bessel function of the first kind for integer order "n":

1)

n : Is odd $\Rightarrow J_n(x) = -J_n(-x) \Rightarrow J_n(x)$ the function is odd.

n : Is even $\Rightarrow J_n(x) = J_n(-x) \Rightarrow J_n(x)$ the function is even.

Therefore, in both cases, we have: $J_n(x) = (-1)^n J_n(-x)$

2) $\sum\limits_{n=-\infty}^{+\infty} J_{2n+1}(z) = 0$

3) $\sum\limits_{n=-\infty}^{+\infty} J_n(z) = 1$

6) $\sum\limits_{n=-\infty}^{+\infty} J_{2n}(z) = 1$

98

Appendix 4: Elastic constants

In the science of materials, numbers that quantify the response of a particular material to elastic or non-elastic deformation when a stress load is applied to that material are known as Elastic Constants. These last are:

- The Modulus of Elasticity (Young's modulus) E.

- The Modulus of rigidity (Shear modulus) G.

- The Bulk Modulus K.

- Poisson's Ratio ν.

- The Lamé parameters: Lamé's first parameter G_1

   Lamé's second parameter $G_2 = G$

For homogeneous isotropic materials simple relation exists between elastic constants that allow calculating them all as long as two are known:

$$E = 2 \cdot G_2(1+\nu) = 3 \cdot K(1-2\nu) = \frac{G_1(1+\nu)(1-2\nu)}{\nu}$$

The two known values.	$E =$	$\nu =$	$G_2 =$	$K =$	$G_1 =$
E, ν	E	ν	$\dfrac{E}{2 \cdot (1+\nu)}$	$\dfrac{E}{3 \cdot (1-2\nu)}$	$\dfrac{\nu E}{(1+\nu)(1-2\nu)}$
E, G_2	E	$\dfrac{E - 2 \cdot G_2}{2 \cdot G_2}$	G_2	$\dfrac{E G_2}{3 \cdot (3G_2 - E)}$	$\dfrac{G_2(E - 2G_2)}{(3G_2 - E)}$
E, K	E	$\dfrac{3K - E}{6K}$	$\dfrac{6KE}{9K - E}$	K	$\dfrac{3K(3K - E)}{9K - E}$
E, G_1	E	$\dfrac{2G_1}{E + G_1 + R}$	$\dfrac{E - 3G_1 + R}{4}$	$\dfrac{E + 3G_1 + R}{6}$	G_1
ν, G_2	$2G_2(1+\nu)$	ν	G_2	$\dfrac{2G_2(1+\nu)}{3(1-2\nu)}$	$\dfrac{2G_2\nu}{(1-2\nu)}$
ν, K	$3K(1-2\nu)$	ν	$\dfrac{3K(1-2\nu)}{2(1+\nu)}$	K	$\dfrac{3K\nu}{(1+\nu)}$
ν, G_1	$\dfrac{(1+\nu)(1-2\nu)G_1}{\nu}$	ν	$\dfrac{(1-2\nu)G_1}{2\nu}$	$\dfrac{(1+\nu)G_1}{3\nu}$	G_1

$$R = \sqrt{E^2 + 9G_1^2 + 2EG_1}$$

1) Young's modulus (modulus of elasticity): denoted by E, can be calculated by dividing the tensile stress σ, by the extensional strain ε :

$$E = \frac{\sigma}{\varepsilon} = \frac{F/A}{\Delta L/L}$$

Where:

E: Is the Young's modulus.

L: Is the original length of the object.

F: Is the force exerted on an object under tension.

ΔL: Is the amount by which the length of the object changes.

A: Is the actual cross-sectional area through which the force is applied.
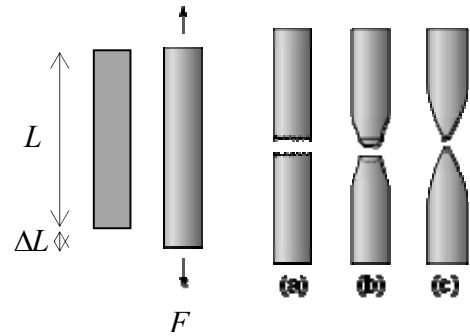
Schematic appearance of round metal bar after tensile testing

(a) Brittle fracture

(b) Ductile fracture

(c) Completely ductile fracture

Material	Typical values for Young's modulus (GPa)
Aluminum	69
Brass	100–125
Bronze	96–120
Copper (Cu)	117
Diamond	1050–1210
Glass	50–90
Magnesium metal (Mg)	45
Nylon	2–4
Osmium (Os)	525–562
Rubber	0.01–0.1
Silicon carbide (SiC)	450
Steel (ASTM-A36)	200
Titanium (Ti)	110.3
Tungsten (W)	400–410
Wood	11

Peak strength

Rupture strength

Ductile behavior

Elastic behavior

100
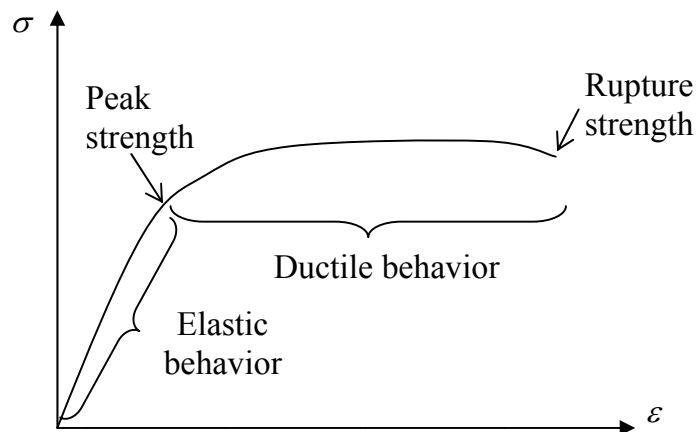
2) Shear modulus (modulus of rigidity): denoted by G, is defined as the ratio of shear stress σ to the shear strain ε:

$$G = \frac{\sigma}{\varepsilon} = \frac{F/A}{\Delta x/l}$$
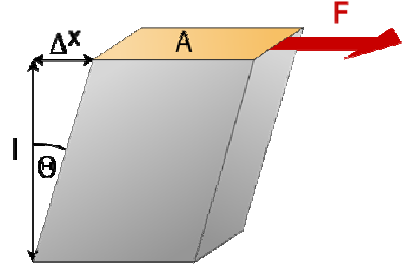
Material	Typical values for shear modulus (GPa) (at room temperature)
Diamond	478.0
Steel	79.3
Copper	44.7
Titanium	41.4
Glass	26.2
Aluminium	25.5
Iron	52.5

3) Bulk modulus: denoted by $K > 0$, can be formally defined by the equation:

$$K = -v_0 \frac{dp}{dv} = \rho_0 \frac{dp}{d\rho}$$

Where:

v_0: Is original pressure.

dp/dv: Denotes the derivative of pressure with respect to volume.

ρ_0: Is original density.

$dp/d\rho$: Denotes the derivative of pressure with respect to density.

The inverse of the bulk modulus gives a substance's compressibility.

Material	Values for bulk modulus
Glass	35 to 55 GPa
Steel	160 GPa
Diamond	443 GPa
Water	2.2 GPa
Methanol	823 MPa
Air	142 KPa
Solid helium	50 MPa

4) Poisson's Ratio: denoted by ν, is the signed ratio of transverse strain to axial strain.

Material	Values for Poisson's Ratio
Rubber	0.4999
gold	0.42–0.44
Saturated clay	0.40–0.49
Copper	0.33
Aluminum-alloy	0.32
Clay	0.30–0.45
Stainless steel	0.30–0.31
Steel	0.27–0.30
Titanium	0.265-0.34
Magnesium	0.252-0.289
Cast iron	0.21–0.26
Sand	0.20–0.45
Glass	0.18–0.3
Foam	0.10–0.50
Concrete	0.1-0.2
Cork	0.0

Appendix 5: Differential operator [25]

A) The Nabla: It's noted ∇, and defined $\nabla = \dfrac{\partial}{\partial x}\vec{i} + \dfrac{\partial}{\partial y}\vec{j} + \dfrac{\partial}{\partial z}\vec{k}$

Where $\dfrac{\partial}{\partial x}, \dfrac{\partial}{\partial y}$ and $\dfrac{\partial}{\partial z}$ are the first partial derivatives of function and the vectors i, j, and k

are the unit vectors in the positive x, y, and z directions, respectively.

This vectorial operator has properties similar to those of ordinary vectors (scalar product, vectorial product, etc.). It is used to define special differential operators include the gradient, divergence, curl, and Laplace operator.

B) The Gradient: In mathematics, a differential operator applied to a three-dimensional vector-valued function to yield a vector whose three components are the partial derivatives of the function with respect to its three variables. The symbol for gradient is $grad$. Thus, the gradient of a function $\phi(x, y, z)$, written $\nabla\phi = grad\phi$, is:

$$\nabla\phi = \left(\frac{\partial}{\partial x}\vec{i} + \frac{\partial}{\partial y}\vec{j} + \frac{\partial}{\partial z}\vec{k} \right)\phi = \frac{\partial\phi}{\partial x}\vec{i} + \frac{\partial\phi}{\partial y}\vec{j} + \frac{\partial\phi}{\partial z}\vec{k}$$

If in physics, for example, $\phi(x, y, z)$ is a temperature field, $\nabla\phi$ is the direction of the heat-flow vector in the field.

C) Divergence: In mathematics, a differential operator applied to a three-dimensional vector-valued function. The result is a function that describes a rate of change. The divergence of a vector $\vec{E}$ is given by:

$$\nabla.\vec{E} = \left(\frac{\partial}{\partial x}\vec{i} + \frac{\partial}{\partial y}\vec{j} + \frac{\partial}{\partial z}\vec{k} \right)\left(E_x\vec{i} + E_y\vec{j} + E_z\vec{k} \right) = \nabla.\vec{E} = \left(\frac{\partial E_x}{\partial x}\vec{i} + \frac{\partial E_y}{\partial y}\vec{j} + \frac{\partial E_z}{\partial z}\vec{k} \right)$$

In which E_x, E_y and E_z are the vector components of $\vec{E}$.

D) Curl: In mathematics, a differential operator that can be applied to a vector-valued function in order to measure its degree of local spinning. It consists of a combination of the function's first partial derivatives. It's noted $\nabla \wedge \vec{E} = \vec{rot}\,\vec{E}$ and defined

$$\nabla \wedge \vec{E} = \left(\frac{\partial}{\partial x} \vec{i} + \frac{\partial}{\partial y} \vec{j} + \frac{\partial}{\partial z} \vec{k} \right) \wedge \left(E_x \vec{i} + E_y \vec{j} + E_z \vec{k} \right) = \begin{vmatrix} \vec{i} & \vec{j} & \vec{k} \\ \frac{\partial}{\partial x} & \frac{\partial}{\partial y} & \frac{\partial}{\partial z} \\ E_x & E_y & E_z \end{vmatrix}$$

$$\Rightarrow \overrightarrow{rot}\vec{E} = \left(\frac{\partial E_z}{\partial y} - \frac{\partial E_y}{\partial z} \right) \vec{i} - \left(\frac{\partial E_z}{\partial x} - \frac{\partial E_x}{\partial z} \right) \vec{j} + \left(\frac{\partial E_y}{\partial x} - \frac{\partial E_x}{\partial y} \right) \vec{k}$$

Some properties: If ϕ and Ψ are differentiable scalar functions and if $\vec{E}$ and $\vec{H}$ are differentiable vector functions, then:

1) $\nabla(\phi + \Psi) = \nabla\phi + \nabla\Psi$

2) $\nabla.\left(\vec{E} + \vec{H} \right) = \nabla.\vec{E} + \nabla.\vec{H}$

3) $\nabla \wedge \left(\vec{E} + \vec{H} \right) = \nabla \wedge \vec{E} + \nabla \wedge \vec{H}$

4) $\nabla.\left(\phi\vec{E} \right) = (\nabla\phi).\vec{E} + \phi\left(\nabla.\vec{H} \right)$

5) $\nabla \wedge \left(\phi\vec{E} \right) = (\nabla\phi) \wedge \vec{E} + \phi\left(\nabla \wedge \vec{H} \right)$

6) $\nabla.\left(\vec{E} \wedge \vec{H} \right) = \vec{H}.\left(\nabla \wedge \vec{E} \right) - \vec{E}.\left(\nabla \wedge \vec{H} \right)$

7) $\nabla \wedge \left(\vec{E} \wedge \vec{H} \right) = \left(\vec{H}.\nabla \right)\vec{E} - \vec{H}\left(\nabla.\vec{E} \right) - \left(\vec{E}.\nabla \right)\vec{H} + \vec{E}\left(\nabla.\vec{H} \right)$

8) $\nabla\left(\vec{E}.\vec{H} \right) = \left(\vec{H}.\nabla \right)\vec{E} + \left(\vec{E}.\nabla \right)\vec{H} + \vec{H} \wedge \left(\nabla \wedge \vec{E} \right) + \vec{E} \wedge \left(\nabla \wedge \vec{H} \right)$

9) $\nabla^2\phi = div\ grad\phi = \frac{\partial^2\phi}{\partial x^2} + \frac{\partial^2\phi}{\partial y^2} + \frac{\partial^2\phi}{\partial z^2}$

10) $\nabla \wedge (\nabla\phi) = 0$

11) $div\ \overrightarrow{rot}\vec{E} = 0$

12) $\nabla^2\vec{E} = grad\ div\vec{E} - \overrightarrow{rot}\ \overrightarrow{rot}\vec{E} = \nabla^2 E_x\ \vec{i} + \nabla^2 E_y\ \vec{j} + \nabla^2 E_z\ \vec{k}$

Appendix 6: POCKELS's and KERR's coefficients [30-31-32]

Crystals are divided into seven crystal systems: triclinic, monoclinic, orthorhombic, tetragonal, trigonal, hexagonal and cubic. Each system is divided into classes. In total there are 32 crystal classes.

The table below presents, one class for each crystal systems, the linear electro-optic matrix coefficients corresponding to the POCKELS effect and the quadratic electro-optic matrix coefficients characterizing the Kerr effect.

Anisotropic medium	POCKELS's coefficients	KERR's coefficients
Triclinic (1)	$$\begin{pmatrix} r_{11} & r_{12} & r_{13} \\ r_{21} & r_{22} & r_{23} \\ r_{31} & r_{32} & r_{33} \\ r_{41} & r_{42} & r_{43} \\ r_{51} & r_{52} & r_{53} \\ r_{61} & r_{62} & r_{63} \end{pmatrix}$$	$$\begin{pmatrix} R_{11} & R_{12} & R_{13} & R_{14} & R_{15} & R_{16} \\ R_{21} & R_{22} & R_{23} & R_{24} & R_{25} & R_{26} \\ R_{31} & R_{32} & R_{33} & R_{34} & R_{35} & R_{36} \\ R_{41} & R_{42} & R_{43} & R_{44} & R_{45} & R_{46} \\ R_{51} & R_{52} & R_{53} & R_{54} & R_{55} & R_{56} \\ R_{61} & R_{62} & R_{63} & R_{64} & R_{65} & R_{66} \end{pmatrix}$$
Monoclinic (mm^2)	$$\begin{pmatrix} r_{11} & 0 & r_{13} \\ r_{21} & 0 & r_{23} \\ r_{31} & 0 & r_{33} \\ 0 & r_{42} & 0 \\ r_{51} & 0 & r_{53} \\ 0 & r_{62} & 0 \end{pmatrix}$$	$$\begin{pmatrix} R_{11} & R_{12} & R_{13} & 0 & R_{15} & 0 \\ R_{21} & R_{22} & R_{23} & 0 & R_{25} & 0 \\ R_{31} & R_{32} & R_{33} & 0 & R_{35} & 0 \\ 0 & 0 & 0 & R_{44} & 0 & R_{46} \\ R_{51} & R_{52} & R_{53} & 0 & R_{55} & 0 \\ 0 & 0 & 0 & R_{64} & 0 & R_{66} \end{pmatrix}$$
Orthorhombic (222)	$$\begin{pmatrix} 0 & 0 & 0 \\ 0 & 0 & 0 \\ 0 & 0 & 0 \\ r_{41} & 0 & 0 \\ 0 & r_{52} & 0 \\ 0 & 0 & r_{63} \end{pmatrix}$$	$$\begin{pmatrix} R_{11} & R_{12} & R_{13} & 0 & 0 & 0 \\ R_{12} & R_{11} & R_{13} & 0 & 0 & 0 \\ R_{31} & R_{31} & R_{33} & 0 & 0 & 0 \\ 0 & 0 & 0 & R_{44} & 0 & 0 \\ 0 & 0 & 0 & 0 & R_{55} & 0 \\ 0 & 0 & 0 & 0 & 0 & R_{66} \end{pmatrix}$$

	POCKELS's coefficients	KERR's coefficients
Tetragonal (422)	$\begin{pmatrix} 0 & 0 & 0 \\ 0 & 0 & 0 \\ 0 & 0 & 0 \\ r_{41} & 0 & 0 \\ 0 & -r_{41} & 0 \\ 0 & 0 & 0 \end{pmatrix}$	$\begin{pmatrix} R_{11} & R_{12} & R_{13} & 0 & 0 & 0 \\ R_{12} & R_{11} & R_{13} & 0 & 0 & 0 \\ R_{31} & R_{31} & R_{33} & 0 & 0 & 0 \\ 0 & 0 & 0 & R_{44} & 0 & 0 \\ 0 & 0 & 0 & 0 & R_{44} & 0 \\ 0 & 0 & 0 & 0 & 0 & R_{66} \end{pmatrix}$
Trigonal (32)	$\begin{pmatrix} r_{11} & 0 & 0 \\ -r_{11} & 0 & 0 \\ 0 & 0 & 0 \\ r_{41} & 0 & 0 \\ 0 & -r_{41} & 0 \\ 0 & -r_{11} & 0 \end{pmatrix}$	$\begin{pmatrix} R_{11} & R_{12} & R_{13} & R_{14} & 0 & 0 \\ R_{12} & R_{11} & R_{13} & -R_{14} & 0 & 0 \\ R_{13} & R_{13} & R_{33} & 0 & 0 & 0 \\ R_{41} & -R_{41} & 0 & R_{44} & 0 & 0 \\ 0 & 0 & 0 & 0 & R_{44} & R_{41} \\ 0 & 0 & 0 & 0 & R_{14} & R_{66} \end{pmatrix}$
Hexagonal $(6mm)$	$\begin{pmatrix} 0 & 0 & r_{13} \\ 0 & 0 & r_{13} \\ 0 & 0 & r_{33} \\ 0 & r_{51} & 0 \\ r_{51} & 0 & 0 \\ 0 & 0 & 0 \end{pmatrix}$	$\begin{pmatrix} R_{11} & R_{12} & R_{13} & 0 & 0 & 0 \\ R_{12} & R_{11} & R_{13} & 0 & 0 & 0 \\ R_{31} & R_{31} & R_{33} & 0 & 0 & 0 \\ 0 & 0 & 0 & R_{44} & 0 & 0 \\ 0 & 0 & 0 & 0 & R_{44} & 0 \\ 0 & 0 & 0 & 0 & 0 & R_{66} \end{pmatrix}$
Cubic (23)	$\begin{pmatrix} 0 & 0 & 0 \\ 0 & 0 & 0 \\ 0 & 0 & 0 \\ r_{41} & 0 & 0 \\ 0 & r_{41} & 0 \\ 0 & 0 & r_{41} \end{pmatrix}$	$\begin{pmatrix} R_{11} & R_{12} & R_{13} & 0 & 0 & 0 \\ R_{13} & R_{11} & R_{12} & 0 & 0 & 0 \\ R_{12} & R_{13} & R_{11} & 0 & 0 & 0 \\ 0 & 0 & 0 & R_{44} & 0 & 0 \\ 0 & 0 & 0 & 0 & R_{44} & 0 \\ 0 & 0 & 0 & 0 & 0 & R_{44} \end{pmatrix}$
Isotropic medium	POCKELS's coefficients	KERR's coefficients
	$\begin{pmatrix} 0 & 0 & 0 \\ 0 & 0 & 0 \\ 0 & 0 & 0 \\ 0 & 0 & 0 \\ 0 & 0 & 0 \\ 0 & 0 & 0 \end{pmatrix}$	$\begin{pmatrix} R_{11} & R_{12} & R_{12} & 0 & 0 & 0 \\ R_{12} & R_{11} & R_{12} & 0 & 0 & 0 \\ R_{12} & R_{13} & R_{11} & 0 & 0 & 0 \\ 0 & 0 & 0 & R_{44} & 0 & 0 \\ 0 & 0 & 0 & 0 & R_{44} & 0 \\ 0 & 0 & 0 & 0 & 0 & R_{44} \end{pmatrix}$

Appendix 7: Photo-elastic coefficients [30-31-32]

The table below presents the photo-elastic matrix coefficients for some class of the crystal systems as well as the isotropic media.

Anisotropic medium	The photo-elastic coefficients
Triclinic	$\begin{pmatrix} p_{11} & p_{12} & p_{13} & p_{14} & p_{15} & p_{16} \\ p_{21} & p_{22} & p_{23} & p_{24} & p_{25} & p_{26} \\ p_{31} & p_{32} & p_{33} & p_{34} & p_{35} & p_{36} \\ p_{41} & p_{42} & p_{43} & p_{44} & p_{45} & p_{46} \\ p_{51} & p_{52} & p_{53} & p_{54} & p_{55} & p_{56} \\ p_{61} & p_{62} & p_{63} & p_{64} & p_{65} & p_{66} \end{pmatrix}$
Monoclinic	$\begin{pmatrix} p_{11} & p_{12} & p_{13} & 0 & p_{15} & 0 \\ p_{21} & p_{22} & p_{23} & 0 & p_{25} & 0 \\ p_{31} & p_{32} & p_{33} & 0 & p_{35} & 0 \\ 0 & 0 & 0 & p_{44} & 0 & p_{46} \\ p_{51} & p_{52} & p_{53} & 0 & p_{55} & 0 \\ 0 & 0 & 0 & p_{64} & p_{65} & p_{66} \end{pmatrix}$
Orthorhombic	$\begin{pmatrix} p_{11} & p_{12} & p_{13} & 0 & 0 & 0 \\ p_{21} & p_{22} & p_{23} & 0 & 0 & 0 \\ p_{31} & p_{32} & p_{33} & 0 & 0 & 0 \\ 0 & 0 & 0 & p_{44} & 0 & 0 \\ 0 & 0 & 0 & 0 & p_{55} & 0 \\ 0 & 0 & 0 & 0 & 0 & p_{66} \end{pmatrix}$
Tetragonal (422)	$\begin{pmatrix} p_{11} & p_{12} & p_{13} & 0 & 0 & 0 \\ p_{12} & p_{11} & p_{13} & 0 & 0 & 0 \\ p_{31} & p_{31} & p_{33} & 0 & 0 & 0 \\ 0 & 0 & 0 & p_{44} & 0 & 0 \\ 0 & 0 & 0 & 0 & p_{44} & 0 \\ 0 & 0 & 0 & 0 & 0 & p_{66} \end{pmatrix}$

Trigonal (32) $p_{66} = \dfrac{p_{11} - p_{12}}{2}$	$\begin{pmatrix} p_{11} & p_{12} & p_{13} & p_{14} & 0 & 0 \\ p_{12} & p_{11} & p_{13} & -p_{14} & 0 & 0 \\ p_{31} & p_{31} & p_{33} & 0 & 0 & 0 \\ p_{41} & -p_{41} & 0 & p_{44} & 0 & 0 \\ 0 & 0 & 0 & 0 & p_{44} & p_{41} \\ 0 & 0 & 0 & 0 & p_{14} & p_{66} \end{pmatrix}$
Hexagonal $(6mm)$ $p_{66} = \dfrac{p_{11} - p_{12}}{2}$	$\begin{pmatrix} p_{11} & p_{12} & p_{13} & 0 & 0 & 0 \\ p_{12} & p_{11} & p_{13} & 0 & 0 & 0 \\ p_{31} & p_{31} & p_{33} & 0 & 0 & 0 \\ 0 & 0 & 0 & p_{44} & 0 & 0 \\ 0 & 0 & 0 & 0 & p_{44} & 0 \\ 0 & 0 & 0 & 0 & 0 & p_{66} \end{pmatrix}$
Cubic (23)	$\begin{pmatrix} p_{11} & p_{12} & p_{12} & 0 & 0 & 0 \\ p_{12} & p_{11} & p_{12} & 0 & 0 & 0 \\ p_{12} & p_{12} & p_{11} & 0 & 0 & 0 \\ 0 & 0 & 0 & p_{44} & 0 & 0 \\ 0 & 0 & 0 & 0 & p_{44} & 0 \\ 0 & 0 & 0 & 0 & 0 & p_{44} \end{pmatrix}$
Isotropic medium	KERR's coefficients
$p_{44} = \dfrac{p_{11} - p_{12}}{2}$	$\begin{pmatrix} p_{11} & p_{12} & p_{12} & 0 & 0 & 0 \\ p_{12} & p_{11} & p_{12} & 0 & 0 & 0 \\ p_{12} & p_{12} & p_{11} & 0 & 0 & 0 \\ 0 & 0 & 0 & p_{44} & 0 & 0 \\ 0 & 0 & 0 & 0 & p_{44} & 0 \\ 0 & 0 & 0 & 0 & 0 & p_{44} \end{pmatrix}$

ABSTRACT:

The using of acousto-optic interaction led to appear a variety of optical devices such as acousto-optic deflectors (AODs), which have in turn widespread applications in many fields. In this thesis, we theoretically demonstrate and experimentally confirmed one of this AOD. This last is obtained using a laser beam interaction with a frequency modulated ultrasonic sinusoidal wave in a liquid medium. The obtained results show that each diffracted order position varies sinusoidally around its central position, in the same rhythm as the modulating signal. Moreover, the scanning frequency of the diffraction order increases linearly according to the modulating signal frequency. Furthermore, the increase in the frequency excursion leads to the increase of the angular excursion. All the theoretical results are confirmed experimentally. Finally, the frequency modulation index has been easily obtained with good precision using experimental measurements of the diffracted order angular excursion.

ملخص:

إن استخدام التداخل الضوئي-الصوتي أدى إلى ظهور العديد من الأجهزة البصرية مثل الماسح الضوئي-الصوتي، والذي بدوره له تطبيقات كثيرة في العديد من المجالات. في هذا الأطروحة نبرهن نظريا ونؤكد تجريبيا واحد من هذه الأجهزة. هذا الأخير يتحصل عليه عندما يتداخل الليزر مع مع موجة فوق صوتية متغيرة تواتريا في وسط سائل. النتائج المحصل عليها تظهر بأن كل موضع كل بقعة منعرجة يتغير جيبيا حول موضعه المركزي، بنفس تواتر المعلومة. ضف إلى ذلك فإن تواتر إهتزاز البقع المنعرجة يتزايد خطيا وفق تواتر المعلومة. أبعد من ذلك، فإن الزيادة في مجال تغير التواتر تؤدي إلى الزيادة في مجال التغير الزاوي. كل النتائج النظرية تم تأكيدها تجريبيا. في الأخير، معامل الترميز التواتري تحصل عليه بطريقة سهلة وبدقة عالية وذلك باستغلال القياسات التجريبية لمجال التغير الزاوي.

RESUME :

L'utilisation de l'interaction acousto-optique a conduit à apparaître une variété de dispositifs optiques tels que les déflecteurs acousto-optiques (DAO), qui ont à leur tour des applications répandues dans de nombreux domaines. Dans cette thèse, nous démontrons théoriquement et nous confirmons expérimentalement l'un de ces DAO. Ce dernier est obtenu en utilisant l'interaction du faisceau laser avec une onde sinusoïdale ultrasonore modulée en fréquence dans un milieu liquide. Les résultats obtenus montrent que la position de chaque ordre diffracté varie sinusoïdalement autour de sa position centrale, au même rythme du signal de modulant. En outre, la fréquence de balayage de l'ordre de diffraction augmente linéairement en fonction de la fréquence du signal de modulant. De plus, l'augmentation de l'excursion de fréquence conduit à l'augmentation de l'excursion angulaire. Tous les résultats théoriques sont confirmés expérimentalement. Enfin, l'indice de modulation de fréquence a été facilement obtenu avec une bonne précision en utilisant des mesures expérimentales de l'excursion angulaire de l'ordre diffracté.